

Agradecimientos

Quiero expresar mi más sincero agradecimiento a los Doctores Mónica Alonso y Juan Carlos Abanades, bajo cuya dirección se ha efectuado el presente trabajo, por el asesoramiento brindado durante su desarrollo, por su dedicación, por la continua motivación y la confianza depositada en mí.

Al Consejo Superior de Investigaciones Científicas (CSIC) por permitir el desarrollo de este trabajo en el Instituto Nacional del Carbón (INCAR) y, en especial, a los Directores de este Centro durante la realización del trabajo, Dra. Rosa Menéndez López y Dr. Carlos Gutiérrez Blanco.

A la Consejería de Educación y Ciencia del Gobierno del Principado de Asturias, por la concesión de una beca predoctoral a través del programa “Severo Ochoa” con cargo a fondos del Plan de Ciencia, Tecnología e Innovación (PCTI).

A los proyectos y contratos que con su financiación han permitido el desarrollo de gran parte de los trabajos realizados en esta Tesis Doctoral: C3-Capture y CaOling del 6º y 7º Programa Marco de la UE, respectivamente. Contrato HUNOSA-CSIC 23/02/2007, contrato Unión Fenosa-CSIC (dentro del módulo 3 del proyecto CENIT CO2) y Agrupación de Interés Económico “La Pereda CO2” entre ENDESA, HUNOSA y CSIC.

A todos los integrantes del “Grupo de Captura de CO₂” del INCAR por su colaboración en los experimentos realizados, especialmente a Fernando Fuentes (eres un crack). A Gemma Grasa y Ramón Murillo del ICB-CSIC de Zaragoza por su ayuda y colaboración en muchos trabajos llevados a cabo en común.

A mis amigos, mis chicas de Ponfe, mis amigos del INCAR, los de siempre, los que acaban de llegar, los que he ido a buscar. Muchas gracias por ir por ahí alegrándome la vida.

Especial agradecimiento a mis padres, a mis hermanas, a mi sobrina. Me encanta teneros como referencia. Me encanta saber de dónde vengo y a dónde puedo volver siempre que quiera, porque estaréis ahí. Muchas gracias.

Resumen

El CO₂ proveniente del uso de combustibles fósiles para la obtención de energía es el principal causante del cambio climático. La captura y el almacenamiento de CO₂ de grandes fuentes estacionarias se plantea como una de las principales opciones de mitigación del cambio climático a corto y medio plazo. En este contexto se enmarca esta memoria de Tesis, en concreto dentro de la temática de captura de CO₂ postcombustión mediante carbonatación-calcinación.

Durante la investigación se ha realizado un análisis básico de diseño y de estructura de costes de dos procesos de captura de CO₂; uno de ellos mediante carbonatación-calcinación, y el otro mediante la obtención de una corriente separada de CO₂ que proviene de la calcinación de CaCO₃ en cementeras.

Con la instalación de una planta piloto experimental compuesta por dos lechos fluidizados circulantes interconectados se han llevado a cabo ensayos de carbonatación y calcinación en continuo para demostrar el proceso de captura de CO₂ con CaO. Se ha desarrollado un modelo del reactor de carbonatación basado en sencillas suposiciones fluidodinámicas, en el que se ha incluido el comportamiento del CaO como sorbente de CO₂. Además se ha realizado un modelo más general para el cálculo de la conversión media máxima de los sólidos que llegan al carbonatador. Por último, se han validado los datos obtenidos de la experimentación en planta piloto con un modelo del

carbonatador. Se ha encontrado que el comportamiento que presentan los datos experimentales concuerda con las tendencias predichas por el modelo.

Abstract

The CO₂ emitted from fossil fuel use for energy production is the main cause of climate change. CO₂ capture and storage from large stationary sources can be one of the main options for climate change mitigation in a short and medium term. This is the general framework for this PhD, which is mainly focused on the CO₂ post-combustion capture process by carbonation and calcination.

During the investigation of this emerging capture process a basic analysis of the design characteristics and the cost structure of two CO₂ capture processes has been carried out. One of these processes is based on capturing CO₂ from flue gases by means of carbonation-calcination cycles, and the other one is aimed at the separation of a pure stream of CO₂ resulting from calcination of CaCO₃ in cement plants.

An experimental pilot plant of two interconnected circulating fluidized beds has been used to test the carbonator reactor in these systems. Many tests of carbonation and calcination have been carried out in continuous mode to demonstrate the viability of CO₂ capture with a bed of CaO. A carbonation reactor model based on simple fluid dynamic assumptions, which includes the behavior of CaO as a CO₂ sorbent, has been developed. In addition, a more general model for calculating the maximum average conversion of solids reaching the carbonator has been accomplished. Finally, the experimental data obtained from pilot plant experiments have been validated with a carbonation

reactor model and the trends of the experimental results are shown to agree with the expected trend predicted by the model.

Tabla de Contenidos

Agradecimientos.....	i
Resumen.....	iii
Abstract	v
Tabla de Contenidos	vii
Lista de Publicaciones.....	ix
Lista de Tablas y Figuras.....	xii
1 Introducción.....	1
1.1 Clima, Energía y CO ₂	2
1.2 Captura, Transporte y Almacenamiento de CO ₂	9
1.2.1 Captura de CO ₂	10
1.2.2 Transporte de CO ₂	12
1.2.3 Almacenamiento de CO ₂	13
1.3 Tecnologías de Captura de CO ₂ Postcombustión	16
1.4 Captura de CO ₂ Postcombustión con CaO a Alta Temperatura	22
1.4.1 Captura de CO ₂ postcombustión. Sistema de dos lechos fluidizados circulantes (carbonatador y calcinador oxifuel)	24
1.4.2 Captura de CO ₂ de la calcinación de CaCO ₃ para cementeras	26
1.4.3 Captura de CO ₂ de gases de combustión. Sistema de tres lechos (combustor, carbonatador y calcinador).....	27
2 Objetivos y Justificación de la Tesis	31
3 Análisis de Procesos de Captura de CO ₂ por Carbonatación – Calcinación	
¡Error! Marcador no definido.	

3.1	Análisis de la Demanda de Calor del Calcinador en el Proceso de Captura de CO ₂ Postcombustión por Carbonatación-Calcinación.....	¡Error! Marcador no definido.
3.2	Análisis de la Pre-calcinación de CaCO ₃ con Captura de CO ₂ para Aplicación a Cementeras.....	¡Error! Marcador no definido.
3.3	Estructura de Costes del Proceso de Captura de CO ₂ con CaO Aplicado a Centrales Térmicas de Carbón y Cementeras..	¡Error! Marcador no definido.
3.4	Publicaciones Relacionadas.....	¡Error! Marcador no definido.
3.4.1	Publicación I.....	¡Error! Marcador no definido.
3.4.2	Publicación II.....	¡Error! Marcador no definido.
3.4.3	Publicación III	¡Error! Marcador no definido.
4	Experimental.....	¡Error! Marcador no definido.
4.1	Descripción de la Planta Piloto de Lechos Fluidizados Circulantes Interconectados	¡Error! Marcador no definido.
4.2	Metodología Experimental.....	¡Error! Marcador no definido.
4.3	Publicaciones Relacionadas.....	¡Error! Marcador no definido.
4.3.1	Publicación IV.....	¡Error! Marcador no definido.
5	Modelo de Reactor de Carbonatación	¡Error! Marcador no definido.
5.1	Descripción del Modelo del Carbonatador	¡Error! Marcador no definido.
5.2	Estimación de la Actividad Media de las Partículas del Sorbente	¡Error! Marcador no definido.
5.3	Validación y Análisis de Tendencias de Datos Experimentales.....	¡Error! Marcador no definido.
5.4	Publicaciones Relacionadas.....	¡Error! Marcador no definido.
5.4.1	Publicación V.....	¡Error! Marcador no definido.
5.4.2	Publicación VI.....	¡Error! Marcador no definido.
5.4.3	Publicación VII.....	¡Error! Marcador no definido.
6	Conclusiones.....	151
	Referencias	157

Lista de Publicaciones

Esta Tesis Doctoral está basada en el trabajo contenido en los siguientes artículos*:

- I. Rodríguez, N., Alonso, M., Grasa, G., Abanades, J. C., 2008. "Heat requirements in a calciner of CaCO₃ integrated in a CO₂ capture system using CaO". *Chemical Engineering Journal*, 138, pp. 148-154.
- II. Rodríguez, N., Alonso, M., Grasa, G., Abanades, J. C., 2008. "Process for capturing CO₂ arising from the calcination of the CaCO₃ used in cement manufacture". *Environmental Science & Technology*, 42, pp. 6980-6984.
- III. Abanades, J. C., Grasa, G., Alonso, M., Rodríguez, N., Anthony, E. J., Romeo, L. M., 2007. "Cost structure of a postcombustion CO₂ capture system using CaO". *Environmental Science & Technology*, 41, pp. 5523-5527.
- IV. Alonso, M., Rodríguez, N., González, B., Grasa, G., Murillo, R., Abanades, J. C., 2009. "Carbon dioxide capture from combustion flue gases with a calcium oxide chemical loop. Experimental results

* La referencia a estos artículos en el texto se hará utilizando los números romanos.

and process development". *International Journal of Greenhouse Gas Control*, 4 (2), pp. 167-173.

- V. Alonso, M., Rodríguez, N., Grasa, G., Abanades, J. C., 2009. "Modelling of a fluidized bed carbonator reactor to capture CO₂ from a combustion flue gas". *Chemical Engineering Science*, 64, pp. 883-891.
- VI. Rodríguez, N., Alonso, M., Abanades, J. C., 2010. "Average activity of CaO particles in a calcium looping system". *Chemical Engineering Journal*, 156 (2), pp. 388-394.
- VII. Rodríguez, N., Alonso, M., Abanades, J. C., 2010. "Experimental investigation of a circulating fluidized bed reactor to capture CO₂ with CaO". *AIChE Journal* (pendiente de publicación)

Los siguientes artículos también han sido publicados durante el periodo de realización de este trabajo pero no son incluidos en esta memoria puesto que su contenido está fuera del objetivo de esta Tesis, o se superponen parcialmente con el trabajo incluido en los anteriores:

- Abanades, J. C., Alonso, M., Rodríguez, N., 2010. "Experimental validation of *in situ* CO₂ capture with CaO during the low temperature combustion of biomass in a fluidized bed reactor". *International Journal of Greenhouse Gas Control* (en prensa).
- Martínez, I., Murillo, R., Grasa, G., Rodríguez, N., Abanades, J. C., 2010. "Conceptual design of a three bed fluidized bed combustion system capturing CO₂ with CaO". *International Journal of Greenhouse Gas Control* (en prensa).

- Murillo, R., Grasa, G., Martínez, I., Rodríguez, N., Abanades J. C., 2009. "Conceptual design of a three bed fluidized bed combustion system capturing CO₂ with CaO". *Proceedings of: 5th Trondheim Conference on CO₂ Capture, Transport and Storage* (Trondheim, Noruega).
- Alonso, M., Abanades, J. C., Rodríguez, N., González, B., Fuentes, F., Rodríguez, I., 2009. "In situ CO₂ capture with CaO during the combustion of biomass in a fluidized bed. Experimental results in a lab scale fluidized bed facility". *Proceedings of: 5th Trondheim Conference on CO₂ Capture, Transport and Storage* (Trondheim, Noruega).
- Alonso, M., Rodríguez, N., González, B., Grasa, G., Murillo, R., Abanades, J. C., 2009. "Postcombustion capture of CO₂ with CaO in a Circulating fluidized bed carbonator". *Proceedings of: 20th International Conference on Fluidized Bed Combustion* (Sian, China).
- Abanades, J. C., Alonso, M., Rodríguez, N., González, B., Grasa, G., Murillo, R., 2008. "Capturing CO₂ from combustion flue gases with a carbonation calcination loop. Experimental results and process development". *Proceedings of: 9th International Conference on Greenhouse Gas Control Technologies* (Washington DC, USA).
- Rodríguez, N., Alonso, M., Abanades, J. C., Grasa, G., Murillo, R., 2008. "Analysis of a process to capture the CO₂ resulting from the pre-calcination of the limestone feed to a cement plant". *Proceedings of: 9th International Conference on Greenhouse Gas Control Technology* (Washington D. C., USA).

Lista de Tablas y Figuras

Tabla 1.1. Descripción de las principales tecnologías de captura de CO ₂ postcombustión.....	18
Figura 1.1. Evolución de la concentración de CO ₂ y CH ₄ en la atmósfera. (Fuente: (TheCopenhagenDiagnosis 2009).....	4
Figura 1.2. Evolución de la demanda de energía primaria mundial y previsiones de la IEA en ausencia de políticas de mitigación. (Fuente: International Energy Agency 2009).....	5
Figura 1.3. Emisiones globales de CO ₂ del uso de combustibles fósiles en un escenario sin políticas de mitigación (línea roja) y en un escenario cuyo objetivo es limitar las emisiones a una concentración de 450 ppm de CO ₂ equivalente (línea verde). (Fuente: International Energy Agency 2009).....	6
Figura 1.4. Esquema general de los procesos y los sistemas de captura de CO ₂	10
Figura 1.5. Esquema general de los principales procesos de separación para la captura de CO ₂ postcombustión.....	17
Figura 1.6. Esquema del sistema de carbonatación- calcinación para gases de combustión de una central existente.	25
Figura 1.7. Esquema del proceso de separación de CO ₂ procedente de la calcinación de CaCO ₃ mediante una corriente de CaO a alta temperatura.....	27

Figura 1.8. Esquema del sistema de carbonatación- calcinación para gases de una cámara de combustión que transfiere calor al calcinador mediante un flujo de CaO a alta temperatura.....	28
Figura 3.1. Esquema comparativo del CO ₂ generado y emitido en una planta convencional y en una planta con CAC.....	¡Error! Marcador no definido.
Figura 4.1. Fotografía de la planta piloto experimental de 30 kW instalada en el INCAR-CSIC.....	¡Error! Marcador no definido.
Figura 4.2. Detalle del funcionamiento de la válvula <i>loop-seal</i> que se sitúa en las tuberías de reciclo del carbonatador y calcinador.	¡Error! Marcador no definido.

1 Introducción

En la última década, se han hecho grandes progresos para comprender mejor el cambio climático y su impacto a largo plazo. Es hoy un hecho probado que la temperatura media de la superficie terrestre se ha incrementado en los últimos 200 años como consecuencia de las emisiones de gases de efecto invernadero (GEI) de origen antropogénico (IPCC-AR4 2007).

El CO₂ se considera el GEI de mayor importancia debido al volumen de sus emisiones a la atmósfera, principalmente por el uso de combustibles fósiles para obtener energía. Por tanto, la energía se halla en el centro del problema del cambio climático y es, por ello, parte esencial de la solución. Asegurar un suministro de energía fiable y asequible, y pasar rápidamente a un nuevo sistema de suministro de energía con bajas emisiones de carbono, eficiente y respetuoso con el medio ambiente son dos de los principales desafíos a los que se enfrenta la humanidad en la primera mitad del siglo XXI.

Se deben tomar medidas políticas inmediatamente para limitar las emisiones de GEI y mitigar así el cambio climático. De lo contrario, todas las previsiones apuntan a un aumento de la demanda mundial de energía primaria promovido fundamentalmente por los países en vías de desarrollo como China, India y Oriente Medio, con incrementos de las emisiones de CO₂ que causarían una elevación de la temperatura media mundial de hasta 6 °C (IPCC-AR4 2007).

En este siglo se requiere una *revolución energética*, que ha de pasar en las próximas décadas por importantes mejoras en la eficiencia de los procesos, el desarrollo de las energías renovables y el impulso de las tecnologías de bajas emisiones de carbono, tales como la captura y el almacenamiento de CO₂ (CAC).

1.1 *Clima, Energía y CO₂*

El clima ha cambiado a lo largo de la vida de la Tierra. Una causa conocida son las variaciones en la intensidad de la energía solar que llega al planeta, consecuencia de las variaciones cíclicas de la excentricidad de la órbita de la Tierra y de la inclinación del eje de rotación de la misma. Además, los eventos catastróficos como choques de meteoritos o erupciones volcánicas generalizadas han ocasionado también impredecibles cambios en el clima. Por tanto, la alteración del clima es permanente y debida a numerosas causas tanto externas como internas al sistema climático. Pero el “cambio climático” del que hoy se habla se define como el cambio del clima atribuido directa o indirectamente a la actividad humana, que altera la composición de la atmósfera terrestre y que se suma a la variabilidad natural del clima observada durante períodos de tiempo comparables (definición utilizada en la Convención Marco de la Naciones Unidas sobre el Cambio Climático (CMNUCC, 1992)).

La atmósfera tiene un papel determinante en la temperatura media de la Tierra debido al efecto invernadero que tiene lugar gracias a los gases que la constituyen. Estos gases, llamados gases de efecto invernadero (GEI), absorben parte de la radiación infrarroja que emite la Tierra para disipar la energía recibida desde el sol. Así, se produce un calentamiento en las capas bajas de la atmósfera alcanzándose una temperatura media de 15°C en la superficie terrestre, en lugar de los -18°C que habría en ausencia de los mismos en la atmósfera. El principal responsable de este efecto invernadero, esencial para el desarrollo de la vida que hoy conocemos, es el vapor de agua

(aproximadamente en un 80% del efecto total) y el segundo es el dióxido de carbono. Así, es comprensible que cualquier alteración de los componentes de la atmósfera responsables del efecto invernadero conllevará un cambio en la cantidad de radiación absorbida y, por ende, un cambio en la temperatura media de la superficie terrestre.

En las últimas décadas se ha detectado una aceleración del incremento de la temperatura de la Tierra con una media en torno a 0,19°C por década desde 1970. El aumento de la temperatura media del planeta se acerca a los 0,8°C desde que empezara la revolución industrial (IPCC-AR4 2007).

Por otro lado, la humanidad ha experimentado un cambio significativo en sus hábitos y costumbres, incrementando su demanda de energía. Como consecuencia de la actividad humana, se han incrementado las emisiones de GEI de larga permanencia como CO₂, CH₄ y N₂O. En la actualidad las concentraciones de estos gases en la atmósfera mundial exceden con mucho de los valores pre-industriales (IPCC-AR4 2007). La concentración de CO₂ en la atmósfera ha alcanzado un valor de 385 ppm en 2008, 105 ppm más que la concentración de CO₂ de la era pre-industrial. La concentración de CH₄ ha aumentado desde 715 ppb en la era pre-industrial hasta 1800 ppb en el año 2008 (ver Figura 1.1), y el N₂O ha aumentado de 270 ppb a 321 ppb.

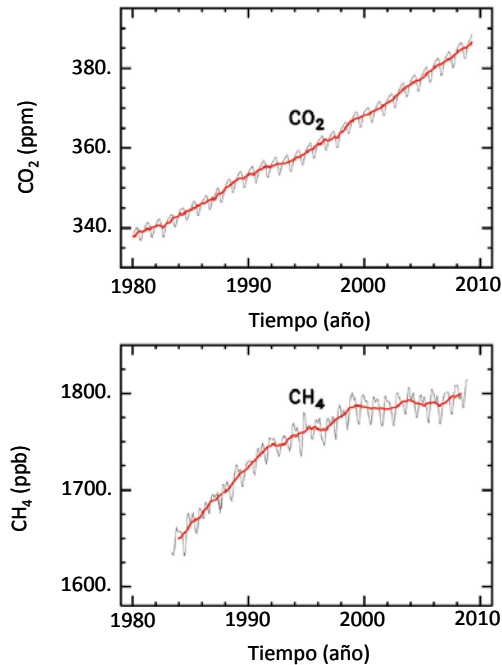


Figura 1.1. Evolución de la concentración de CO₂ y CH₄ en la atmósfera. (Fuente: (TheCopenhagenDiagnosis 2009))

Científicos expertos en clima de todo el mundo han sido capaces de establecer una relación causa-efecto entre las emisiones masivas de GEI en el último siglo y el cambio climático observado (IPCC-AR4 2007).

El incremento de la concentración de GEI como consecuencia de la actividad humana se debe principalmente al uso de combustibles fósiles para dotarnos de bienes y productos energéticos. Como se puede ver en la Figura 1.2, en la actualidad, el 81% de la energía primaria proviene de reacciones de combustión de combustibles fósiles: petróleo, carbón y gas natural. En un escenario de referencia sin políticas de mitigación, la Agencia Internacional de la Energía (IEA) prevé que la demanda mundial de energía primaria aumente un 40% entre 2007 y 2030, y pasar así de algo más de 12.000 millones de toneladas equivalentes de petróleo (tep) a 16.800 millones de tep (IEA 2009). Todas las fuentes de energía crecerán. Sin embargo, los combustibles fósiles

continuarán siendo la base del *mix* energético mundial. Quemar carbón, petróleo y gas, a pesar de sus precios crecientes, seguirán siendo la fuente de energía primaria más barata y accesible, tanto para países desarrollados como para grandes países en vía de desarrollo con enormes reservas de carbón. De todos ellos, el carbón continuará siendo el combustible esencial para la producción eléctrica, y su participación en el *mix* de generación mundial aumentará hasta representar el 44% en 2030. Se puede ver en la Figura 1.2 que las previsiones actuales se han modificado ligeramente respecto al año 2008 (representado por la línea negra punteada) debido a una disminución del consumo energético mundial como consecuencia de la recesión económica. Pero todas las previsiones apuntan a que el crecimiento continuará tan pronto como se inicie la recuperación económica.

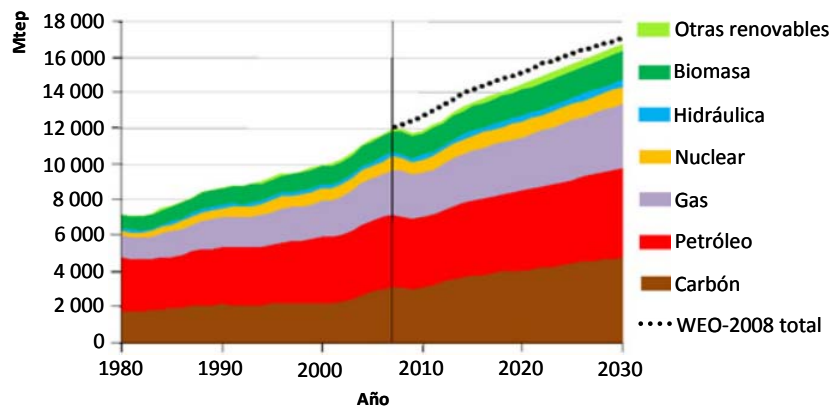


Figura 1.2. Evolución de la demanda de energía primaria mundial y previsiones de la IEA en ausencia de políticas de mitigación. (Fuente: International Energy Agency 2009)

Atendiendo a la demanda energética actual, el CO₂ emerge como el GEI antropogénico de mayor importancia. En la Figura 1.3 se observan las emisiones actuales de CO₂ en millones de toneladas (Gt) y la previsión del incremento de las mismas si se continúa con la senda energética actual. Las previsiones de la IEA, dadas por la línea roja, muestran un aumento rápido y continuo de las emisiones de CO₂, relacionadas con la energía, hasta 2030 como

resultado del incremento general de la demanda de energía fósil. Se calcula que las emisiones de CO₂ alcanzarán 34,5 Gt en 2020 y 40,2 Gt en 2030. Y aunque todos los datos apuntan a que las emisiones de CO₂ relacionadas con la energía se han reducido en 2009 (en torno a un 3%) como consecuencia de la recesión económica, se prevé que retomen una trayectoria al alza a partir de 2010. Si la tasa de crecimiento del consumo de energías fósiles no cambia, la concentración de GEI en la atmósfera aumentará hasta alcanzar una concentración superior a 1000 ppm de CO₂ equivalentes. Esto llevará a una elevación media de la temperatura mundial de hasta 6°C, que provocaría un severo cambio climático de consecuencias irreparables para el planeta.

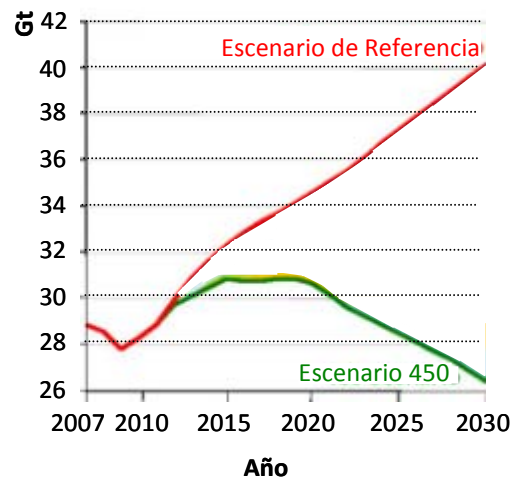


Figura 1.3. Emisiones globales de CO₂ del uso de combustibles fósiles en un escenario sin políticas de mitigación (línea roja) y en un escenario cuyo objetivo es limitar las emisiones a una concentración de 450 ppm de CO₂ equivalente² (línea verde). (Fuente: International Energy Agency 2009)

En los últimos años se ha experimentado un creciente consenso mundial sobre la necesidad de reducir las emisiones de GEI. En el 4º Informe de Evaluación del Panel Intergubernamental de Cambio Climático de Naciones Unidas (IPCC-AR4

² Concentración de CO₂ que causaría el mismo flujo neto de energía hacia la superficie de la Tierra que una mezcla dada de CO₂ y otros GEI.

2007) se consideraba necesario la reducción de entre el 50-80% de gases de efecto invernadero para el año 2050, respecto del año 1990. En la reciente Cumbre de las Naciones Unidas sobre el Cambio Climático celebrada en Copenhague en diciembre de 2009, participaron 189 países cuyo objetivo era llegar a un acuerdo vinculante sobre las medidas a tomar para mitigar el cambio climático y que permitiera relevar el protocolo de Kyoto que expira en 2012. La finalidad última era conseguir un acuerdo refrendado por la mayoría de países para lograr una reducción sustancial de los gases de efecto invernadero. El resultado final de la Cumbre celebrada no fue del todo satisfactorio, pues no se llegó a un acuerdo en el que se estableciesen las cantidades de emisiones que cada país debe reducir y, por otro lado, tampoco se refrendó el compromiso de reducir un 50% las emisiones de cara al 2050, respecto al valor de 1990. A pesar de esto, lo que sí se forjó en el Acuerdo de Copenhague fue un consenso en torno a la necesidad de limitar la elevación de la temperatura global a 2°C, y se estableció limitar la temperatura con objetivos voluntarios de reducción de emisiones que los países habían de presentar antes de febrero de 2010.

Para limitar el incremento de la temperatura por debajo de 2°C sería necesario estabilizar la concentración de gases de efecto invernadero en la atmósfera a un nivel cercano a 450 ppm de CO₂ equivalente. En este escenario, denominado *Escenario 450* en la Figura 1.3, las emisiones mundiales de CO₂ relacionadas con la energía alcanzarían un máximo de 30,9 Gt justo antes de 2020 para disminuir a partir de ese punto hasta 26,4 Gt en 2030.

A pesar del consenso mundial para mitigar el cambio climático a través de la reducción de las emisiones de CO₂, la tarea para llevarlo a cabo no es fácil. Su problemática se percibe atendiendo a las tendencias de los términos de la ecuación de Kaya:

$$\text{Emisiones de CO}_2 = \text{Población} \left(\frac{\text{PIB}}{\text{Población}} \right) \left(\frac{\text{Energía}}{\text{PIB}} \right) \left(\frac{\text{Emisiones de CO}_2}{\text{Energía}} \right)$$

La evolución de la población humana (Cohen 1995) muestra un crecimiento exponencial sostenido durante casi un millón de años, con un despegue particularmente notable desde el siglo XVIII. Las previsiones de Naciones Unidas indican que este crecimiento continuará hasta 9.000-10.000 millones de personas hacia el 2050 (Duarte et al. 2009). El segundo término (PIB/población) hace referencia a la renta per cápita. La renta per cápita tiende a crecer en casi todo el mundo, y debe crecer más rápidamente en aquellos países que están en vías de desarrollo. El tercer término es la intensidad energética o la cantidad de energía necesaria para generar una unidad de riqueza (energía/PIB). Este factor es alto en los países en vías de desarrollo, y solo puede disminuir ligeramente hacia un valor constante en economías muy desarrolladas gracias al ahorro y la eficiencia energética. El último factor, emisiones de CO₂ por unidad de energía, es prácticamente una constante química que corresponde al *mix* de combustibles fósiles utilizados en el mundo para dotarnos de energía primaria. Puesto que los tres primeros factores son difíciles de reducir drásticamente, se puede decir que el problema de las emisiones de CO₂ es hoy un problema de energía primaria. Por tanto, el factor “emisiones/energía” en la ecuación de Kaya es el que encierra la única esperanza para la reducción drástica de emisiones de CO₂. Como queda patente en la Figura 1.2, se usa un gran flujo de energía primaria y, hasta la fecha, no se han encontrado alternativas de bajo coste y continuidad de suministro que puedan sustituir a los combustibles fósiles. Se están investigando en todo el mundo prometedores procesos, sistemas más eficaces y baratos de aprovechar las fuentes dispersas e intermitentes de energía renovable y transformarlas en electricidad o hidrógeno. Estas investigaciones deberían suministrar soluciones a largo plazo de obtención de energía para sostener y aumentar el grado de bienestar de las sociedades futuras. Pero no parece que estas tecnologías vayan a llegar a tiempo para resolver el desafío de reducción de emisiones que debe

abordarse en las próximas décadas para estabilizar la concentración de CO₂ en no más de 450 ppm, y así prevenir calentamientos medios superiores a 2°C.

Las opciones reales de reducción de emisiones de CO₂ que se plantean a medio plazo se basan en la mejora de la eficiencia energética, la extensión de la utilización de energías renovables, la utilización de energía nuclear y la captura y almacenamiento de CO₂ (CAC). Pero teniendo en cuenta nuestro sistema energético actual, la captura y almacenamiento geológico permanente de CO₂ se considera una de las más poderosas herramientas de mitigación del cambio climático a medio plazo. La CAC ocupa de modo muy prioritario las agendas de políticos y científicos de muy diversos ámbitos en todo el mundo. El IPCC ha evaluado las tecnologías existentes y emergentes de captura y almacenamiento de CO₂ (IPCC 2005) y ha concluido que, en la mayor parte de los escenarios, las tecnologías CAC contribuirían entre el 15 y el 55% del esfuerzo mundial de mitigación acumulativo hasta el 2100.

1.2 Captura, Transporte y Almacenamiento de CO₂

Las grandes centrales térmicas, cementeras, refinerías, acerías etc. son procesos diseñados hasta hoy para obtener uno o varios productos energéticos (electricidad, calor) o químicos a gran escala, emitiendo CO₂ a la atmósfera como subproducto. El desafío para cualquier tecnología de captura es transformar estos procesos existentes (o "sistemas de referencia") en sistemas que generan el mismo producto pero con una corriente de CO₂ separada y comprimida para su confinamiento ("sistema con captura"). Por tanto, un sistema con captura de CO₂ es el proceso completo necesario para producir el mismo producto que los sistemas actuales, pero generando una corriente concentrada de CO₂ susceptible de compresión, transporte y almacenamiento permanente. Los principales destinatarios de las tecnologías de captura son procesos estacionarios que hacen uso de combustibles fósiles a gran escala, pero hay que destacar que las tecnologías CAC podrían ser igualmente

aplicadas en el futuro a grandes centrales e industrias que hacen uso de biomasa, haciendo de estas centrales sumideros netos de CO₂ de la atmósfera por eliminar permanentemente el CO₂ absorbido por la biomasa durante su crecimiento.

1.2.1 Captura de CO₂

Por definición, todos los sistemas de captura de CO₂ incluyen siempre un proceso de separación de gases a gran escala, que suele suponer $\frac{3}{4}$ partes del coste total de mitigación. Esta separación de gases no es necesariamente una separación de CO₂, de hecho, los sistemas de captura de CO₂ se suelen clasificar en función del lugar donde se sitúa la gran etapa de separación de gases en el sistema y del tipo de gas que se separa en los mismos. La Figura 1.4 esquematiza los sistemas de captura según este criterio para el caso de grandes centrales térmicas. Otros sistemas de captura para otros procesos distintos a los de generación de energía eléctrica suelen poder adaptarse a esta clasificación (postcombustión, precombustión, oxicomustión), pero se han incluido por simplicidad en la línea de "procesos industriales" de la Figura 1.4.

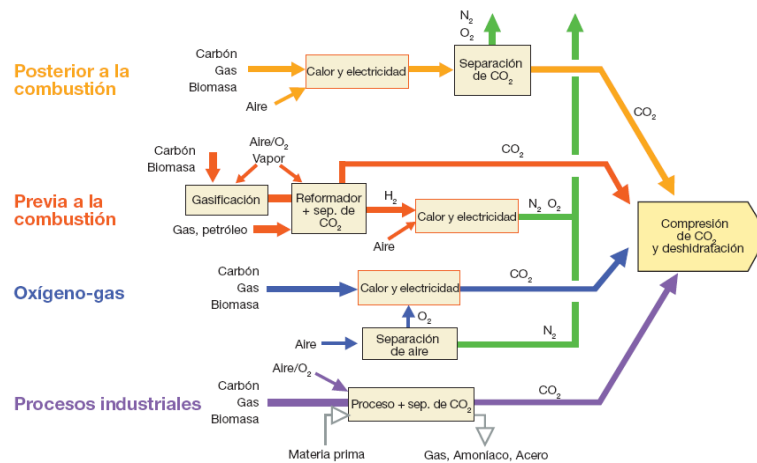


Figura 1.4. Esquema general de los procesos y los sistemas de captura de CO₂.

(Fuente: IPCC, 2005)

Post-combustión. El objetivo de los sistemas de captura de post-combustión es separar el CO₂ que se encuentra diluido en la corriente de gases producidos de la combustión de combustibles fósiles y biomasa en aire. En general, se hace pasar el gas a través de un equipo que sea capaz de separar la mayor parte del CO₂, mientras que el resto de gases son descargados a la atmósfera. La infraestructura energética actual en España y en el mundo se basa en procesos mayoritariamente de combustión con aire, por lo que estas tecnologías de captura son las únicas viables para centrales existentes de reciente construcción.

Actualmente existen varias tecnologías disponibles para capturar el CO₂ de gases de combustión. Algunos estudios muestran que los procesos de absorción basados en solventes químicos son una opción muy atractiva debido a la alta eficacia de captura de CO₂ y a la alta selectividad que presentan. Varias tecnologías emergentes están actualmente en investigación y desarrollo en todo el mundo, como los procesos de captura mediante adsorción, membranas o sorbentes sólidos, y otros procesos llamados de *emisiones negativas* que son aquellos diseñados para capturar el CO₂ generado de la combustión de biomasa. Puesto que es ésta la familia de procesos en los que se enmarca el trabajo realizado en esta Tesis, en la sección 1.3 se realizará una introducción más detallada a estas tecnologías.

Pre-combustión. Los sistemas de captura de CO₂ en precombustión suelen constar de dos etapas principales. La primera etapa consiste en transformar el combustible en un gas rico en H₂ y CO, añadiendo vapor de agua u oxígeno. La siguiente etapa es la llamada reacción de desplazamiento de gas de agua, en la que el CO reacciona con vapor de agua para producir más H₂ y CO₂. Posteriormente, se ha de separar el CO₂ de la mezcla CO₂/H₂ que suele presentarse en una concentración en base seca del 15-60%. Puesto que estas reacciones se llevan a cabo a altas presiones, se facilita el proceso de separación de estos gases físicamente. A estos sistemas de captura se les suele reconocer una gran importancia estratégica porque podrían alimentar la llamada

economía del hidrógeno, o la producción de combustibles de automoción con bajo contenido en carbono, siempre que se capture y almacene el CO₂ resultante en la producción de dichos combustibles limpios.

Oxi-combustión. Consiste en la combustión del combustible en presencia de oxígeno diluido en CO₂ en lugar de aire, lo que da lugar a un gas muy rico en CO₂ que facilita su purificación final antes del almacenamiento. Por tanto, en este sistema de captura de CO₂, la etapa crítica de separación de gases es la obtención de O₂ de elevada pureza a partir del aire.

El IPCC evaluó en un informe especial sobre captura y almacenamiento de CO₂ (IPCC 2005) todas las tecnologías en desarrollo de captura y almacenamiento de CO₂. En la actualidad se están desarrollando en todo el mundo importantes proyectos de CAC utilizando diferentes tecnologías. En Europa, los primeros grandes proyectos de demostración (a escala de varios centenares de MWe) se han anunciado ya en varios países. Uno de ellos demostrará a gran escala en la central de Compostilla de Endesa (León) la tecnología de Foster Wheeler de oxicomcombustión de lecho fluido circulante. La captura y el almacenamiento de CO₂ puede ser especialmente importante en países como España, muy intensivos en el uso de recursos fósiles (80% de nuestra energía primaria) y que han aumentado masivamente sus emisiones de CO₂, incumpliendo así el protocolo de Kyoto.

1.2.2 Transporte de CO₂

Salvo en caso de que las plantas CAC estén ubicadas directamente sobre un lugar de almacenamiento geológico, el CO₂ capturado debe ser transportado desde el punto de captación hasta un lugar de almacenamiento. El CO₂ gaseoso se comprime a una presión superior a 8 MPa, con el fin de aumentar su densidad y así, facilitar y abaratar su transporte. Otra opción, es el transporte de CO₂ en forma líquida mediante buques.

El transporte de gases no es algo novedoso. En la actualidad existen ejemplos de ambos tipos de transporte. El transporte de CO₂ a alta presión se hace a gran escala y de forma rutinaria en campos petrolíferos de EE.UU y Canadá. El primer gasoducto de CO₂ de larga distancia entró en funcionamiento a principios de los años 70. En EE.UU más de 2500 km de gasoductos transportan más de 40 Mt de CO₂ al año desde fuentes naturales y antropógenas hasta emplazamientos donde el CO₂ es utilizado para la recuperación mejorada de petróleo. El transporte por buques puede resultar más atractivo desde el punto de vista económico, especialmente si el CO₂ tiene que ser transportado largas distancias en ultramar. Por ejemplo, los gases de petróleo licuados (propano y butano, principalmente) son transportados en buques cisterna a escala comercial.

El IPCC ha realizado una estimación de los costes tanto para el transporte por gasoductos como para el transporte marítimo de CO₂. En cada caso, los costes dependen en gran medida de la distancia y de la cantidad transportada. El coste del transporte de CO₂ para una distancia nominal de 250 km se estima entre 1 y 8 US\$ por tonelada de CO₂ (IPCC 2005). El coste del acero, en el caso del gasoducto representa una fracción significativa del coste total, por lo que las fluctuaciones en el coste del mismo podrían afectar de manera significativa a la economía general de los gasoductos y habrían de ser tenidas en cuenta.

1.2.3 Almacenamiento de CO₂

La etapa final del proceso de captura de CO₂ es el confinamiento permanente del CO₂. La opción que se maneja de forma más común y que presenta mayores posibilidades es la del almacenamiento en formaciones geológicas profundas. Para el almacenamiento geológico de CO₂ se requiere su inyección en forma condensada. La inyección de CO₂ en formaciones geológicas profundas comprende muchas de las tecnologías que se han desarrollado en la industria de la prospección del petróleo y del gas. Por lo general, se estima almacenar el CO₂ a una profundidad por debajo de los 800 m. A estas profundidades, la

presión y la temperatura darán lugar a que el CO₂ esté en estado líquido supercrítico. En estas condiciones, la densidad del CO₂ será similar a la de un líquido (oscilará entre el 50 y el 80% a la densidad del agua), mientras que mantendrá la viscosidad propia de un gas. En estas condiciones 1 tonelada de CO₂ ocupa un volumen 400 veces menor que en la superficie.

En la actualidad, el almacenamiento geológico de CO₂ se está practicando en proyectos a escala industrial en Noruega, Canadá y EE.UU. Un ejemplo es el de Sleipner (en el mar del Norte), la compañía Statoil inyecta del orden de 1 Mt de CO₂ al año desde 1996. Con la totalidad de los proyectos vigentes (en Noruega, Canadá y EE.UU), entre 3 y 4 Mt de CO₂ son captados y almacenados en formaciones geológicas. Además de estos proyectos de CAC, se inyectan alrededor de 30 Mt de CO₂ al año para la recuperación mejorada de petróleo.

Actualmente, los grandes yacimientos de gas y de petróleo agotados son la opción más atractiva de almacenamiento masivo de CO₂, ya que son formaciones sedimentarias en las que ha habido fluidos a altas presiones almacenados durante millones de años. Las capas de carbón también pueden utilizarse para almacenar CO₂ cuando sea poco probable que el carbón sea explotado posteriormente y siempre que la permeabilidad sea suficiente. En España, al no haber grandes yacimientos de gas o de petróleo, la opción más atractiva son las formaciones salinas profundas (capas de sedimentos porosos que alojan en sus poros gran cantidad de agua salada o salmuera). Estas formaciones salinas son capaces de aceptar grandes cantidades de CO₂ dependiendo del tamaño y características de la capa y del mecanismo por el que el CO₂ es retenido.

Otra posible opción de almacenamiento consiste en inyectar el CO₂ captado directamente en los fondos oceánicos (a más de mil metros de profundidad). Así, la mayor parte del CO₂ quedaría aislada de la atmósfera durante siglos. Ello puede lograrse mediante el transporte de CO₂ por gasoductos o buques a un lugar de almacenamiento oceánico, donde se inyecta en la columna de agua del

océano o en los fondos marinos. Posteriormente, el CO₂ disuelto y disperso se convertiría en parte del ciclo global del carbono. El almacenamiento oceánico, tiene grandes problemas y dudas sin resolver ya que no se sabe en qué manera la adición de CO₂ puede dañar a los organismos marinos y de qué alcance serían las repercusiones en el ecosistema oceánico de una inyección masiva de CO₂.

El almacenamiento de CO₂ en formaciones geológicas profundas en el subsuelo marino o en tierra firme utiliza muchas de las tecnologías desarrolladas por la industria petrolera y del gas, y ha demostrado ser económicamente viable en condiciones específicas. Las tecnologías y los equipos utilizados para el almacenamiento geológico son de uso generalizado en los sectores del petróleo y el gas, por lo que las estimaciones de los costes para esta opción tienen un grado de confianza relativamente alto. No obstante, hay una escala y una variabilidad de los costes debido a factores específicos de cada emplazamiento como el almacenamiento marítimo frente al terrestre, la profundidad del depósito y las características geológicas de la formación de almacenamiento.

Las estimaciones de costes de almacenamiento en formaciones salinas y yacimiento petrolíferos y de gas agotados suelen oscilar entre 0.5 y 8 US\$ por tonelada de CO₂ inyectado. Los costes de vigilancia, que serían adicionales, varían entre 0.1-0.3 US\$ por tonelada de CO₂. Los costes más bajos corresponden a los depósitos terrestres de poca profundidad y alta permeabilidad, y/o lugares de almacenamiento en que los pozos y la infraestructura de yacimientos petrolíferos y de gas existentes pueden ser reutilizados. Cuando el almacenamiento se combina con la recuperación mejorada de petróleo o de gas, el valor económico del CO₂ puede reducir los costes totales de la CAC. Podría generar incluso beneficios netos de 10 a 16 US\$ por tonelada de CO₂ (según datos anteriores a 2003) (IPCC 2005).

1.3 *Tecnologías de Captura de CO₂ Postcombustión*

Como se ha indicado anteriormente, el ámbito de trabajo de esta Tesis es el de la captura de CO₂ en sistemas de postcombustión, por lo que se ha considerado de interés realizar aquí una introducción más detallada de esta familia de tecnologías de captura.

La mayor parte de las emisiones de CO₂ de grandes fuentes estacionarias proceden de sistemas de combustión como centrales térmicas, cementeras o la industria de producción de acero. En estos procesos, la energía se extrae quemando el combustible en aire, y los gases de combustión presentan contenidos de CO₂ con concentraciones que varían dependiendo del tipo de combustible usado. Suelen variar entre el 3% y el 15% en volumen para gas natural de ciclo combinado y para la combustión en aire de carbón, respectivamente.

La captura de CO₂ de grandes fuentes estacionarias de combustión con fines de almacenamiento todavía no se ha desarrollado a gran escala. Sin embargo, tal y como apunta el (IPCC 2005) los sistemas de postcombustión se plantean como una de las opciones más viables para mitigar el cambio climático si se tiene como objetivo mantener el abastecimiento de la demanda de energía eléctrica en el corto y medio plazo a partir de los sistemas de combustión. Estos sistemas se pueden utilizar en centrales existentes y ser incorporados realizando mínimas modificaciones sobre las mismas.

Existen varias tecnologías para la captura de CO₂ de una corriente de gases de combustión que son comerciales en algunas aplicaciones industriales o están siendo investigadas en la actualidad. Un esquema general de los principales procesos de separación para captura de CO₂ postcombustión se puede observar en la Figura 1.5. En la Tabla 1.1 se resumen los métodos de captura de CO₂ que están más desarrollados y que presentan mayor potencial para tratar gases de

combustión a gran escala. En la Tabla se indican además, las ventajas e inconvenientes de cada método.

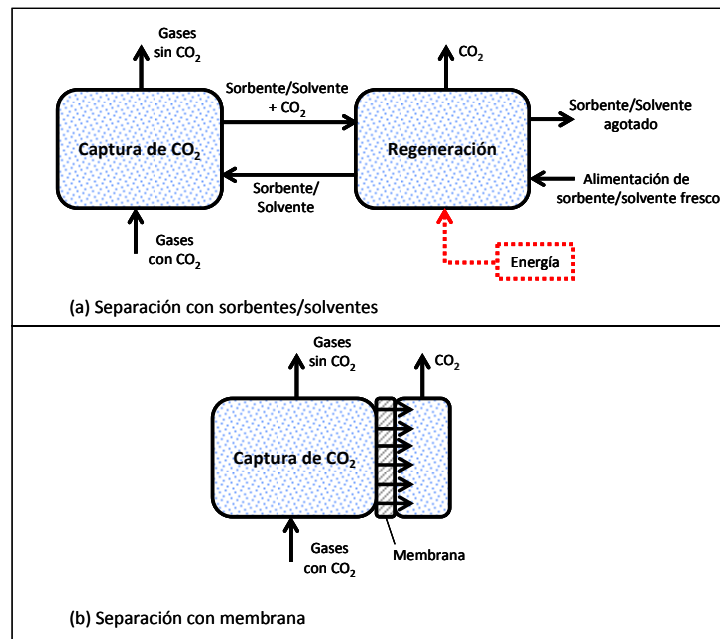


Figura 1.5. Esquema general de los principales procesos de separación para la captura de CO₂ postcombustión.

Los métodos de absorción química se basan en la reacción química de un solvente con el CO₂ disuelto en los gases. La absorción química se usa en la industria petroquímica y en la producción de gas natural o amoníaco para eliminar el CO₂ de las corrientes de gases. La absorción para captura de CO₂ postcombustión presenta mayores dificultades puesto que el CO₂ se encuentra en menor concentración en la corriente de gases, a alta temperatura y en presencia de partículas y otras especies gaseosas que hacen el proceso más caro y complicado (Ebner y Ritter 2009).

Tabla 1.1. Descripción de las principales tecnologías de captura de CO₂ postcombustión.

	Descripción del Proceso	Ventajas	Inconvenientes	Estado del Arte
ABSORCIÓN <ul style="list-style-type: none"> Disoluciones de aminas (principalmente MEA^a) Disoluciones inorgánicas: disolución acuosa de amoníaco 	<p>El gas de combustión, se pone en contacto con el solvente químico en un absorbedor a temperaturas moderadas (40-60°C). Posteriormente el solvente se regenera en una torre a 100-140°C y a presión cercana a la atmosférica, y vuelve hacia la torre de absorción</p>	<p>Tecnología muy desarrollada.</p> <p>Utilizada comercialmente durante décadas en procesos de limpieza de gas natural, gas de refinería y obtención de amoníaco.</p>	<p>La presión parcial del CO₂ en los gases de combustión es inferior que en otras aplicaciones en las que se usa esta tecnología. El O₂, SO_x, NO_x, cenizas y hollín presentes en los gases de combustión pueden desactivar el absorbente. La regeneración del sorbente conlleva alta penalización energética</p>	<p>Se buscan absorbentes que logren reducir el consumo en la etapa de regeneración, así como que consigan altas cinéticas de la reacción química para acelerar la transferencia de masa en el absorbedor.</p>
ADSORCIÓN <ul style="list-style-type: none"> Lechos de alúmina, zeolitas o carbón activado 	<p>El CO₂ presente en el gas de combustión interacciona con un sólido adsorbente mediante fuerzas superficiales. La regeneración tiene lugar a baja presión, en el caso del PSA^b, o a alta temperatura, caso del TSA^c.</p>	<p>La PSA y TSA ya se utilizan para la purificación de hidrógeno y para la separación de CO₂ del gas natural antes de ser comercializado</p>	<p>Requiere operación con gases a alta presión. Si hay que comprimir gases antes del adsorbente esto conlleva gran penalización energética.</p>	<p>El desarrollo de nuevos materiales adsorbentes que puedan adsorber eficientemente CO₂ mejorará la competitividad de este método de separación.</p>
MEMBRANAS <ul style="list-style-type: none"> Membranas poliméricas Membranas porosas inorgánicas, metálicas o cerámicas 	<p>El CO₂ difunde a través de una membrana porosa o semiporosa.</p>	<p>Los procesos de captura de CO₂ basados en el uso de membranas son usados comercialmente para tratar gas natural a alta presión con alta concentración de CO₂.</p>	<p>La menor presión parcial de CO₂ en los gases de combustión desfavorece el proceso (menor fuerza impulsora de la separación)</p>	<p>Se buscan nuevos materiales para el desarrollo de membranas con alta permeabilidad y selectividad del CO₂, y que reduzcan el coste del proceso actual.</p>
SORBENTES SÓLIDOS <ul style="list-style-type: none"> Óxidos de sodio y potasio y los carbonatos soportados sobre un sustrato sólido. Sorbentes basados en litio Sorbentes basados en óxido de calcio. 	<p>Se basa en poner en contacto los gases de combustión con el sorbente en un reactor a alta temperatura de manera que la reacción sólido-CO₂ gas tenga lugar. El sólido formado se separa fácilmente de la corriente de gases y el sorbente se regenera en un reactor diferente para ser usado en un proceso cíclico.</p>	<p>El uso de altas temperaturas permite reducir la penalización energética.</p>	<p>La estabilidad química y mecánica del sorbente ha de ser elevada para soportar numerosos ciclos de operación. El coste del sorbente es un factor crítico a la hora de decidir si el proceso es rentable a gran escala.</p>	<p>Se buscan sorbentes con buena capacidad de absorción de CO₂, así como estabilidad química y mecánica para largos periodos de operación en repetidos ciclos.</p>

^a MEA: monoetanolamina, amina primaria muy utilizada para captura de CO₂ postcombustión.^b PSA: Adsorción con oscilación de presión (de las siglas en inglés de *pressure swing adsorption*)^c TSA: Adsorción con oscilación de temperatura (de las siglas en inglés de *temperature swing adsorption*)

En los procesos de absorción para la captura de CO₂ postcombustión, el gas de combustión, una vez enfriado, se pone en contacto con el solvente químico (generalmente disoluciones acuosas de aminas) en un absorbedor a temperaturas entre 40 y 60°C. Posteriormente el solvente con el CO₂ es

bombeado a través de un intercambiador de calor a la torre de regeneración. El solvente se regenera a 100-140°C y a presiones cercanas a las atmosféricas. Una vez regenerado, vuelve hacia la torre de absorción a través del intercambiador de calor por el que pasa el solvente con el CO₂. La mayor penalización energética de este proceso se atribuye al calor necesario para la regeneración del sorbente. Por ello, la elección de un solvente adecuado es clave para la viabilidad de una planta de absorción química de CO₂. Los más utilizados son las aminas, entre ellas la monoetanolamina (MEA). Otros solventes utilizados son disoluciones acuosas de amoníaco.

La aplicación de la captura de CO₂ por absorción química como tecnología CAC a sistemas de combustión conlleva unos 10-15 puntos de pérdida de rendimiento neto, y esto puede hacerlas indeseables desde el punto de vista económico ya que, incluso para centrales de combustión de última generación, implementar las tecnologías actuales de captura implica aumentar el consumo de combustible un 20-35% para generar la misma potencia eléctrica (IPCC 2005).

Aunque no a la escala requerida para centrales térmicas, la absorción química ha alcanzado la etapa comercial de operación para sistemas de captura de CO₂ postcombustión. Un ejemplo es la planta comercial de Mitsubishi Heavy Industries Ltd. en Malasia. Esta planta opera con absorción de CO₂ para la producción de urea desde 1999 y captura alrededor de 200 toneladas de CO₂ al día, que equivale a las emisiones de una central termoeléctrica de carbón pulverizado de 10 MW térmicos (IPCC 2005).

Otros métodos no comerciales y todavía en fase de investigación para aplicaciones de postcombustión son la adsorción con sólidos, el uso de membranas o la reacción con sorbentes sólidos. Algunos de estos métodos, aunque menos desarrollados, presentan cualidades que los hacen posibles candidatos a reducir el coste y la penalización energética asociada a la captura de CO₂ con solventes químicos.

Los procesos de captura de CO₂ basados en métodos de adsorción se basan en la interacción del CO₂ presente en el gas con un sólido adsorbente mediante fuerzas superficiales. Para la regeneración del CO₂ adsorbido existen dos métodos comerciales: PSA (*pressure swing adsorption*) and TSA (*temperature swing adsorption*) que se basan en el cambio de presión y temperatura, respectivamente, en la etapa de regeneración. Algunos de los adsorbentes utilizados para separar CO₂ de corrientes de gases son zeolitas, carbones activados, alúmina e hidrotalcitas.

La adsorción se utiliza en procesos industriales, como la purificación de hidrógeno y del gas natural, sin embargo no existen procesos comerciales para captura de CO₂ postcombustión (Ebner y Ritter 2009). El principal inconveniente que presentan es la necesidad de tratar la corriente de gases antes de la separación de CO₂ en el adsorbedor. En muchos casos los gases tienen que ser enfriados y secados antes, lo que conlleva penalización energética y limita el atractivo de estos procesos. El desarrollo de nuevos materiales adsorbentes con alta capacidad de adsorción de CO₂ a alta temperatura, con adecuada cinética de adsorción/desorción y con estabilidad mecánica ante repetidos ciclos mejorará la competitividad de este método de separación (Yong et al. 2002).

La separación de CO₂ de la corriente de gases con membranas se basa en la penetración del gas a través de la misma. Las membranas son materiales porosos o semiporosos que transportan los gases mediante un mecanismo de difusión. Aunque una gran variedad de membranas se están desarrollando para las aplicaciones de separación y purificación de CO₂ de corrientes de gases (membranas poliméricas, de transporte facilitado (FTM), inorgánicas e híbridas), actualmente las tecnologías comerciales de membranas para separación de CO₂ se basan en materiales poliméricos con aplicación a la purificación del gas natural (Ebner y Ritter 2009).

Los procesos basados en membranas para la separación de CO₂ del uso de combustibles fósiles presentan un menor potencial de aplicación a gran escala debido a la alta penalización energética y la baja eficacia de captura de CO₂ comparada con otros procesos (Feron 1994), principalmente por la baja presión parcial de CO₂ en los gases de combustión. El desarrollo de esta tecnología se basa en la investigación de nuevos materiales para el desarrollo de membranas (Yang et al. 2008), o métodos híbridos que combinen las ventajas de las membranas con las ventajas de la absorción (Eide et al. 2005).

Muchos procesos de captura de CO₂ en postcombustión están desarrollando tecnologías que usan sólidos regenerables como sorbentes de CO₂ a alta temperatura. El uso de altas temperatura en la separación de CO₂ presenta una gran ventaja intrínseca, ya que la integración del sistema de captura con la propia central emisora de los gases conllevará una reducción de la penalización energética. Para el desarrollo de estos sistemas, y su escalado, se requiere un estudio de los posibles sorbentes candidatos. Las cualidades que se buscan en el sorbente serán, además de la buena capacidad de absorción de CO₂, estabilidad química y mecánica para soportar largos periodos de operación en repetidos ciclos. El coste del sorbente es también un factor crítico a la hora de decidir si el proceso es rentable a gran escala o no (Abanades et al. 2004b).

Algunos de los sólidos regenerables novedosos que se están investigando para aplicaciones de captura de CO₂ a alta temperatura son sorbentes basados en óxidos de litio, calcio, sodio y potasio.

Los estudios realizados con sorbentes basados en litio, como el Li₂ZrO₃ (Fauth et al. 2005) o Li₄SiO₄ (Kato et al. 2005), ponen de manifiesto las buenas características que presentan para capturar CO₂ a través de la formación de Li₂CO₃. Estos sorbentes tienen alta reactividad en un amplio intervalo de temperaturas por debajo de los 700°C, se regeneran rápidamente y presentan durabilidad tras repetidos ciclos de captura y regeneración (Yang et al. 2008). Puesto que los compuestos basados en litio son caros, deben demostrar

estabilidad durante miles de ciclos para ser competitivos con sistemas comerciales (Abanades et al. 2004b).

Otros sorbentes en desarrollo son los basados en sodio, como el desarrollado por investigadores de NETL (National Energy Technology Laboratory) que contiene una mezcla de NaOH y CaO. El hidróxido de sodio presenta alta capacidad de captura de CO₂ a 200-400 °C formándose Na₂CO₃. La regeneración del carbonato de sodio se da a 800°C, sin embargo cuando el NaOH se mezcla con CaO, el sorbente puede ser regenerado en torno a 700°C (Siriwardane et al. 2007).

También se están estudiando sorbentes basados en potasio, como el SorbKX35 que consiste en K₂CO₃ soportado para darle resistencia mecánica (Seo et al. 2009). La reacción de K₂CO₃ con CO₂ y H₂O para obtener KHCO₃ es reversible y altamente exotérmica. Por ello, el control de la temperatura será un factor fundamental en el escalado del proceso.

Puesto que en esta Tesis se estudia, principalmente, el proceso de captura de CO₂ de una corriente de gases de combustión mediante CaO, se dedica a continuación una sección especial para introducir este tipo de procesos, también llamados de carbonatación-calcinación.

1.4 Captura de CO₂ Postcombustión con CaO a Alta Temperatura

Estos procesos se basan en la reacción reversible del CO₂ con CaO como sólido sorbente. La captura de CO₂ usando CaO se propuso en numerosos procesos durante el siglo XIX. El principio básico de separación haciendo uso de este ciclo de carbonatación-calcinación ya se llevó a cabo con éxito en los años 60 en una planta piloto de gasificación de carbón de 40 toneladas al día para el desarrollo

del Acceptor Coal Gasification Process (Curran et al. 1967). Con la separación de CO_2 en este proceso se obtenían gases de mayor poder calorífico y contenido en hidrógeno haciendo uso de dos lechos fluidos interconectados. Shimizu et al. propusieron por primera vez la utilización del ciclo de carbonatación con CaO como sistema de postcombustión realizando la regeneración del sorbente en un lecho fluidizado quemando parte del combustible con mezclas de O_2/CO_2 (Shimizu et al. 1999). El CSIC ha trabajado desde las mismas fechas en la demostración de ese concepto y en el desarrollo de otros procesos avanzados de captura de CO_2 con CaO que se describirán a continuación. La reacción de carbonatación de CaO para capturar CO_2 de una corriente de gases de combustión a temperatura elevada (temperaturas en torno a los 650°C) es muy rápida y la regeneración del sorbente mediante calcinación de CaCO_3 en CaO y CO_2 se encuentra favorecida a temperaturas por encima de los 900°C a presiones parciales de CO_2 de 0,1 MPa (Baker 1962).

La captura de CO_2 mediante ciclos de carbonatación-calcinación se puede llevar a cabo en distintas configuraciones del proceso. Todas las configuraciones presentan una serie de características que hacen a estos procesos muy atractivos. La principal característica es que son procesos que se llevan a cabo a alta temperatura por lo que es posible generar potencia extra mediante la integración energética de los flujos del ciclo de captura con la planta emisora. El material utilizado como sorbente, la piedra caliza (precursor del CaO), es barato, abundante y está bien distribuido geográficamente. El CaO tiene una cinética de reacción rápida con el CO_2 a temperaturas en torno a los 650°C , por tanto se requerirán reactores compactos. El CaO, además de reaccionar con el CO_2 , presenta la posibilidad de reducir el azufre de los gases de combustión en la propia unidad de separación del CO_2 mediante su reacción con SO_2 . Con este mismo fin, el CaO se usa en centrales térmicas de carbón. Por otro lado, el CaO es también utilizado en cementeras para la fabricación del cemento. Por lo tanto es un material conocido y manejado a gran escala. Además, los equipos empleados son mecánicamente similares a los combustores de lecho fluidizado circulantes, reactores comerciales utilizados a gran escala.

Un punto débil de este tipo de procesos es la rapidez con la que decae la actividad del sorbente (calizas y dolomitas) para reaccionar con CO_2 , con el consiguiente elevado consumo de sorbente fresco que se ha de aportar al ciclo para reponer el flujo desactivado (Abanades et al. 2004a). Sin embargo, se podría obtener crédito por el sorbente desactivado si se le da algún uso como subproducto, por ejemplo en la industria cementera.

Dentro de los procesos de captura de CO_2 postcombustión denominados emergentes, se considera que el ciclo de carbonatación-calcinación mediante CaO puede resolver dificultades que presentan otros procesos descritos en el apartado anterior, como son el elevado coste del absorbente, problemas con los contaminantes de los gases de combustión o instalaciones demasiado costosas.

Se presentan en esta parte del trabajo tres procesos que tienen en común la obtención de una corriente pura de CO_2 lista para ser tratada para el posterior almacenamiento. En los tres procesos el material clave utilizado para la obtención de dicha corriente es el CaCO_3 . Dos de los procesos se basan en la sorción-desorción de CO_2 de gases de combustión con CaO , y se propone otro proceso para la obtención de una corriente pura de CO_2 a partir de la calcinación de CaCO_3 para su aplicación en cementeras.

1.4.1 Captura de CO_2 postcombustión. Sistema de dos lechos fluidizados circulantes (carbonatador y calcinador oxifuel)

El proceso de captura de CO_2 que se muestra en la Figura 1.6 se basa en el tratamiento de los gases de combustión procedentes de una central convencional de carbón mediante un sistema de reactores de lecho fluidizado circulante interconectados. El CO_2 de los gases de combustión (F_{CO_2}) de una central térmica reacciona en el carbonatador con un flujo de óxido de calcio (F_{CaO}) a 600-700°C, y se forma CaCO_3 . La eficacia de captura de CO_2 mediante

esta reacción depende de la actividad del sorbente y del diseño del reactor de carbonatación. Los gases de combustión, ahora con baja concentración de CO_2 , son expulsados a la atmósfera. La corriente sólida, compuesta por CaCO_3 y CaO no reaccionado, es dirigida hacia el calcinador donde, a temperaturas en torno a los 900°C , el CaCO_3 se descompone en CaO y CO_2 . El CaO vuelve al carbonatador para empezar de nuevo el ciclo y el CO_2 gas se obtiene concentrado en una corriente que está lista para ser purificada y tratada para su posterior compresión, transporte y almacenamiento permanente.

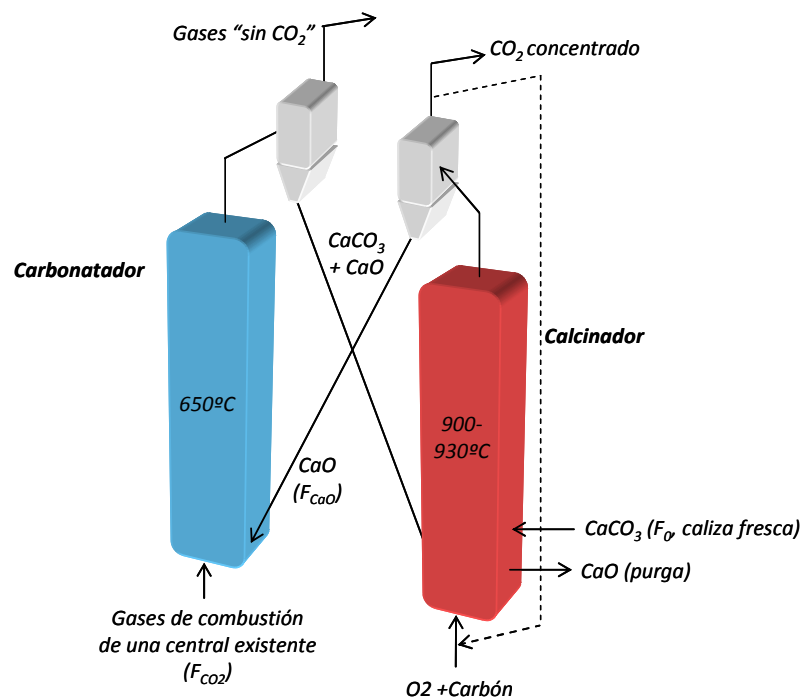


Figura 1.6. Esquema del sistema de carbonatación- calcinación para gases de combustión de una central existente.

Como se ha comentado, el óxido de calcio como sorbente de CO_2 pierde capacidad de captura con el número de carbonataciones y calcinaciones sufridas. Por tanto, en la práctica, es importante dotar al sistema de una alimentación de caliza fresca (F_0) y una purga de CaO desactivado y cenizas.

En este sistema el calcinador demanda una fracción importante de la energía total que requiere el proceso completo (en torno al 40-50%), entendido éste como central térmica existente más sistema de carbonatación-calcinación de la Figura 1.6. Como se ha comentado, la energía invertida en el calcinador abandona el proceso en corrientes de materia a alta temperatura, por tanto es posible recuperar este calor en forma de energía adicional. En realidad, el calcinador se puede considerar una nueva central térmica de oxidación en lecho fluidizado circulante que aporta, entonces, más energía a la central existente al mismo tiempo que captura la mayor parte del CO_2 que se genera en ella gracias al ciclo de carbonatación-calcinación.

1.4.2 Captura de CO_2 de la calcinación de CaCO_3 para cementeras

Con el esquema de la Figura 1.7 se plantea un proceso para descomponer el carbonato cálcico mediante un flujo de CaO a alta temperatura precalentado en un combustor. El procedimiento consiste en sobrecalentar una corriente de material calcinado (CaO) hasta una temperatura superior a la temperatura de calcinación, y hacer circular esta corriente sobrecalentada de material calcinado hasta el calcinador, donde los sólidos ceden su calor de modo que el CaCO_3 se descompone en CO_2 y CaO . Este método de generar el calor necesario para la calcinación en una cámara separada del calcinador hace que el CO_2 que se obtiene de la calcinación de CaCO_3 se obtenga en una corriente pura, mientras que el CO_2 resultante de la combustión en aire en la cámara de combustión sea emitido a la atmósfera.

La obtención de una corriente pura de CO_2 de la descomposición de CaCO_3 utilizando CaO como transportador de calor fue propuesta por (Abanades et al. 2005). Esta manera de obtener una corriente pura de CO_2 es una alternativa a la oxidación que presenta menor penalización energética, puesto que se evita el alto consumo de energía de la unidad de separación de aire (ASU).

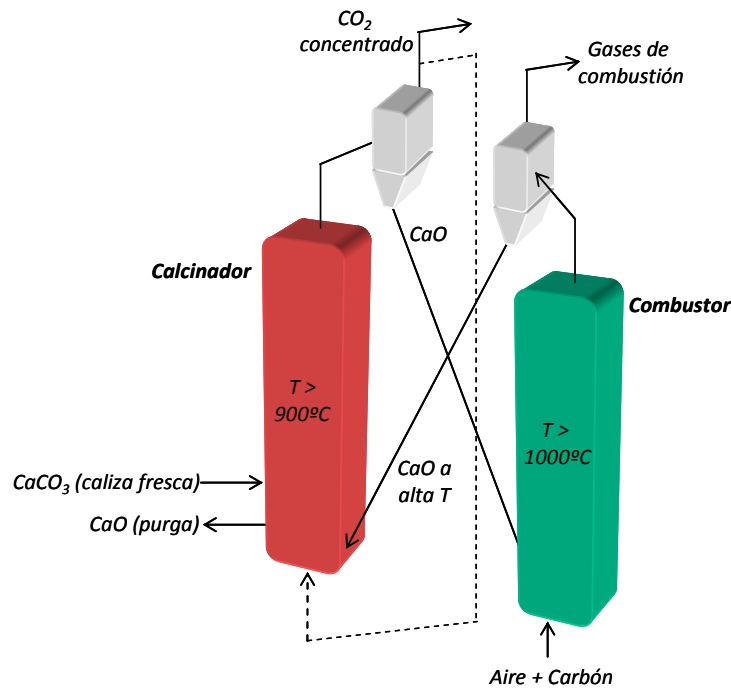


Figura 1.7. Esquema del proceso de separación de CO_2 procedente de la calcinación de CaCO_3 mediante una corriente de CaO a alta temperatura.

Este esquema se podría aplicar a las plantas de producción de cemento, donde una gran parte del CO_2 emitido en las mismas proviene de la calcinación de CaCO_3 para obtener CaO . El análisis de este proceso y su integración con la cementera es uno de los objetivos de esta memoria, y se detalla en el apartado 3.2.

1.4.3 Captura de CO_2 de gases de combustión. Sistema de tres lechos (combustor, carbonatador y calcinador)

El sistema de tres lechos que se muestra en la Figura 1.8, constituye un nuevo concepto de central térmica con separación integrada de CO_2 . Este proceso es una combinación de los procesos explicados en los apartados 1.4.1 y 1.4.2

El sistema de la Figura 1.8 consta de dos bucles. El bucle de la derecha compuesto por combustor-calcinador sería el equivalente al proceso mostrado en la Figura 1.7, en el que el calor para la calcinación lo transmite una corriente de CaO a alta temperatura que ha sido sobrecalentada en una cámara de combustión a temperatura en torno a 1000°C.

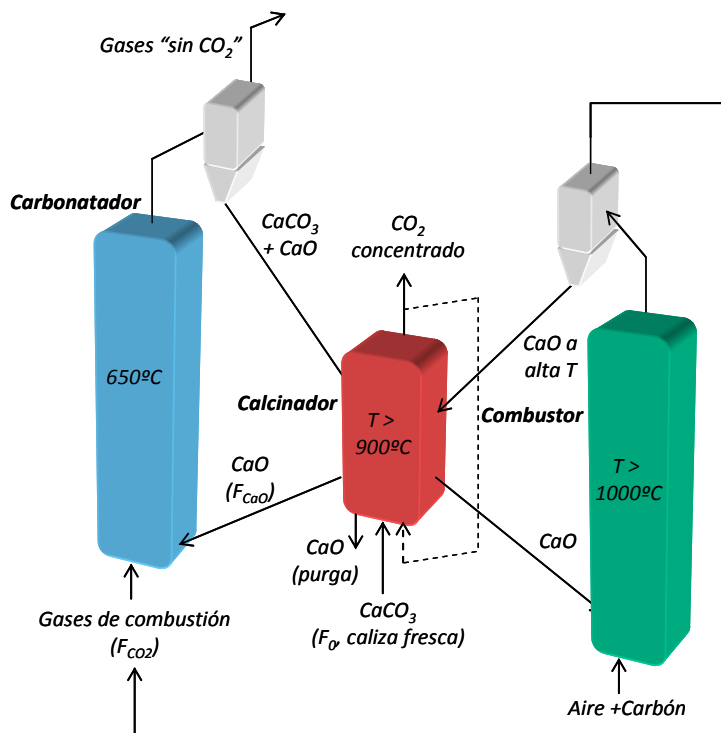


Figura 1.8. Esquema del sistema de carbonatación- calcinación para gases de una cámara de combustión que transfiere calor al calcinador mediante un flujo de CaO a alta temperatura.

Los gases de combustión generados en el combustor se dirigen al segundo bucle, compuesto por carbonatador-calcinador (Figura 1.6). En el carbonatador los gases que contienen CO_2 (F_{CO_2}) reaccionan con un flujo de CaO (F_{CaO}) y se forma CaCO_3 a una temperatura de 650°C . La corriente sólida, compuesta principalmente por CaCO_3 y CaO no reaccionado, se dirige al calcinador donde se descompone gracias al calor transmitido por el flujo de CaO a alta

temperatura, en nuevo CaO y CO₂. La temperatura de operación del calcinador, para asegurar la calcinación completa, es ligeramente superior a los 900°C. De esta manera el CO₂ se obtiene del calcinador en una corriente pura susceptible de compresión y almacenamiento. Parte del CO₂ obtenido se recircula para fluidizar el calcinador. Si fuese necesario aumentar la velocidad de la reacción de calcinación y/o moderar la temperatura del reactor, sería posible reducir la presión parcial de CO₂ en el calcinador alimentando, además, vapor de agua al calcinador.

Cabe la duda de si la alta temperatura del bucle de la derecha de la Figura 1.8 podría afectar al comportamiento del CaO como sorbente de CO₂ en el bucle de la izquierda. Estudios recientes evidencian que la temperatura de calcinación no afecta al sorbente mientras no sobrepase temperaturas en torno a los 1000°C (González et al. 2008). Estos estudios apoyan otros trabajos desarrollados anteriormente (Curran et al. 1967) en los que se obtuvieron curvas de desactivación del CaO tratado en combustores de lecho fluidizado a temperaturas superiores a 1060°C, similares a las que se obtienen tras la operación en condiciones más moderadas.

Este proceso presenta un gran atractivo en comparación con otros procesos de generación de energía y captura de CO₂. Se obtiene una corriente pura de CO₂ sin necesidad de obtener el calor de la reacción de combustión, de esta manera no hay necesidad de quemar en oxígeno puro, y por tanto se evita la penalización energética asociada a la unidad de separación de aire (ASU). La principal ventaja de este proceso está en la disponibilidad de flujos de calor de gran calidad y en la ausencia de otras penalizaciones energéticas que no sean la purificación y compresión de CO₂, que, por otro lado, son penalizaciones comunes a todos los procesos de CAC.

Recientemente ha sido publicado un trabajo en el que se hace la integración energética de este proceso aplicado a un combustor de 1GWt, con un ciclo de vapor supercrítico (Martínez et al. 2010). La integración se hace con el

simulador comercial de procesos Aspen Hysys, y se consideran para ella tres reactores de lecho fluidizado interconectados, un ciclo supercrítico de vapor y una unidad de purificación y compresión de CO₂. En el trabajo publicado se comprueba la baja penalización energética asociada a esta configuración. Martínez et al. demuestran que es posible diseñar una integración adecuada del proceso de la Figura 1.8, con la que se consigue generar potencia eficazmente (eficiencia en torno al 38%, incluyendo la fase de compresión de CO₂) y altas eficacias de captura de CO₂ (en torno al 90%).

2 Objetivos y Justificación de la Tesis

El presente trabajo se enmarca en el contexto del desarrollo de los procesos de captura de CO₂ en sistemas postcombustión con CaO a alta temperatura. Por tanto, el objetivo principal de esta Tesis es avanzar en el conocimiento de los sistemas de captura de CO₂ mediante carbonatación-calcinación con óxido de calcio, buscando las condiciones óptimas de operación teórica y experimentalmente que demuestren la viabilidad técnica y económica de estos procesos a gran escala.

El índice de esta memoria abarca tres grandes bloques con objetivos concretos que han sido objeto de distintas publicaciones a lo largo del desarrollo de esta Tesis Doctoral. Por ello, se ha decidido presentar este trabajo como un compendio de las publicaciones realizadas, situando cada una de ellas dentro del bloque que le corresponde.

El primer bloque atiende al análisis de procesos de captura de CO₂ por carbonatación-calcinación y su estructura de costes. El análisis de dos procesos, uno de ellos orientado a la captura de CO₂ postcombustión y otro con posible aplicación a cementeras, se hace principalmente con la presentación de tres trabajos ya publicados, y en los que se recoge en gran medida las aportaciones originales de la autora en este campo.

El segundo bloque del índice tiene que ver con el trabajo experimental realizado. La descripción de la planta piloto instalada, el protocolo experimental que se sigue para la realización de cada experimento y algunos ejemplos de los resultados experimentales obtenidos quedan recogidos en la cuarta publicación presentada en esta parte de la memoria.

Para finalizar, el último bloque del índice recoge lo que tiene que ver con el modelado del reactor de carbonatación y la validación de los resultados experimentales realizados en una planta piloto. A esta parte de la memoria se aportan tres publicaciones originales; una en la que se describe un modelo de carbonatador de lecho fluidizado para capturar CO_2 de gases de combustión con CaO , que se basa en simples suposiciones en lo que se refiere al comportamiento fluidodinámico y de reactividad de las partículas; otra publicación, que podría suponer una mejora del modelo del carbonatador que se describe, es la que se presenta en este último bloque sobre la capacidad media de captura de CO_2 de las partículas de CaO que se encuentran dentro del sistema, atendiendo a los flujos de sólidos y a la extensión de las reacciones de calcinación y carbonatación. Por último, se adjunta una publicación en la que se recogen los datos experimentales obtenidos de la planta piloto, y se validan haciendo un estudio de la tendencia de la eficacia de captura de CO_2 con la variación de diferentes parámetros que intervienen en el proceso.

**EXPERIMENTAL INVESTIGATION OF A
CIRCULATING FLUIDIZED BED REACTOR TO
CAPTURE CO₂ WITH CAO**

Pendiente de publicación en:
AIChE Journal

Año 2010

3 Análisis de Procesos de Captura de CO₂ por Carbonatación – Calcinación

El primer paso para realizar el análisis conceptual de un proceso es realizar los balances de materia y energía de los mismos en condiciones de operación razonables. Para ello, en los procesos de captura de CO₂ por carbonatación-calcinación se debe incluir el conocimiento sobre el comportamiento del sorbente y tener en cuenta las restricciones impuestas por las condiciones de operación (velocidad de gas y caudal de circulación de sólidos) en sistemas similares de lecho fluidizado circulantes.

3.1 Análisis de la Demanda de Calor del Calcinador en el Proceso de Captura de CO₂ Postcombustión por Carbonatación-Calcinación

De los muchos aspectos a estudiar sobre el sistema de captura de CO₂ postcombustión mediante carbonatación-calcinación mostrado en la **¡Error! No se encuentra el origen de la referencia.**, en esta memoria se ha realizado un análisis de los balances de materia y de energía del proceso. Aunque los balances puntuales de materia y energía sobre casos concretos de aplicación ya se habían realizado con anterioridad (Abanades 2002; Wang et al. 2004), en

este estudio se ha incorporado el comportamiento del CaO como sorbente de CO₂. De esta manera, se han obtenido las ecuaciones de diseño que permiten garantizar una cierta capacidad de captura en la corriente de CaO que circula del calcinador al carbonatador (F_{CaO} en la **¡Error! No se encuentra el origen de la referencia.**) minimizando el flujo de caliza fresca (F_0) al proceso.

Como se ha explicado anteriormente, la regeneración del sorbente en el calcinador requiere aporte de calor al proceso. El flujo de calor que demanda el calcinador es tanto para la reacción endotérmica de calcinación como para calentar las corrientes de gas y sólidos que entran al calcinador. La fracción de calor que requiere el calcinador es una variable clave para la viabilidad técnica y económica de este proceso. Por tanto, el análisis detallado de la demanda de calor del calcinador en función de las propiedades del sorbente, de la composición del combustible y de las condiciones de operación del sistema, ha sido objeto de estudio y discusión en la *Publicación 1* que se adjunta en la sección 3.4.1 y que forma parte del contenido de esta Tesis.

En esta publicación se presenta la resolución de los balances de materia y de energía del proceso de la **¡Error! No se encuentra el origen de la referencia.**, con el objetivo de conocer cómo varía la demanda energética del calcinador en función de la actividad del CaO para reaccionar con CO₂. En este trabajo no se define cuál es la fuente de calor al calcinador, simplemente se define la demanda de energía del calcinador (H_{in}) como la suma de dos factores: calor de calcinación (para calcinar tanto el carbonato que se ha formado en el carbonatador y que llega en la corriente de reciclo al calcinador, como la caliza fresca que se alimenta al sistema para mantener la actividad del sorbente) y calor sensible para calentar las corrientes de sólidos y de gases que llegan al calcinador.

La composición del combustible utilizado en la central térmica y en el calcinador, en su caso, determina el volumen de purga necesario y, por ende, de la alimentación de caliza fresca. La purga estará compuesta principalmente por

una mezcla de cenizas del combustible utilizado, de CaO desactivado y del sulfato de calcio (CaSO₄) formado si el combustible presenta azufre en su composición. El SO₂ reacciona con CaO para formar CaSO₄ en ambientes con exceso de oxígeno. Ha sido demostrado experimentalmente que el SO₂ disminuye la capacidad de captura del CaO (Li 2005). En este trabajo se ha supuesto que, en caso de presencia de azufre en la composición del combustible, el SO₂ reacciona sólo con CaO activo para la captura de CO₂. Con lo cual, la presencia de azufre en el sistema afecta de manera notable a la demanda de calor del calcinador (bien por acumulación de inertes en el sistema, bien por el incremento de la alimentación de caliza fresca para mantener la actividad global del sorbente que ha sido desactivado).

El efecto de la presencia de azufre y de cenizas en la demanda de calor del calcinador se analiza a partir de cuatro combustibles con diferente contenido de azufre y ceniza en sus composiciones. Por tanto, en la *Publicación 1* se puede observar el efecto de la composición de los gases de combustión a tratar en el sistema de captura de CO₂ planteado en la **¡Error! No se encuentra el origen de la referencia..**

3.2 Análisis de la Pre-calcinación de CaCO₃ con Captura de CO₂ para Aplicación a Cementeras

Las emisiones de CO₂ de la industria del cemento son el 5% de las emisiones totales de fuentes estacionarias (IEA 2008). La producción de cemento consume gran cantidad de combustible para alcanzar las altas temperaturas asociadas al proceso. La piedra caliza es materia prima principal en el proceso de fabricación de cemento. Por lo tanto, además del CO₂ que procede del combustible utilizado, se emite a la atmósfera el CO₂ generado en la calcinación de la caliza para transformar el CaCO₃ en CaO. En las más nuevas y eficientes cementeras, con una alta integración energética y necesidad mínima de

consumo de combustible, casi el 70% de las emisiones de CO₂ provienen de la descomposición de CaCO₃ a CaO (Gartner 2004). En este contexto, el proceso de la **¡Error! No se encuentra el origen de la referencia.** podría aplicarse a procesos de fabricación de cemento como un sustituto de la etapa de pre-calcinación. La ventaja está en la obtención de una corriente concentrada de CO₂ que proviene de la descomposición de CaCO₃ a CaO. Una parte del CaO resultado de la calcinación podrá ser utilizado para la fabricación del clinker (precursor del cemento), mientras que el resto se recicla al combustor para ser sobrecalentado.

Aunque con este proceso no hay una etapa de “captura de CO₂” propiamente dicha (no hay reacción de carbonatación), el CO₂ generado en la etapa de calcinación se obtiene de forma pura o fácilmente purificable y es por tanto susceptible de tratamiento para su posterior confinamiento.

En la *Publicación II*, que se adjunta en la sección 3.4.2, se hace un análisis de este proceso. En primer lugar, se estudian los flujos netos de materia y calor necesarios para la fabricación de 1 tonelada de cemento Portland en las cementeras convencionales. A partir de estos flujos se plantean unas condiciones de operación que permiten cerrar los balances de materia y calor para integrar el esquema de la **¡Error! No se encuentra el origen de la referencia.** en una planta de fabricación de cemento como un sistema que sustituya al pre-calcinador convencional. La obtención de una corriente pura de CO₂ tiene como penalización el mayor consumo de combustible por tonelada de cemento fabricado, puesto que se necesita generar suficiente calor como para conducir la reacción endotérmica de calcinación sólo con un flujo de sólidos a alta temperatura. Por tanto, es clave minimizar el consumo de combustible en la cámara de combustión de la **¡Error! No se encuentra el origen de la referencia.** El estudio realizado en la *Publicación II* analiza el efecto de la temperatura de precalentamiento de las corrientes que entran al proceso de la **¡Error! No se encuentra el origen de la referencia.** y el efecto de la diferencia de temperatura entre combustor y calcinador atendiendo al flujo de sólidos que

circula entre reactores (parámetro clave en todos los sistemas de lecho fluidizado circulante).

En la *Publicación II* además se hace un análisis de costes de este proceso. Esta parte de la publicación será comentada en la sección 3.3.

3.3 Estructura de Costes del Proceso de Captura de CO₂ con CaO Aplicado a Centrales Térmicas de Carbón y Cementeras

Durante la realización de esta Tesis se ha realizado una primera evaluación económica de los procesos descritos en los apartados 1.4.1 y 1.4.2, con el objeto de apoyar y justificar mejor la decisión de demostrar estas tecnologías a escala industrial. Estos estudios se han realizado aprovechando la información disponible en la literatura sobre sistemas análogos, especialmente sobre costes de calderas comerciales de lecho fluido circulante (NELT 2007; Nsakala ya et al. 2007). Los análisis realizados se han desarrollado definiendo unos entornos de costes comparables a los utilizados para otros sistemas de captura analizados en el (IPCC 2005).

En la Figura 3.1 se muestra un esquema ilustrativo para comparar la diferencia entre la generación de CO₂ en un sistema convencional y en el mismo sistema con captura de CO₂ integrada. Todo sistema de captura de CO₂ llevará consigo un consumo de energía adicional, por lo tanto el “CO₂ generado por unidad de energía útil” en una planta con captura y almacenamiento de CO₂ (barra inferior de la Figura 3.1) será mayor que en una planta sin captura (barra superior). Por ello, hablar de “CO₂ capturado” para distintas propuestas de captura de CO₂ puede resultar engañoso, ya que es un valor referido al CO₂ generado con la nueva planta. Sin embargo, el término “CO₂ evitado” relaciona el CO₂ emitido en una planta de referencia con el emitido en una planta con captura, y es más

utilizado para realizar comparaciones entre distintas tecnologías de captura. Así, el coste de captura de CO₂ puede estimarse de diferentes maneras. Las más extendidas en la literatura son el coste de producto (\$/ unidad de producto) y el coste del CO₂ evitado (\$/t CO₂ evitado) (IPCC 2005). Estas definiciones se han tenido en cuenta a la hora de presentar los resultados obtenidos.

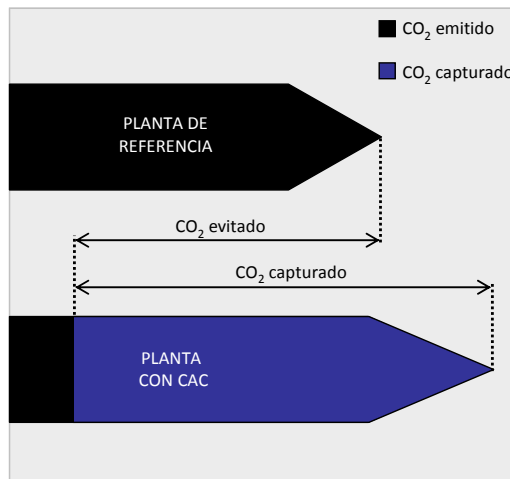


Figura 3.1. Esquema comparativo del CO₂ generado y emitido en una planta convencional y en una planta con CAC.

En primer lugar, se ha realizado una evaluación de los costes del sistema de captura de CO₂ en postcombustión descrito en el apartado 1.4.1, integrando a una ecuación de costes sencilla los resultados obtenidos sobre los consumos de energía en el calcinador (presentados en la *Publicación I*). La estructura de costes desarrollada para este proceso se presenta de manera detallada en la *Publicación III*, que se adjunta en el apartado 3.4.3 de esta memoria. Para analizar este proceso, la planta de captura de CO₂ en postcombustión se ha desglosado en tres bloques principales de coste: la planta de referencia (o central existente), la planta de oxidación (que se refiere al calcinador oxidante) y el reactor de carbonatación. Gracias a este desglose es posible obtener una estimación de costes de los dos primeros bloques cercana a la realidad, relegando la mayor incertidumbre al reactor de carbonatación. Sin

embargo, es posible acotar el coste del carbonatador teniendo en cuenta que este equipo es similar a las cámaras de combustión de lecho fluidizado circulante de las centrales actuales. En la *Publicación III* se incluye toda la serie de suposiciones que se han adoptado y que justifican los costes obtenidos (en \$/kWhe producido) para el caso de una central existente sin captura, una central de oxidación de lecho fluido circulante y el sistema completo de captura de CO₂ compuesto por: central existente, calcinador oxidador y carbonatador. Además, con las mismas suposiciones, se obtiene el coste por tonelada de CO₂ evitada para el caso de una central de oxidación de lecho fluido circulante y para el sistema completo de captura de CO₂ por carbonatación-calcinación.

Del mismo modo, se realizó un análisis de los costes del sistema de captura de CO₂ de la calcinación de CaCO₃ para aplicar a cementeras (apartado 1.4.2). Para este caso se ha de tener en cuenta que el producto obtenido es el cemento, por ello los costes unitarios para reducir las emisiones de CO₂ se dan por unidad de cemento producido. El análisis realizado, e incluido en la *Publicación II* adjunta en el apartado 3.4.2, se realiza comparando las emisiones de CO₂ por unidad de cemento producido de una cementera convencional, con las emisiones de una nueva cementera en la que la calcinación se lleva a cabo en una atmósfera independiente de la del combustor mediante el aporte de calor con CaO sobrecalentado en un combustor (ver **¡Error! No se encuentra el origen de la referencia.**).

3.4 Publicaciones Relacionadas

3.4.1 Publicación I

**HEAT REQUIREMENTS IN A CALCINER OF
CaCO₃ INTEGRATED IN A CO₂ CAPTURE
SYSTEM USING CaO**

Publicado en:
Chemical Engineering Journal
Volumen 138
Año 2008

HEAT REQUIREMENTS IN A CALCINER OF CaCO₃ INTEGRATED IN A CO₂ CAPTURE SYSTEM USING CAO

N. Rodríguez^a, M. Alonso^{a*}, G. Grasa^b, J. Carlos Abanades^a

^a *Instituto Nacional del Carbón, CSIC, Oviedo 33011, Spain*

^b *Instituto de Carboquímica, CSIC, Zaragoza 50015, Spain*

Abstract

Several systems for CO₂ capture using CaO as regenerable sorbent are under development. In addition to a carbonation step, they all need a regeneration step (calcination of CaCO₃) to produce a concentrated stream of CO₂. Different options for calcination may be possible, but they all share common operating windows that appear when the mass and heat balances in the system are solved incorporating equilibrium data, sorbent performance information, and fuel composition (sulphur and ash content). These relatively narrow operating windows are calculated and discussed in this work. Due to sorbent performance limitations, low carbonation levels of the sorbent in the carbonator are expected and the heat demand in the calciner is dominated by the heating of inert solids flowing in the carbonation chemical loop. High make up flows of fresh limestone reduce this effect by increasing the average reactivity of the sorbent, but they also increase the heat demand in the calciner to calcine the fresh feed of limestone. Hence, an optimum level of sorbent activity appears under different operating conditions, processes and fuel characteristic, and these are discussed in this work.

Keywords: CO₂ capture; Coal combustion; Carbonation; Calcination

*Corresponding author e-mail address: mac@incar.csic.es; Tel.: +34 985119090; Fax; +34 985297662

1. Introduction

Capturing (separating) the CO₂ from large stationary sources (like power plants, cement plants, steel mills, refineries, etc.) and storing it permanently in suitable geological formations, can be a major mitigation option for climate change¹. It is generally agreed that CO₂ capture and storage can be done by putting together technologies that are already in place today in large industrial applications¹. However, it is also generally agreed that there is time and scope to explore and develop alternative CO₂ capture systems, better suited for specific power plant boundary conditions. The driving force for these R&D efforts must be to lower the cost and to lower the energy penalties associated with the separation step. Several of these novel systems are based on the carbonation/calcination loop to separate CO₂ at high temperature using the reversible reaction:



This reaction can be applied in pre-combustion routes, aimed at large scale production of H₂ from coal, natural gas or other carbonaceous materials like biomass (see review^{1,2} for further references, and more recent^{3,4}). But our main focus in this paper is on a range of postcombustion systems⁵ that have shown a large potential for low capture cost⁶⁻⁹. Large combustion plants (in particular coal combustion plants) are by far the largest CO₂ sources in the world and they dominate the power generation sector in most countries. They are likely to continue to do so in the next few decades, considering the long life span of these large infrastructures, and the high rate at which these are being built in some developing countries with plenty of coal resources like China. The market potential for new, cost effective CO₂ postcombustion systems is therefore vast.

The schematic process considered in this work is shown in Fig. 1. Flue gases from an existing power plant (or any other large source) will enter the carbonator, react with CaO to form CaCO₃, and leave the system as flue gas depleted in CO₂ (depending on the capture efficiency in the carbonator). All the

solids including the carbonate carrying the CO₂ are then directed through standpipes to a calciner. Due to the endothermic reaction of calcination and the need to heat up solid streams, a large heat flow has to be supplied to the calciner. Several options could be feasible, but the nearest option to demonstration is to choose a calciner to operate like an oxy-fired circulating fluidized bed combustor (which has its own developing path in several large projects in US and Europe). The concept of Fig. 1 was first published by Shimizu et al.¹⁰.

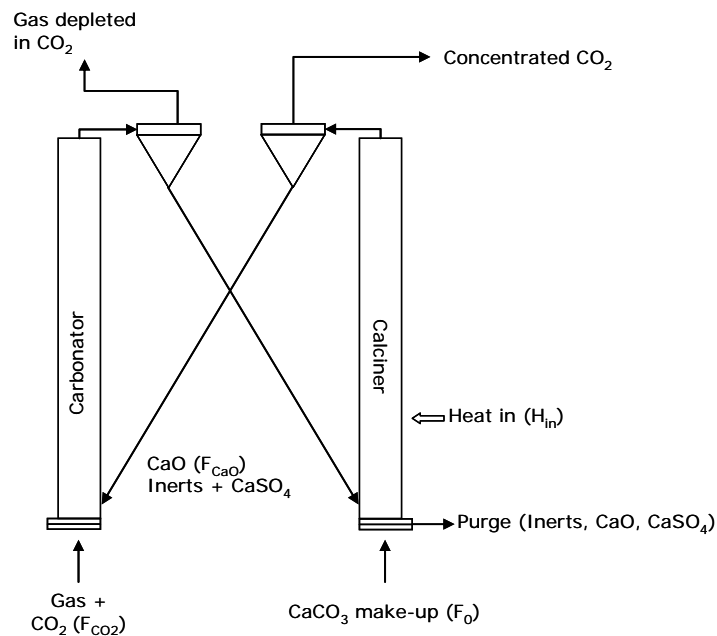


Figure 1: Scheme of the process for CO₂ capture using the carbonation-calcination loop of CaO.

All CO₂ capture system incorporating the carbonation-calcination loop share a common challenge: to supply to a fluidised bed of solids a large amount of heat to drive the calcinations reactions in an atmosphere with a high concentration of CO₂. The equilibrium of CaO/CaCO₃ that is plotted in Fig. 2 for the temperature range of interest for this work¹¹ imposes a temperature for calcination higher than 900 °C for regeneration in CO₂ at 1 atm. The rapid development expected by key manufacturers^{9,12} for oxy-fired combustion using

circulating fluidized bed combustors (CFBCs), should facilitate soon this calcinations option. In fact, it could be argued that operation of these oxyfired CFBC systems should be easier (in terms of temperature control in the bed at high O₂ concentration) when there is an endothermic reaction like calcination of CaCO₃ taking place in the combustor. Therefore, the discussion that follows can be carried out irrespective of the calcination method, but keeping also in mind that the heat requirements in the calciner need to be kept to the minimum irrespective of the calcination method.

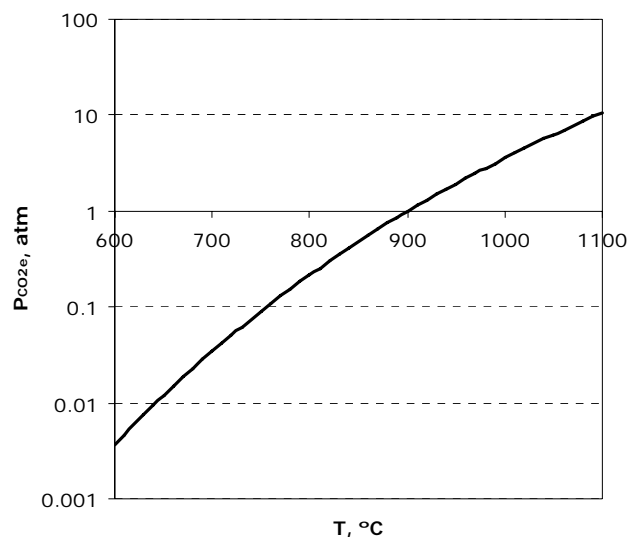


Figure 2: The equilibrium pressure of CO₂ on CaO.

The purpose of this work is to analyse how the heat demand in the calciner changes for different operating conditions and design fuels when using the carbonation–calcination loop of Fig. 1. Or in other words, what set of operating conditions can be chosen for a given fuel and process scheme to minimize the heat requirements in the calciner. To answer this question we need to solve the mass and heat balances in the system of Fig. 1, incorporating equilibrium and sorbent performance and reactor data as well as fuel composition (sulphur and ash content in the incoming fuels or flue gases).

2. The circulating mass flows of CaO required for effective CO₂ capture

The purpose of a system as depicted in Fig. 1 is to separate CO₂ in concentrated form in the calciner so that this is suitable for geological storage, after purification and compression (not shown in the diagram). Ideally, most of the carbon in the CO₂ stream leaving the calciner, should originate from the carbon contained in the carbonate. Some CO₂ will also originate from the decomposition of the limestone fed to system to maintain the activity of the sorbent in the carbonation reactor (see below). CO₂ may also come from the oxy-combustion of the coal fed to the calciner to drive regeneration reactions. Therefore, as indicated in Fig. 1, there is a flow of CO₂ entering the carbonator reactor and reacting with CaO (F_{CaO}) contained in the solid flow coming from the calciner. In the most general case, this stream will be composed of CaO, CaSO₄, ash and any other inert material present in the incoming solid streams to the system (fuels and fresh sorbent make up). The resulting solid stream from the carbonator will contain a certain fraction, X_{carb} , of the total calcium converted to CaCO₃ that will determine the efficiency in the capture of CO₂ from the combustion gases in the carbonator.

$$F_{CaCO_3} = F_{CO_2 \text{ captured}} = F_{CaO} \times X_{carb} \quad (2)$$

This carbonate will be regenerated back to CO₂ and CaO in the calciner. The heat input, H_{in} , to the calciner is required to drive the endothermic calcination reaction of CaCO₃ and heat up all the solids from the carbonation temperature to the calcinations temperature.

In principle, X_{carb} can take any value from zero to the maximum average carbonation conversion achievable by the CaO particles cycling in the system. We call this the maximum average conversion, X_{ave} , because it represents the average conversion of the solid attained when a sufficient large inventory of solids in the carbonator is maintained, to allow sufficiently high residence times of the solids. As reviewed in previous works, the carbonation reaction of CaO can progress in a fast reaction regime at temperatures over 600 °C¹³⁻¹⁵ and

typical concentrations of CO₂ in flue gases. A solid residence time of a few minutes should therefore be enough to achieve conversions close to X_{ave} . However, it is important to understand the limits to the value of X_{ave} ¹⁶ imposed by the poor sorbent performance of CaO as regenerable sorbent submitted to many carbonation–calcination cycles. It has been well documented from early works, including continuous pilot testing in interconnected fluidized beds¹⁷, that natural calcium oxide and dolomites are able to carbonate in the fast reaction regime up to a maximum level of conversion, X_N that decays with an increasing number of cycles. In a recent paper¹⁸ we have shown that the trend of this decay, up to 500 cycles, follows the equation proposed by Wang and Anthony¹⁹ adding a residual activity:

$$X_N = \frac{1}{\frac{1}{(1-X_r)} + kN} + X_r \quad (3)$$

This equation is based on a second order sintering mechanism of the sorbent, and it fits well with $k = 0.52$ and $X_r = 0.075$ most data available for many limestones, and a wide variety of operating conditions (limestone type, particle sizes, carbonation atmosphere and temperature, calcination atmosphere and temperature up to 950 °C). The value of X_r in Eq. (3) would be the maximum carbonation conversion of the sorbent in a continuous system with no make up flow of sorbent (no consumption of fresh limestone), and no deactivation agents of sorbent (like SO₂). Although this is a modest value of conversion, it still translates into a CO₂ capture capacity of 60 mg/g of sorbent, which compares very favourably with most adsorbents proposed to capture CO₂²⁰. However, the solids entering the carbonator of Fig. 1 can be tailored to yield much higher carbonation conversions, by adding a make up flow of fresh limestone (the end of the fast carbonation for the first calcine takes place at values of X_1 around 0.7, 10 times higher than X_r). A mass balance for this CaO recycle system with make up flow of fresh CaO was solved elsewhere¹⁶ and

provides an expression for the fraction of solids entering the carbonator that have circulated N times through the loop of Fig. 1:

$$r_N = \frac{F_0 / F_{CaO}}{(1 + F_0 / F_{CaO})^N} \quad (4)$$

So, the fraction of particles that are been in the system at least N cycle is:

$$S_N = 1 - \sum_{N=1}^{\infty} r_N = \left(\frac{1}{\frac{F_0}{F_{CaO}} + 1} \right)^N \quad (5)$$

Fig. 3 represents this function together with Eq. (3), for values of F_0/F_{CaO} reasonable for the loop of Fig. 1. Although low values of F_0/F_{CaO} are always desirable in any sorption-desorption system (low consumption of fresh sorbent make up), it has been discussed elsewhere²¹ that the very low cost of limestones allows for high F_0/F_{CaO} (in the order of 0.1) without escalating the sorbent cost. As can be seen in Fig. 3, for low values of F_0/F_{CaO} the representative conversion of the sorbent is given by X_r . For high values of F_0/F_{CaO} the largest fraction of sorbent particles in the loop can correspond to those that have been in the system only a few times and can yield much higher conversions.

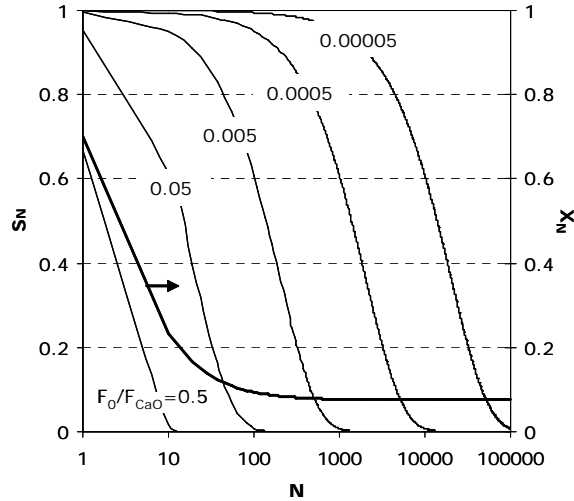


Figure 3: X_N and S_N , as a function of number of cycles at different ratios of F_0/F_{CaO}

The average capture capacity of the CaO circulating in the system is given by:

$$X_{ave} = \sum_{N=1}^{N=\infty} r_N X_N \quad (6)$$

For the case of sorbent deactivation by CaSO₄ formation, it is assumed that all the sulphur present in the fuel reacts quantitatively with the active part of CaO, and therefore all the sulphur leaves the system in the solid drain (F_0):

$$X_{ave} = \sum_{N=1}^{N=\infty} r_N X_N - \frac{F_{CO_2}}{F_0 r_{C/S}} \quad (7)$$

where $r_{C/S}$ is the C/S mol ratio in the fuel. New data²¹ indicate that this may be an excessively conservative assumption because part of the CaO not active for the carbonation can actually be active for the sulphation reaction as well. Furthermore, since the CaSO₄ formed on the free surfaces of CaO of the sorbent is always in low conversion (the Ca/S ratio entering the system is at least one order of magnitude higher than the used for desulphuration systems, because

the C/S ratio is very high even in high sulphur fuels) the SO₂ cannot introduce pore blocking mechanism, that are known to reduce the availability of more CaO in the reaction with SO₂. In the absence of better quantitative information, the Eq. (7) is adopted in this work, assuming that the fate of all S entering the system will be to irreversibly deactivate only the “CO₂ active” part of CaO (fraction defined by Eq. (4)) forming CaSO₄. Fig. 4 represents X_{ave} for a range of conditions of interest. Clearly, the CO₂ capture capacity of the sorbent (X_{ave}) could be kept high in the carbonator despite the decay in sorbent activity, by increasing the fresh feed ratio (F_0/F_{CO_2}). Values of X_{ave} below zero in Fig. 4 correspond to a lack of sufficient fresh limestone to maintain the capture of the sulphur contained in the fuel as CaSO₄. The mass balances for the system of Fig. 1 can now be completed for different fuels and sorbent make up flow ratios, in order to calculate all the solid and gas streams in the system, necessary to achieve a certain CO₂ capture efficiency (Eq. (2)). This has been done for 4 different ideal fuel compositions, characteristic of different sulphur and ash contents and associated flue gas compositions. The calculations have been carried out using a Matlab code that yields identical solutions to those used with commercial process simulation software used in previous works⁵, but has the benefit of integrating new sorbent performance models like Eqs. (6) and (7) and allow a fast evaluation of the model for different sorbent flow ratios (Figs. 5–8). The ratio F_0/F_{CaO} represents the make up flow of limestone to the system. This defines through the infinite sum of Eq. (7) the maximum capture capacity of the solids circulating between calciner and carbonator, X_{ave} . The conversion of a real carbonator reactor will always have to be lower than X_{ave} . But as mentioned before, if the carbonator was designed with sufficient solid residence time (1–3 min) it should be possible to yield conversions close to the maximum. This was the case in pilot test conducted during the development of the Acceptor Gasification Process¹⁷, although in their case, the high partial pressures of CO₂ would have favoured faster carbonation rates. The actual conversion in the carbonator, X_{carb} , will determine the necessary flow of sorbent between reactors (F_{CaO}) to achieve a given capture efficiency (Eq. (2)) of the reference flow of CO₂ entering the carbonator, F_{CO_2} .

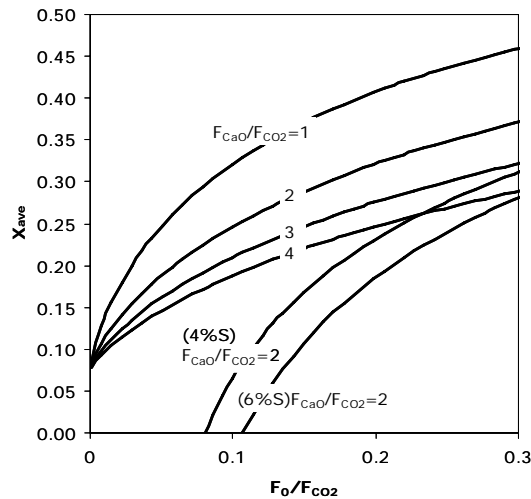


Figure 4: X_{ave} as a function of ratios F_0/F_{CO_2} and F_{CaO}/F_{CO_2} including the effect of S at low 4% and high 6% fraction.

3. Heat requirements for sorbent regeneration

The choice of CaO flow ratios (F_0/F_{CO_2} and F_{CaO}/F_{CO_2}) to achieve the desired capture capacity in the carbonator is not free, because the heat balance in the system will impose further limits on these solid ratios. The calcination of the $CaCO_3$ contained in the solid stream ($F_{CaO} + F_{inert} + F_0$) will involve the supply of heat, H_{in} , to drive the endothermic calcination of the $CaCO_3$ contained in that stream and to heat up to the calcination temperature all the mass streams fed into the calciner (mainly the solid stream from the carbonator). The heat input to the calciner, H_{in} , and the heat input to the combustor (H_{comb}) are defined as:

$$\begin{aligned}
 \frac{H_{in}}{F_{CO2}} = & \Delta H_{carb} \left(\frac{F_{CaO}}{F_{CO2}} X_{carb} + \frac{F_0}{F_{CO2}} \right) + \\
 & + \Delta T_{cal} \left[\begin{array}{l} C_{pCaO} \frac{F_{CaO}}{F_{CO2}} (1 - X_{carb}) + C_{pCaCO3} \frac{F_{CaO}}{F_{CO2}} X_{carb} + \\ C_{pCaSO4} \frac{F_{CaSO4}}{F_{CO2}} + C_{pAsh} \frac{F_{Ash}}{F_{CO2}} \end{array} \right] + \\
 & + \frac{F_0}{F_{CO2}} C_{pCaCO3} \Delta T_{F0}
 \end{aligned} \tag{9}$$

$$H_{comb} = \Delta H_{LHV} \frac{12}{w_c} F_{CO2} \tag{10}$$

where F_{CaSO4} and F_{Ash} are the molar flowrates of $CaSO_4$ and ash between both reactors. It is assumed for the discussion below that all the individual reactor designs and conditions for the calciner are such that full calcination of the sorbent particles are attained in the calciner.

Figs. 5–8 were all built assuming a carbonation efficiency of 70%. Each point in the figure corresponds to a choice of F_0/F_{CO2} and X_{carb} . When these two parameters are fixed, the mass balance of Eq. (2) allows the calculation of F_{CaO}/F_{CO2} . Eq. (7) is used to set the limit imposed by the poor sorbent performance equation (X_{carb} can only vary from zero to X_{ave}) and Eq. (9) can then be used to estimate the heat requirements for the chosen set of X_{carb} and F_0/F_{CO2} .

Fig. 5 plots the heat ratio defined as the fraction of heat input to the calciner relative to the total heat input to the power plant, $H_{in}/(H_{comb} + H_{in})\%$, as a function of different values of X_{carb} . Fig. 5 has been built for a characteristic example of a flue gas with no ashes and no sulphur (fuel of case 1 in Table 1), and with a temperature gradient between carbonation and calcination units (T_{cal}) of 300K (650 °C for carbonator and 950 °C for the calciner). The limit that X_{carb} can reach when all particles in the system reach their maximum conversion is represented as a dotted line, X_{ave} . As discussed above, this

conversion limit is only a function of the F_0/F_{CO_2} ratio when a capture efficiency is imposed. If the X_{ave} is not reached in the system (as will be the case in real reactor systems with incomplete sorbent conversion) the F_{CaO}/F_{CO_2} must increase to achieve a certain level of CO₂ capture efficiency from the gas phases. Therefore, as the solid lines indicate, the heat requirements in the calciner increase as X_{carb} diminishes, due to the increasing demand of heat for heating up a the unconverted solid stream from the carbonator.

Table 1. Fuel compositions for the references cases

	CASE1 (%w)	CASE 2 (%w)	CASE 3 (%w)	CASE 4 (%w)
C	83	65	83	52
H	5	3	5	3
S	0	0	4	6
O	3	8	3	9
N	4	0	0	1
H2O	5	8	5	0
ASH	0	16	0	29
TOTAL	100	100	100	100
LHV (MJ/kg)	34	25	34	21

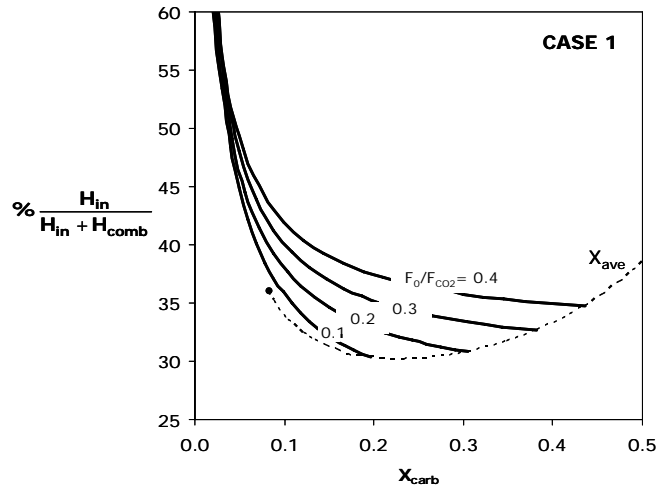


Figure 5: Heat ratio as a function of CaO conversion at different F_0/F_{CO_2} ratios for reference case 1.

There is a characteristic point in Fig. 5 (at $X_{carb} = 0.075$) that has been marked with a solid dot and that corresponds to a situation with no make up flow of limestone ($F_0/F_{CO_2} = 0$). This would be an ideal system, where the residual activity of the sorbent (CO₂ capture capacity for an infinite number of cycles) would be used (with a $F_{CaO}/F_{CO_2} = 9.3$ in this example) to capture the CO₂ in the carbonator (capture efficiency of 70% in this example). This ideal case is only possible if there is no sulphur in the flue gas and no ash accumulation in the carbonation–calcination cycle. The heat requirements are 36.9% of total heat input to the plant for this ideal case. The dotted line of Fig. 5 represents the series of minimum heat requirements for a given make up flow of fresh sorbent to the system. For each F_0/F_{CO_2} , this corresponds to the case where X_{carb} reaches its maximum value allowed by Eq. (6). Fig. 5 shows that this dotted line also has a minimum, where the heat requirements to the calciner is reduced to 30.2% (this correspond to $X_{carb} = X_{ave} = 0.23$ for a $F_{CaO}/F_{CO_2} = 3.0$ and a $F_0/F_{CO_2} = 0.13$ in this example). These molar flows correspond to 0.90 kg of fresh limestone/kg of coal fed to the power plant to generate the flue gas entering the carbonator. This minimum appears because the opposite effect that an increase in the make up flow of fresh limestone, F_0/F_{CO_2} , has on the two main components in the definition of H_{in} (Eq. (9)). Low values of F_0/F_{CO_2} lead to low

values of X_{ave} , and this means that more heat is required to heat up to the calcination temperature the inert CaO ($1-X_{ave}$). An increase of F_0/F_{CO_2} will tend to improve the capture capacity (higher X_{ave}) of the solids flowing between carbonator and calciner. With higher X_{ave} , less solids will be required to circulate between reactors, and the heat requirements for heating solid streams will be reduced. However, the necessary heat to calcine the fresh make up flow, F_0 , will increase, giving rise to the optimum value of F_0/F_{CO_2} that minimizes the overall heat requirement in the calciner.

The quantification of these optimum values of solid flow ratios to minimize the heat requirements in the calciner is important for the design of these systems, because in order to minimize limestone consumption, the economic optimum is likely to be a function of this minimum.

In the discussion above we have not defined the source of the heat input to the calciner. As indicated in the introduction, the most plausible solution at present is to burn a certain amount of coal with O₂ to produce a highly concentrated stream of CO₂ from this calciner¹⁰. The value of H_{in} will increase slightly in these conditions depending on the level of the preheating of the additional solid and gas streams (coal, make up, O₂, CO₂ recycle) entering the calciner.

Fig. 6 presents similar simulation when introducing a fuel containing ash (but negligible sulphur content) into the mass and heat balances. In practice, this can be the case when the carbonator system is treating flue gases before dedusting equipment. The solid lines of Fig. 6 follow similar qualitative trends as in Fig. 5, with the heat demand increasing rapidly as X_{carb} diminishes for a fixed value of make up flow ratio F_0/F_{CO_2} . The dotted line of Fig. 6 represents again the minimum heat requirements for each make up flow ratio F_0/F_{CO_2} , that shows a minimum for this particular case at 32.5%, with $F_0/F_{CO_2} = 0.16$ and $F_{CaO}/F_{CO_2} = 2.63$. The presence of inert ashes in the carbonation–calcination loop will increase as the make up flow ratio (and associated purge rate) diminishes. Therefore, the dark point that marked in Fig. 5 the heat requirements when operating the system with no make up flow has now moved up to $H_{in}/(H_{in} + H_{comb}) = 1$ when $X_{carb} = X_{ave} = X_r$ (which appears when there is no purge rate of solids). The need to purge ashes from the carbonation–calcination loop may

determine the choice of F_0/F_{CO_2} . For the particular boundary conditions of Fig. 6 it would be attractive to choose F_0/F_{CO_2} around 0.16 (0.87 kg limestone/kg coal) to moderate the heat requirements in the calciner and purge the ashes introduced by the fuel in the carbonation–calcination loop.

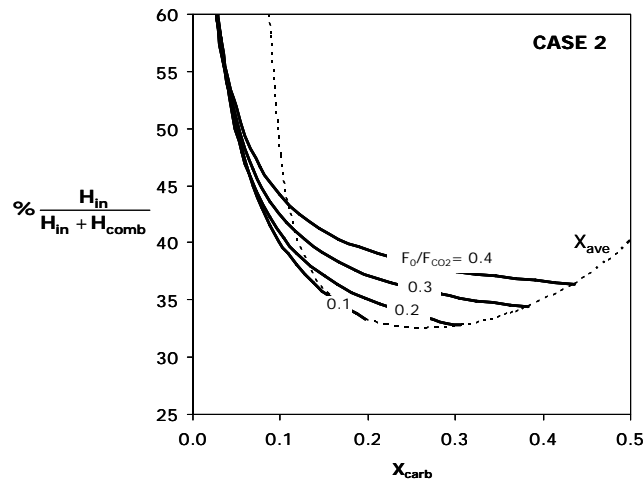


Figure 6: Heat ratio as a function of CaO conversion at different F_0/F_{CO_2} ratios for reference case 2. Fig. 7 presents the solution to the mass and heat balances in a system burning a fuel with no ash but high sulphur content (for example, pet coke). Since all sulphur contained in the fuel is assumed to react with the active part of CaO for carbonation, it is necessary to operate with higher F_0/F_{CO_2} ratios. For the particular fuel of case 3, there is a F_0/F_{CO_2} ratio 0.086) just to capture the sulphur contained in the fuel as $CaSO_4$. In every other aspect, the figure is qualitatively similar to the case of Fig. 6. A higher minimum heat requirement appears around 34.7%, for a solids conversion of 0.27 and a F_0/F_{CO_2} ratio of 0.29 (2 kg fresh limestone per kg fuel). There may be some conditions where the sulfation reaction (exothermic) could take place also in the calciner (for example, when oxyfiring sulfur containing coal in the calciner). In these cases, Eq. (9) should add this term and the heat requirements in the calciner would be reduced slightly.

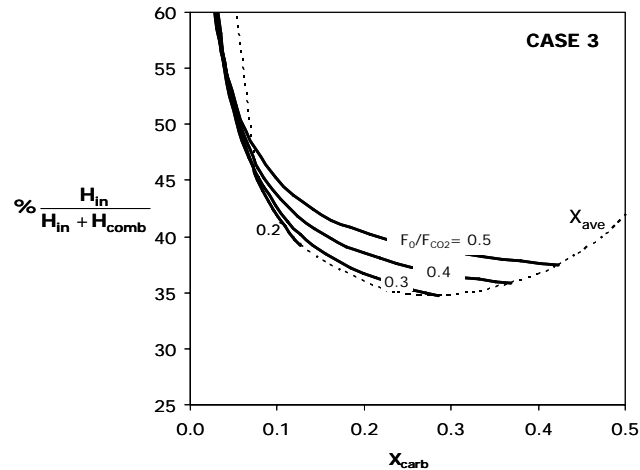


Figure 7: Heat ratio as a function of CaO conversion at different F_0/F_{CO_2} ratios for reference case 3.

Fig. 8 presents the final example with the most challenging fuel in Table 1: a coal with high ash and high sulphur content. This could be the case for highly integrated carbonation–calcination loops (“in situ” CO₂ capture as in reference^{5,22}) when carbonation and CO₂ generation by combustion or gasification are taking place in the same reactor. The conditions of pressure and temperature will change for these cases, but the heat and mass balances will result in solutions as represented in Fig. 8. Large F_0/F_{CO_2} ratios are unavoidable both to purge the ashes and to compensate for the deactivation of active CaO as CaSO₄. The figure is qualitatively similar to the ones above but the minimum heat requirement is now gone up to 39.3% at F_0/F_{CO_2} ratio of 0.43 (1.86 kg of limestone per kg of fuel). The make up is slightly lower than in case 3 because the lower carbon content of the fuel. With cases 3 and 4 the integration of the capture system with a cement plant would be essential, in order to give a use to the large purge of solids, and take credit of the energy spent to calcine the fresh make up flow of limestone⁵.

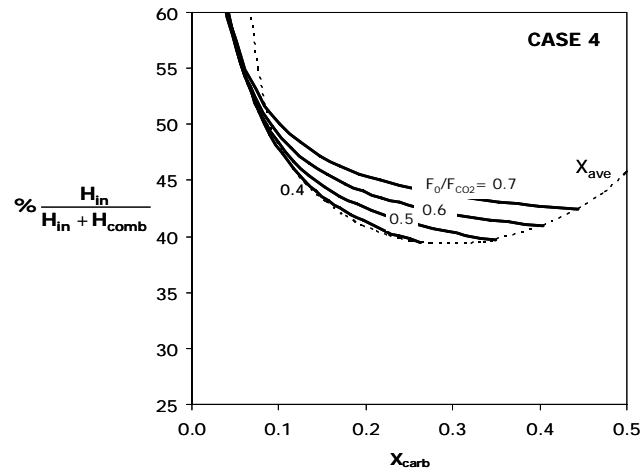


Figure 8: Heat ratio as a function of CaO conversion at different F_0/F_{CO_2} ratios for reference case 4.

4. Conclusions

Emerging CO₂ capture systems using CaO as regenerable sorbent of CO₂ require large flows of heat to be supplied to the calciner in order to regenerate the carbonated sorbent by calcination. Although this heat supply can be effectively recovered in the system because all mass streams are at high temperature, it is always interesting to minimize the heat demand in the calciner. The simultaneous solution of heat and mass balances in a general carbonation–calcination cycles, incorporating sorbent performance data, allow the calculation of the heat requirement in the calciner for different fuels and boundary conditions. For flue gases with no ash and no sulphur, aiming at a 70% CO₂ capture, heat requirement around 37% appears when no make up flow of fresh sorbent is required because the carbonate loop relies on the residual activity (7–8%) of the CaO towards carbonation at very high cycle numbers. This heat requirement decreases down to 30% when increasing the F_0/F_{CO_2} because the fresh limestone addition improves rapidly the average activity of the sorbent up to $X_{carb} = 23\%$. From this point, further increases in make up flow of limestone translate into increasing heat requirements, because the heat demand for the calcination of the fresh make up becomes dominant in

the heat balance around the calciner. The effect of high ash content in the fuel produce an increase of solid amount circulating in the loop, and this tend to increase the heat requirements. The effect of high sulphur content implies an increase of F_0/F_{CO_2} to compensate for the sulphation of the active part of the CaO. For the case of high ash and sulphur fuel, a larger make up flow of sorbent is needed and a synergy with a cement plant may be necessary.

Nomenclature

C_p □ heat capacities (J/° mol), calculated from ref. 23

E_{carb} □ CO₂ capture efficiency in the carbonator

E_{equil} □ carbonation efficiency reaching the equilibrium conditions

F_{CO_2} □ CO₂ from the combustor to the carbonator (kmol/s)

F_0 □ fresh make up of sorbent (kmol/s)

F_{Ash} □ molar flow rate of ashes between carbonator and calciner (kmol/s)

F_{CaO} □ CaO stream between carbonator and calciner (kmol/s)

F_{CaSO_4} □ molar flowrate of CaSO₄ between carbonator and calciner (kmol/s)

H_{in} □ heat requirement in the calciner (MJ)

H_{comb} □ total heat input to the power plant (MJ)

ΔH_{carb} □ calcination heat reaction at 900 °C (MJ/mol)

ΔLHV □ low heat value for the fuel (MJ/kg)

K □ constants proposed in Eq. (3)

N □ number of carbonation/calcination cycles

$r_{C/S}$ □ carbon to sulphur molar ratio in the fuel

r_N □ fraction of sorbent particles that has experienced N calcinations

S_N □ fraction of particles that have been cycling in the carbonation–calcination loop more than N times

T_{calc} □ temperature gradient between calciner and carbonator (K)

T_{F0} □ temperature gradient between calciner and fresh make up stream (K)

w_C □ weight fraction of carbon in the fuel

X_{ave} □ maximum conversion attainable by the average sorbent particle circulating in the carbonation–calcination loop

X_{carb} □ average conversion attained by the sorbent in the carbonator reactor

X_N carbonation conversion of a particle in the N^{th} carbonation–calcination cycle

Acknowledgments

This paper contains work from a project partially funded by the European Commission (C3Capture and ISCC projects) and the project CENIT-CO₂ in Spain, where we acknowledge funding from Union Fenosa SA. GGrasa acknowledges a grant under the “Juan de la Cierva” program.

References

1. B. Metz, O. Davidson, H. de Coninck, M. Loos, L. Meyer (Eds.), Special report on carbon dioxide capture and storage, Intergovernmental Panel on Climate Change, Cambridge University Press, 2005.
2. A.G. Collot, Prospects for Hydrogen from Coal, IEA Clean Coal Centre, 2003 (CCC/78).
3. K. Johnsen, J.R. Grace, S.S.E.H. Elnashaie, L. Kolbeinsen, D. Eriksen, Modeling of sorption-enhanced steam reforming in a dual fluidized bubbling bed reactor, *Ind. Eng. Chem. Res.* 45 (2006) 4133–4144.
4. K. Johnsen, H.J. Ryu, J.R. Grace, C.J. Lim, Sorption-enhanced steam reforming of methane in a fluidized bed reactor with dolomite as CO₂-acceptor, *Chem. Eng. Sci.* 61 (2006) 1195–1202.
5. J.C. Abanades, E.J. Anthony, J. Wang, J.E. Oakey, Fluidized Bed Combustion Systems Integrating CO₂ Capture with CaO, *Environ. Sci. Technol.* 39 (2005) 2861–2866.
6. J.C. Abanades, E.S. Rubin, E.J. Anthony, Sorbent cost and performance in CO₂ capture systems, *Ind. Eng. Chem. Res.* 43 (2004) 3462–3466.
7. J.C. Abanades, G. Grasa, M. Alonso, N. Rodríguez, E.J. Anthony, L.M. Romeo, Cost structure of a postcombustion CO₂ capture system using CaO, *Environ. Sci. Technol.* 41 (2007) 5523–5527.
8. L.M. Romeo, J.C. Abanades, J.C. Ballesteros, A. Valero, J.M. Escosa, A. Giménez, C. Cortés, J. Paño, Process optimization in postcombustion CO₂-capture by means of repowering and reversible carbonation/calcinations cycle, in: 8th

- International Congress on Greenhouse Gas Control Technologies—GHGT-8, Trondheim, Norway, June 2006.
9. N. Nsakala, G. Liljedahl, J. Marion, C. Bozzuto, H. Andrus, R. Chamberland, Greenhouse gas emissions control by oxygen firing in circulating fluidized bed boilers, in: Second Annual National Conference on Carbon Sequestration, Alexandria, VA, USA, May 2003.
 10. T. Shimizu, T. Hiram, H. Hosoda, K. Kitani, M. Inagaki, K. Tejima, Atwin fluid-bed reactor for removal of CO₂ from combustion processes, *Trans. IChemE* 77 (Pt A) (1999) 62–68.
 11. E.H. Baker, The calcium oxide–carbon dioxide system in the pressure range 1–300 atmospheres, *J. Chem. Soc.* (1962) 464–470.
 12. T. Hyppänen, A. Hotta, Development in Oxy-coal combustion boiler: a view from boiler manufacturer, in: Foster Wheeler Inaugural Workshop in Oxyfuel Combustion, Cottbus, Germany, November 2005.
 13. R. Barker, The reversibility of the reaction $\text{CaCO}_3 = \text{CaO} + \text{CO}_2$, *J. Appl. Chem. Biotechnol.* 23 (1973) 733–742.
 14. S.K. Bhatia, D.D. Perlmutter, Effect of the product layer on the kinetics of the CO₂-lime reaction, *AIChE J.* 29 (1983) 79–86.
 15. G.S. Grasa, J.C. Abanades, M. Alonso, B. González, Reactivity of highly cycled particles of CaO in a carbonation/calcination loop, *Chem. Eng. J.* 137 (2008) 561–567.
 16. J.C. Abanades, The maximum capture efficiency of CO₂ using a carbonation/calcination cycle of CaO/CaCO₃, *Chem. Eng. J.* 90 (2002) 303–306.
 17. G.P. Curran, C.E. Fink, E. Gorin, Carbon dioxide-acceptor gasification process. Studies of acceptor properties, *Adv. Chem. Ser.* 69 (1967) 141–165.
 18. G.S. Grasa, J.C. Abanades, CO₂ capture capacity of CaO in long series of carbonation/calcination cycles, *Ind. Eng. Chem. Res* 45 (2006) 8846–8851.
 19. J. Wang, E.J. Anthony, On the decay behavior of the CO₂ absorption capacity of CO₂-based sorbents, *Ind. Eng. Chem. Res.* 44 (2005) 627–629.
 20. Z. Yong, V. Mata, A.E. Rodrigues, Adsorption of carbon dioxide at high temperature, *Sep. Purif. Technol.* 26 (2002) 195–205.

21. P. Sun, J.R. Grace, J.C. Lim, E.J. Anthony, Proceedings of the 18th International Conference on Fluidized Bed Combustion, Toronto, May 2005.
22. J.Wang, E.J. Anthony, J.C. Abanades, Clean and efficient use of petroleum coke for combustion and power generation, Fuel 83 (2004) 1341-1348.
23. R.H. Perry, D. Green, Perry's Chemical Engineers' Handbook, sixth ed. McGraw-Hill, 1984.

3.4.2 *Publicación II*

**PROCESS FOR CAPTURING CO₂ ARISING
FROM THE CALCINATION OF THE CaCO₃
USED IN CEMENT MANUFACTURE**

Publicado en:
Environmental Science & Technology
Volumen 42
Año 2008

PROCESS FOR CAPTURING CO₂ ARISING FROM THE CALCINATION OF THE CaCO₃ USED IN CEMENT MANUFACTURE

N. Rodríguez^a, M. Alonso^a, G. Grasa^b, J. Carlos Abanades^a

^a *Instituto Nacional del Carbón, CSIC, Oviedo 33011, Spain*

^b *Instituto de Carboquímica, CSIC, Zaragoza 50015, Spain*

ABSTRACT

This paper outlines a new CaCO₃ calcination method for producing a stream of CO₂ (suitable for permanent geological storage after purification and compression). The process is based on the use of very hot CaO particles ($T > 1000$ °C) to transfer heat from a circulating fluidized bed combustor (CFBC) to a calciner (fluidized with CO₂ and/or steam). Since the fluidized bed combustor and calciner have separate atmospheres, the CO₂ resulting from the decomposition of CaCO₃ can be captured, while the CO₂ generated in the combustion of the fuel in air is emitted to the atmosphere. We demonstrate that with this system it is possible to reduce the CO₂ emissions of a cement plant by around 60%. Furthermore, since the key pieces of equipment are similar to the commercial CFBCs used in power generation plants, it is possible to establish the additional investment required for the system and to estimate the cost per ton of CO₂ avoided for this process to be about 19 \$/tCO₂ avoided.

INTRODUCTION

Global cement production grew from 594 Mt in 1970 to 2200 Mt in 2005 (1). Average emission intensities are now around 0.81 t CO₂/t cement. This means that about 5% of total CO₂ emissions to the atmosphere come from cement manufacture (1-3). Cement manufacture is an energy-intensive industry due to the large amount of energy required for the calcination of the raw feed (rich in limestone) and the need for very high temperatures (up to 1400 °C) for clinker

reactions. In new, highly efficient cement plants, almost 70% of the CO₂ emissions come from the decomposition of CaCO₃ to CaO, the main raw material for clinker production (2). The total theoretical heat requirement for the manufacture of the Portland cement clinker, assuming no heat loss, has been estimated at 1.76 GJ/t (2) (all raw materials starting at 20 °C). 1.99 GJ/t of clinker are required for the dissociation of calcite and heat is generated (0.31 GJ/t of clinker) through the formation of clinker phases. Currently the best available technology requires 3GJ/t of cement and the potential for improving energy efficiency is very limited in such highly efficient cement plants (4, 5). Even if efficiency could be increased, the overall fraction of CO₂ emitted from the cement plant due to the calcination of the raw feed would only increase from the current 60-70% levels.

Cement plants are large stationary sources of CO₂ (up to several MtCO₂/yr) and therefore they are candidates for implementing CO₂ capture and storage technologies (1). Hendricks et al. (3) reviewed the application of capture technologies to cement manufacture and concluded that oxyfuel combustion was particularly well suited for CO₂ recovery in cement production. Since most CO₂ comes from the decomposition of CaCO₃ and only a fraction of CO₂ originates from the combustion of the fuel, less pure oxygen is required to recover 1 t of CO₂ than for similar oxyfuel processes in power generation (3). However, the avoided costs have been estimated to be higher than 50 \$/tCO₂ avoided, due to the investment required to install the air separation unit and compressors, which consume large quantities of electricity.

Other opportunities for CO₂ capture in cement plants are offered by the potential synergy with emerging concepts of CO₂ capture in power generation by means of a lime carbonation-calcination cycle. Future cement plants could be installed near power plants that use CaO in a chemical loop where CO₂ is captured in one reactor and it is released in pure form in a calciner. Some processes of this type have been proposed for combustion applications (6, 7) and others are being considered for H₂ production routes (8, 9). In all these systems, high CaCO₃ makeup flows and CaO purge rates are required, due to the need to ensure that the activity of the sorbent is sufficiently high. The purge

could be a feedstock used in the cement industry, so that a synergy would be established between the power plant and the cement plant leading to a very low avoided cost (10). However, there may be many situations in which such proximity between the power plant and the cement plant is not possible in practice.

The purpose of this work is to propose a new process aimed at substantially reducing CO₂ emissions from existing and new cement plants without using any chemical reaction of CO₂ capture. This is achieved by focusing only on the CO₂ arising from the decomposition of CaCO₃ to CaO. For this purpose a new type of calciner is analyzed. In this calciner the calcination chamber is separated from the combustion chamber and CaO is used as heat carrier between a fluidized bed combustor and a fluidized bed calciner. Apart from similarities with a concept outlined in our previous work on lime carbonation-calcination cycles (7) we have only found one other reference to this idea (11). Therefore, in this work we explore the potential of a process that exploits the very high capacity of circulating fluidized bed combustors for transferring heat at high temperatures from the combustion chamber to a calciner of CaCO₃, thereby producing a concentrated stream of CO₂ suitable for disposal.

DESCRIPTION OF THE PROCESS

The reference cement plant and the proposed system are illustrated in the schemes of Figure 1. The reference cement plant (Figure 1a) uses a dry process with preheaters and a precalciner before the kiln. This figure shows only the main components of the carbon balance. More details can be found in references 2-5. It is assumed that 1.5 t of raw material are required to produce 1 t of Portland cement, depending on the fuel employed. It is also assumed that a modern reference cement plant requires an energy input of about 3 GJ/t of cement and about 60% of this energy is used in the precalciner to carry out the calcination (2-5). With a clinker/cement ratio of 0.95 and assuming a typical calcination heat requirement of 1.88 GJ/t cement (2), the mass and heat balance of the reference cement plant can be completed (Figure 1a). As can be seen in this figure, a major fraction (63%) of carbon dioxide emissions from the

reference cement plant originates from calcining the limestone present in the raw material.

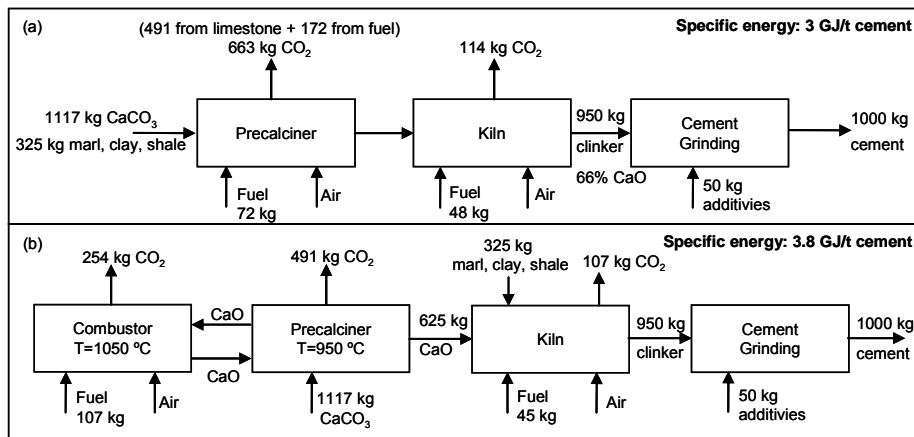


Figure 1. (a) Scheme of a reference cement plant and (b) the system proposed in this paper with the main mass flows for the production of 1 t of cement. (LHV 25 MJ/kg, 10% air excess, combustor temperature 1050 °C, precalciner temperature 950 °C, preheating temperatures for these units 700 °C).

The aim of the alternative process outlined in Figure 1b is to replace the precalciner in Figure 1a by a new arrangement that produces a pure stream of CO₂ (or CO₂/steam). This is achieved in a separate fluidized bed precalciner, where high temperature CaO particles are brought into contact with the raw feed of CaCO₃. The high-temperature CaO particles come from a circulating fluidized bed combustor where coal, or another suitable fuel, such as pet coke, can be burned at high temperatures in the presence of CaO (the recycled stream of CaO shown in Figure 1b). There is a purge of CaO at some point in the recycled stream of CaO that is directed to the clinker oven. Therefore, the result of this process is the calcination (precalcination) of the raw feed before it is fed into the clinker oven (kiln). In principle, the clinker oven and the other components of the cement plant are the same in both diagrams, but a redesign of the overall plant might be required to ensure a better heat integration in the new cement plant. However, this is outside the scope of the present work. Also outside the scope of this work are heat recovery issues (including the possibility of producing steam from excess heat) and the purification and

compression of CO₂. It is assumed that these operations could be carried out as in other CO₂ capture systems for power plants of equivalent thermal scale (12).

Figure 2 shows a possible arrangement for the main interconnected fluidized bed reactors which would allow the delivery of sufficient heat to the calciner (i.e., 1.88 GJ/t cement). This large heat flow required from the combustion chamber to the calciner makes it necessary to use circulating fluidized bed (CFB) technology. Coal burns in the main CFB combustor in an atmosphere of air at temperatures close to 1050 °C and produces the heat necessary to bring the temperature of the recycled solid stream of CaO from that of the calciner up to the reheated temperature. From the mechanical and material point of view, these high-temperature CFB combustors are well-established technology up to operating temperatures of 1150 °C for alumina calcination and other mineral ore roasting processes (13). Such high combustion temperatures may be challenging for some fuels (ash softening) but this is clearly not a problem for many other available fuels such as pet coke which is commonly used in the cement industry. It can be seen from Figure 2 that the CO₂ resulting from the combustion of the fuel in the CFBC is not recovered. It is important, therefore, to minimize the energy requirements in this combustor in order to maximize the fraction of CO₂ captured and avoided. Heat recovery from the hot gas and solid streams leaving the units in Figure 2 offers great opportunities for heat integration. The mass and heat balances in the new system have been solved in a wide variety of cases in order to illustrate the key operating windows that affect the preheating temperatures, the temperature of combustion and calcination, and the fuel characteristics of the combustor. The heat balances are solved assuming adiabatic reactors, but the heat lost in the whole system is assumed to be 1.12 GJ/t. This is the difference between the real heat consumption of 3GJ/t in the reference plant and the theoretical net heat required to calcine the CaCO₃ needed to make 1 t of cement (Figure 1a). In these conditions, the way to minimize the heat requirements, H_R (GJ/t), of the new system is to minimize the heat requirements of the combustor of Figure 2, H_{comb} (GJ/t), which includes the heat necessary for calcination (1.88 GJ/t, to be

transported by the hot CaO to the precalciner) and the heat necessary to heat up the air and fuel fed into the combustor. Figure 3 shows H_R in the range of preheating temperatures of the gases and solid streams entering the combustor for three different heating values and the carbon contents of the solid fuels. Reasonable air preheating temperatures, up to around 700 °C, translate into total heat requirements (taking into account the losses estimated above) between 3.5 and 4 GJ/t cement, depending on the type of fuel employed. For the sake of simplicity, other minor solid components (mainly the ash from the fuel) are ignored in this figure.

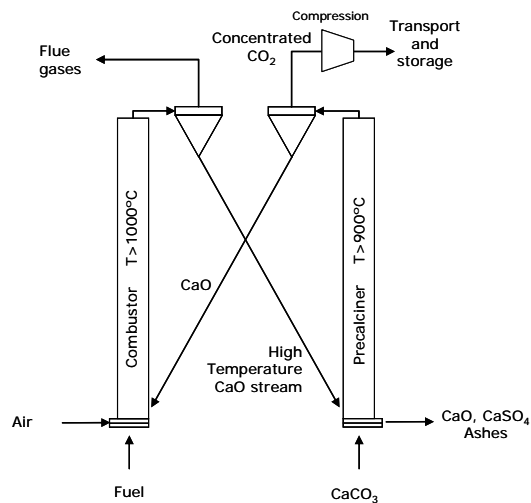


Figure 2. Interconnected circulating fluidized bed reactors proposed in this work to obtain the CO₂ resulting from the calcination of CaCO₃ as a separate stream.

As can be seen in Figure 3, the operation of the system in the conditions selected may translate into a substantial increase in the energy requirements of the cement plant with respect to the reference case in Figure 1a, even with preheating temperatures as high as 700 °C. Some of these heat requirements could be reduced by feeding calcined solids into the kiln at the combustion temperature (1050 °C in the reference case) instead of at the calcination temperature. Further heat integration could be achieved by feeding into the combustion chamber very hot gas streams rich in oxygen from the kiln (effective precalcination temperatures much higher than 700 °C). With the system proposed, heat can also be recovered by producing steam from the very

high temperature gas and solid streams leaving the system. Indeed, opportunities for cogeneration in new and existing cement manufacture plants have been proposed (13), and in this particular process cogeneration may be an interesting option to generate the necessary power for CO₂ purification and compression (3).

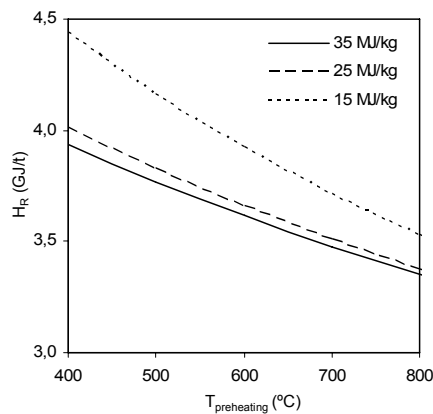


Figure 3. Heat requirements in the cement plant of Figure 1b as a function of the preheating temperatures of the solid and gas streams entering the CFBC for three different solid fuels (10% air excess in all cases).

The flow of solids circulating between the combustor and precalciner of Figure 2 must be restricted to what is standard practice in similar circulating fluidized bed systems. For circulating fluidized bed combustors, solid fluxes can be 10-50 kg/m²s (13, 14) or 5-25 kg solids per kg of gas (S/G), but large-scale CFB boilers usually operate at the lower end of these ranges. As Figure 4 shows, the required solid circulation rate between the combustor and calciner increases rapidly as the temperature difference between the combustor and calciner decreases. These temperatures are subject to limitations. The equilibrium of the calcination reaction in pure CO₂ requires calcination temperatures higher than 900 °C. A 30-50 °C increase in the equilibrium temperature is necessary to achieve a sufficiently fast calcination rate. The use of steam in the calciner, leading to a reduction in the partial pressure of the CO₂ in the calciner, has been proposed (7) in order to reduce the calcination temperature while keeping the calcination rate high. In the combustion chamber, high temperatures may need to be avoided depending on characteristics of the ashes.

There is also a need to minimize heat requirements (Figure 3) and pollutant emissions, both of which increase with increasing combustion temperatures. In particular, SO₂ retention has been shown to be effective only up to 1050 °C according to Anthony et al. (15). There is, therefore, a trade off between the temperature difference between the combustion and precalcination reactor and the solid circulation rate required to achieve the required heat transfer between the reactors. A typical case of this is represented in Figure 4. For the purpose of the preliminary cost analysis that follows, a temperature difference of 100 °C has been assumed, which translates into heat requirements of 2.66 GJ/t cement in the combustor chamber and total heat requirements of 3.8GJ/t (preheating temperature of 700 °C, fuel with LHV= 25 MJ/kg).

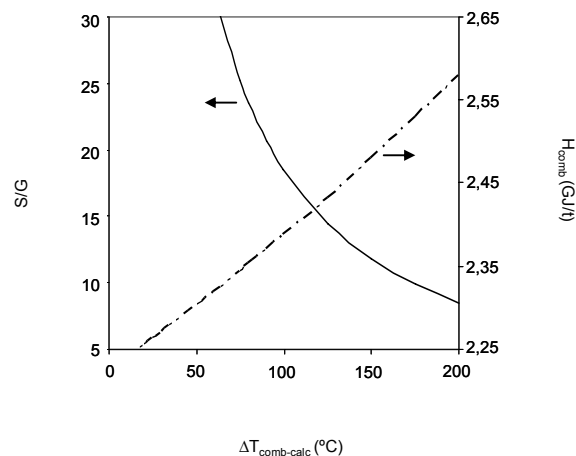


Figure 4. Solid circulation rate required between combustor and calciner (left) and heat required in the CFBC (right) as a function of the temperature in the combustion chamber. (LHV 25 MJ/kg, 65%w C, 10% air excess, T_{calc} 950 °C).

ESTIMATION OF CO₂ AVOIDED

A common method to measure the cost of CO₂ capture and storage systems is the cost of CO₂ avoided. When used correctly, this method makes it possible to compare the average costs of reducing CO₂ emissions for the same amount of useful product (in this case 1 ton of Portland cement from the processes of Figure 1a and b). To facilitate a preliminary analysis of the avoided cost of the proposed system, we assume that both the reference plant (Figure 1a) and the capture plant (Figure 1b) are of the same type and of the same design.

Therefore the specific total capital requirements, TCR (\$ per t of annual cement production capacity) of all those elements in both systems that are not affected by the capture system are the same. The installation of the capture system in the cement plant entails an increase in total capital requirements (ΔT CR), in the consumption of electricity (mainly for CO₂ compression), and in the fuel cost in order to supply the 0.8 GJ/tcement estimated in the previous paragraph as the additional heat requirements (ΔH) in the new system. The avoided cost can then be defined per ton of CO₂ avoided as:

$$AC = \frac{\frac{\Delta TCR \cdot FCF}{CF} + FC \cdot \Delta H + COE_{comp}}{CO_2 t_{cement_{ref}}^{-1} - CO_2 t_{cement_{capture}}^{-1}} \quad (1)$$

where AC is the cost per tonne of CO₂ avoided, FCF is the fixed charge factor (assumed to be 0.1), CF is the capacity factor (assumed to be 0.9), FC is the fuel cost (assumed to be 2 \$/GJ), ΔH is the additional heat requirements per tonne of cement (GJ/t), COE_{comp} is the cost of the electricity used to compress the 0.491 tCO₂/tcement captured (see Figure 1b), and $CO_2 t_{cement}^{-1}$ is the specific CO₂ emissions in the reference cement plant (0.777) and in the cement plant where the CO₂ is captured (0.361).

To estimate ΔTCR we consider two major items:

$$\Delta TCR = TCR_{CFBC} + TCR_{comp} \quad (2)$$

In the absence of detailed cost information, we will make use of its similarity with circulating fluidized bed combustion (CFBC) systems to discuss a reasonable upper limit for the avoided cost. We assume that the TCR_{CFBC} of Equation 2 must not be higher than 30% of the cost of building a full CFBC power plant with an equivalent thermal capacity. This percentage is a reasonable contribution of the boiler to the total capital cost of a CFBC or PC power plants [17, 18]. The TCR of the multi-stage preheater/precalciner kiln that the new system substitutes should be subtracted from Equation 2, since

this is not longer necessary in the cement plant. The information on capital cost of these preheaters in the open literature is scarce, ranging from 8 to 28 \$/(t yr⁻¹) according to Worrell [19], compared to the total TCR of cement plants around 200\$/(t yr⁻¹) (150M€ according to reference [5]). Therefore, and to keep the estimate of Δ TCR reasonably conservative, we have decided to ignore this possible saving of capital cost and leave Equation 2 with the two adding terms.

In order to estimate TCR_{CFBC} in suitable units (\$/(t yr⁻¹) of cement), we consider that a typical cement plant producing about 1 Mt yr⁻¹ of cement requires a total investment of about or TCR_{ref}=200\$/(t yr⁻¹). Assuming heat requirements of 3GJ/t a plant of this capacity requires an annual thermal power supply of 95 MWt, or 106 MWt assuming a capacity factor characteristic of cement plants of 0.9. This means that the specific capital requirements of the cement plant, per units of thermal power, are about TCR_{ref}=1900\$/kWt. Specific TCR_{CFBC} for commercial CFBC power plants are considered to be around 1500 \$/kWe [12, 17]. Assuming a 40% net efficiency in the production of electricity this means 600 \$/kW_t. When the specific capital requirements refer to units of thermal power, a cement plant is more than three times more expensive than a power plant. Following the discussion above, TCR_{CFBC}=200\$/kW_t. The same transformation can be applied in reverse. The thermal power required in a CFBC (such as that in Figure 2) to deliver the heat necessary to manufacture in a year one tonne of cement (estimated to be 2.66 GJ/t cement in the previous paragraphs) is 0.0937 kWt/(t yr⁻¹) where CF=0.9. Therefore, the specific TCR of a CFBC boiler with a thermal input identical to the one required to run the process of Figure 2 would be TCR_{CFBC} = 16.9 \$/(t yr⁻¹).

In order to estimate TCR_{comp} we make use of a recent review of Rubin et al (2007) [20] that estimates CO₂ compression cost for PC postcombustion systems at 86 \$/kW. Assuming a typical CO₂ capture rate of 0.8kgCO₂/kWh for these systems, this indicates a TCR_{comp} of 0.39M\$/kgCO₂ s⁻¹. For the system of Figure 1b, taking into account the reference plant capacity and the 0.49tCO₂ captured per ton of cement produced, it is possible to estimate TCR_{comp}=

6.7\$/tcement yr⁻¹). Adding this number to the TCR_{CFBC} estimated in the previous paragraph yields a $\Delta TCR=23.6\$/(\text{t yr}^{-1})$. According to Equation 1 this translates into a capital cost of 2.6\$/tcement. The fuel cost of the additional heat requirements of 0.8GJ/tcement is 1.6\$/tcement. The electricity cost associated to the compression cost is estimated to be COE_{comp}=3.7\$/tcement. This is estimated assuming a cost of electricity of 0.05\$/kWh and 150 kWh of electricity consumption to compress 1 ton of CO₂ [1, 17].

The specific emissions of the plant with the capture installation are 0.361 tCO₂/tcement and of the reference plant are 0.777 tCO₂/tcement (Figure 1). Substituting these figures into Equation 1 gives an avoided cost of 19.0 \$/t CO₂ avoided, which is a highly competitive estimation compared to the capture costs for power plants [12, 17, 18, 20]. Furthermore, there is the possibility of achieving even lower avoidance costs, considering the conservative assumption adopted for the ΔTCR when ignoring the saving of the precalciner that the new system can substitute.

The main reason why the avoided cost is so low is in the denominator of Equation 1. Specific emissions of cement plants per MJ of heat used in the cement production process are about 2.5 times higher than the specific emissions of CO₂ in the production of electricity. The precalciner which produces pure CO₂ proposed in this work requires only combustion heat to operate. With relatively robust new pieces of equipment, it is possible to capture up to 58% of the CO₂ released in the plant and avoid 54% of the CO₂ emitted in the original cement plant. Although the total energy requirements in the system are high, the additional energy requirements with respect to the reference plant are modest because heat leaves the system in mass streams at high temperature so that they should be suitable for integration in the cement plant.

ACKNOWLEDGEMENT

N. Rodriguez acknowledges a predoctoral research grant from FICYT.

REFERENCES

- [1] Metz B., Davidson O., Bosch P., Dave R., Meyer L., Intergovernmental Panel on Climate Change, Fourth Assessment Report, Climate Change 2007. Mitigation. Chapter 7, 2007, Cambridge Univ. Press.
- [2] Gartner E, Industrially interesting approaches to “low-CO₂” cements. *Cem. Concr. Res.*, 2004, 34, 1489-1498.
- [3] Hendriks C. A., Worrell E., Price L., Martin N., Ozawa Meida L. The reduction of greenhouse gas emission from the cement industry. IEA Greenhouse Gas R&D Programme, 1999.
- [4] Szabó L., Hidalgo I., Ciscar J.C., Soria A., Russ P., Energy consumption and CO₂ emissions from the world cement industry. Institute for Prospective Technological Studies, European Commission, 2003.
- [5] CEMBUREAU, Best available techniques for the cement industry. A contribution from the European Cement Industry to the exchange of information and preparation of IPPC BAT REFERENCE. Document for the cement industry, 1999. Available at www.cembureau.be.
- [6] T Shimizu, T Hiram, H Hosoda, K Kitani, M Inagaki, K Tejima, A twin fluid-bed reactor for removal of CO₂ from combustion processes. *Trans I Chem E*, 1999, 77, Part A, 62-68.
- [7] Abanades J.C., Anthony E.J., Wang J., Oakey J.E., Fluidized bed combustion systems integrating CO₂ capture with CaO. *Environ. Sci. Technol.*, 2005, 39, 2861-2866.
- [8] Collet, A.G.. Prospects for hydrogen from coal. IEA Clean Coal Centre, CCC/78, (2003).
- [9] Weimer T., Berger R., Hawthorne C., Abanades J.C., Lime enhanced gasification of solid fuels: Examination of a process for simultaneous hydrogen production and CO₂ capture. *Fuel*, 2008, (in press, doi:10.1016/j).
- [10] Abanades J.C., Grasa G., Alonso M., Rodríguez N., Anthony E.J., Romeo L.M., Cost structure of a postcombustion CO₂ capture system using CaO. *Environ. Sci. Technol.*, 2007, 41, 5523-5527.
- [11] Hisao H., Kenji S., patent application JP57067013, 1982.

- [12] Metz, B.; Davidson, O.; de Coninck, H.; Loos, M.; Meyer, L. (Eds.). Special Report on Carbon Dioxide Capture and Storage, Intergovernmental Panel on Climate Change; Cambridge Univ. Press, 2005.
- [13] Reh L., New and efficient high-temperature processes with circulating fluid bed reactors. *Chem. Eng. Technol.*, 1995, 18, 75-89.
- [15] Johansson A., Johnsson F., Leckner B., Solids back-mixing in CFB boilers. *Chem. Eng. Sci.*, 2007, 62, 561-573.
- [16] Anthony E.J., Becker H.A., Code R.W., McCleave R.W., Stephenson J.R., Bubbling fluidized bed combustion of syncrude coke. Proceeding of the 1987 International Conference on Fluidized Bed Combustion, Vol I, Boston, May 3-7, 1987.
- [17] Nsakala ya N., Liljedahl G. N., Turek D. G., Greenhouse gas emissions control by oxygen firing in circulating fluidized bed boilers-phase II. Final technical progress report. NO. PPL-04-CT-25. Alstom Power Inc., 2004.
- [18] National Energy Technology Laboratory (NETL). The [Cost and Performance Baseline for Fossil Energy Power Plants study, Volume 1: Bituminous Coal and Natural Gas to Electricity](#), DOE/NETL-2007/1281, 2007.
- [19] Worrell E, Energy Efficiency Improvement Opportunities for the Cement Industry. *Lawrence Berkeley National Laboratory*. Paper LBNL-72E, 2008. Available at: <http://repositories.cdlib.org/lbnl/LBNL-72E>
- [20] Rubin E. S., Yeh S., Antes M., Berkenpas M., Davison J., Use of experience curves to estimate the future cost of power plants with CO₂ capture. *Int. J. Greenhouse Gas Control* 1, 2007, 188-197.

3.4.3 *Publicación III*

**COST STRUCTURE OF A POSTCOMBUSTION
CO₂ CAPTURE SYSTEM USING CaO**

Publicado en:
Environmental Science & Technology
Volumen 41
Año 2007

THE COST STRUCTURE OF A POSTCOMBUSTION CO₂ CAPTURE SYSTEM USING CaO

J. Carlos Abanades¹, G. Grasa², M. Alonso¹, N. Rodríguez¹, E. J. Anthony³, L. M. Romeo⁴

¹ *Instituto Nacional del Carbón, CSIC, Oviedo 33011, Spain*

² *Instituto de Carboquímica, CSIC, Zaragoza 50015, Spain*

³ *CANMET Energy Technology Centre, Ottawa K1A 1M1, Canada*

⁴ *CIRCE, Universidad de Zaragoza, CPS, Zaragoza 50015, Spain*

ABSTRACT

This paper presents the basic economics of an emerging concept for CO₂ capture from flue gases in power plants. The complete system includes three key cost components: a full combustion power plant, a second power plant working as an oxyfired fluidized bed calciner and a fluidized bed carbonator interconnected with the calciner and capturing CO₂ from the combustion power plant. The simplicity in the economic analysis is possible because the key cost data for the two major first components is well established in the open literature. It is shown that there is clear scope for a breakthrough in capture cost to around 15 \$/t of CO₂ avoided with this system. This is mainly because the capture system is generating additional power (from the additional coal fed to the calciner) and because the avoided CO₂ comes from the capture of the CO₂ generated by the coal fed to the calciner and the CO₂ captured (as CaCO₃) from the flue gases of the existing power plant, that is also released in the calciner.

KEY WORDS: CO₂ capture cost, carbonation, calcination, regenerable sorbent

INTRODUCTION

CO₂ capture from power plants and permanent storage in suitable geological formations can become a major mitigation option for climate change [1]. Most of the key elements in the capture, transport and storage chain are already available and demonstrated at large scale. Capture cost can, therefore, be

estimated with reasonable confidence for options really based on “existing technologies” [1]. However, it is widely recognized that there is scope for large reductions in capture cost, and there is a wide variety of R&D efforts around the world to test new concepts to separate CO₂ (or O₂ or H₂). One or more of these large-scale gas separation processes is always at the core of any CO₂ capture system [1].

To get a fair comparison among emerging technologies for CO₂ capture, it is always interesting to analyze the cost structure in these emerging concepts, identifying the critical points for cost reduction and also the dangers for cost escalation. New CO₂ capture technologies have well-defined benchmarks on efficiency and cost, that are established by the “existing technologies” to capture CO₂ [1]. Preliminary cost analysis of emerging CO₂ capture options can help to identify promising paths for development and conclude that some process routes may not have a chance to be competitive against well-established capture options [2] and should be excluded from further support for research and development.

Among the new concepts for CO₂ capture, it is also important to distinguish between two categories. The first refers to totally new concepts, with no analogous reactors at sufficiently large scale in operation today. These technologies require a full scaling up from basic principles tested at laboratory test. The second category refers to new concepts that rely on the use of new functional materials in reactors commercially established at large scale (*e.g.*, a new solvent for absorption columns or a new solid sorbent or gas carrier in a circulating fluidized bed system). Developers of new technologies tend to report cost estimates overly optimistically [1] and always with uncertainty. But it can be argued that the uncertainties are much lower for the second category of new processes. The process discussed in this work falls into this second category.

The CO₂ capture process discussed below was originally proposed by Shimizu *et al.* [3], and uses CaO as a regenerable sorbent to capture CO₂ from combustion flue gases. Other processes using CaO in combustion systems have been proposed [4] but these fall into the first category described above (they require new reactor configurations) and will not be further discussed here. A schematic of the system proposed by Shimizu *et al.* [3] is presented in Fig. 1. CO₂ is captured from the combustion flue gas of an existing power plant in a circulating fluidized bed carbonator operating between 650-700°C. The solids leaving the carbonator (with a certain conversion of CaO to CaCO₃) are directed to a second fluidized bed where calcination/regeneration takes place. Coal burns in the calciner in an atmosphere of O₂/CO₂ at temperatures over 900°C to produce the heat necessary to calcine the CaCO₃ back to CaO and CO₂. This second fluidized bed calciner operates with oxygen supplied by an air separation unit, that consumes power. The CO₂ captured from the flue gases as CaCO₃, and the CO₂ resulting from the oxy-fired combustion of coal in the calciner, is recovered in concentrated form in the calciner gas, suitable for final purification and compression (typically >100 bar), for transport and safe storage in a suitable deep geological formation. The compression step marks the boundary of the capture system for cost estimates [1]. The calciner requires a relevant fraction (40-50%) of the total energy entering the system in order to heat up to the calciner temperatures the incoming gas and solid streams and in order to provide the heat that drives the endothermic calcination of CaCO₃. But this energy leaves the system in mass streams at high temperature (at T>900°C) or is recovered as carbonation heat in the carbonator (at around 650°C). Therefore, the large energy input to the calciner comes out of the system as high quality heat, available for a high-efficiency steam cycle [3, 5,7]. This is a distinctive characteristic of this capture system, with respect to any other postcombustion CO₂ capture system: it is possible to generate additional power (fraction (1-f_p) in Fig. 1) from the various high-temperature sources in the capture system. The calciner is in fact a new oxyfired fluidized bed power plant (dotted boundary in Figure 1).

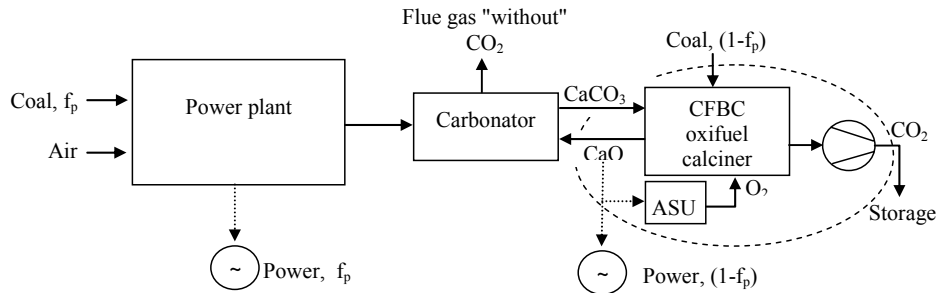


Figure 1. Scheme of power plant incorporating capture of CO₂ with a carbonation loop.

Variants of this carbonation-calcination system are planned to be tested at small pilot scale (10s of kW) in ongoing projects in France, UK, US, Germany, Canada and Spain. We have already demonstrated [5] that capturing CO₂ from flue gases with CaO at atmospheric pressure in a batch fluidized bed of CaO can be done with reasonable gas residence times and bed inventories when compared with those in existing large-scale fluidized bed systems. It has also been shown [4] that the potential for high efficiencies exists for a range of these combustion systems. The purpose of this communication is to justify, with a simple and transparent economic analysis, why to expect a very large reduction in CO₂ capture costs when using these CaO loops in post-combustion applications. Lowering the capture cost is the primary driving force to justify the development of a new capture system.

METHODS AND RESULTS

The cost of CO₂ capture can be estimated in different forms, but the most common are incremental cost of electricity (\$/kWh) and the cost of avoiding CO₂ (\$/t CO₂ avoided).

$$\Delta COE = COE_{capture} - COE_{ref} \tag{1}$$

$$AC = \frac{COE_{capture} - COE_{ref}}{CO_2 kWh_{ref}^{-1} - CO_2 kWh_{capture}^{-1}} \tag{2}$$

The first equation is self-explanatory when referred to a unit of product (\$/kWh) in both the reference plant and the capture plant. This means that the additional energy requirements for the capture step must be incorporated in the estimation of COE_{capture}, not only as the extra cost of fuel, but as an increase in capital cost to be able to deliver the same amount of electricity product (kWh). The avoided costs (AC) are derived from equation (2) when the emission factor (tonnes of CO₂ emitted per kWh of electricity produced in the plants) is known. For a more detailed explanation of these and other measures of capture cost, the reader can consult reference [1].

These cost equations require definition of the reference system without capture. The reference system for the purpose of this work will be a power plant using state-of-the-art components similar to those used in the capture system. For simplicity, and because most measures of capture cost in the literature are referred to 1 kWh of electricity, this is the assumed total power output for the system discussed in this work and for the reference plant. The system of reference for this work could also be an existing power plant with sufficient remaining life span, but to simplify the analysis it is assumed that the reference is a newly built pulverized coal or large-scale circulating fluidized bed (CFB) power plant. For any of these combustion systems, reliable capital cost estimates exist (see for example section 3.7 in reference [1] for a comprehensive review of these costs). Also, a set of financial factors (fuel costs, interest rates, *etc.*) and other technical (operating and maintenance costs) and non-technical factors (capacity factor) have to be defined to estimate COE with a simple equation such as:

$$\text{COE} = \text{Fixed Costs} + \text{Variable Costs} + \text{Fuel Costs} = \frac{\text{TCR} * \text{FCF} + \text{FOM}}{\text{CF} * 8760} + \text{VOM} + \frac{\text{FC}}{\eta} \quad (3)$$

The top section of Table 1 summarizes the parameters chosen for the reference system, largely based on data from reference [1]. To introduce flexibility in the assumptions and allow a quick visualization of their impact on cost figures, three cases have been defined in Table 1 for both the reference plant and the

capture system: optimistic set, best estimate and pessimistic set of cost parameters.

Table 1. Summary of assumptions and cost results. Marked in bold are the input data. All remaining cells can be calculated from equations (1-5)

EXISTING POWER PLANT	Units	Optimistic set	Best estimate	Pessimistic set
Fuel Cost, FC	US\$ GJ ⁻¹	1	1.5	2
Fuel Cost, FC	US\$ kWh ⁻¹	0.0036	0.0054	0.0072
Capital Cost, TCR	US\$ kWe ₁ ⁻¹	1100	1300	1500
Net efficiency, η_{ref}	kWhe kWh ⁻¹	0.45	0.43	0.40
Fixed fraction cost, FOM	-	0.04	0.04	0.04
Capacity factor, CF	-	0.95	0.80	0.65
Fixed charge	yr ⁻¹	0.075	0.100	0.150

factor, FCF				
Variable cost, VOM	US\$ kWh ⁻¹	0.007	0.007	0.007
Emission factor, CO₂kWh	kgCO ₂ kWh ⁻¹	760	795	855
Cost of electricity, COE	US\$ kWh ⁻¹	0.025	0.039	0.066
OXIFUEL CFBC	Units	Optimistic set	Reasonable set	Pessimistic set
Capture efficiency, E_{oxi}	-	0.95	0.95	0.9
Capital cost, TCR_{oxi}	US\$ kWh ⁻¹	2100	2200	2400
Penalty compression	-	0.04	0.05	0.05
Penalty	-	0.06	0.06	0.07

ASU				
Penalty total	-	0.1	0.11	0.12
Net efficiency, η_{oxifuel}	-	0.35	0.32	0.28
Emission factor, CO₂kWh	kgCO ₂ kWh ⁻¹	48.9	53.4	122.1
Cost of electricity, COE	US\$ kWh ⁻¹	0.037	0.057	0.097
Avoided cost, AC	US\$ tCO ₂ ⁻¹	16.4	23.8	44.2
CARBONAT OR WITH OXIFUEL	Units	Optimi stic set	Reaso nable set	Pessim istic set
Carbonato r efficiency, E_{carb}	-	0.9	0.8	0.7

Overall capture efficiency, E	-	0.915	0.86	0.80
Carbonator cost fraction, δ_{carb}	-	0.10	0.20	0.30
Capital cost, $TCR_{capture}$	US\$ kW ^{e-1}	1566	1816	2175
Conventional power fraction, fp	-	0.6	0.6	0.5
Penalty compression	-	0.04	0.05	0.05
Net efficiency, $\eta_{capture}$	-	0.386	0.356	0.315
Emission factor, CO₂kWh	kgCO ₂ kWh ⁻¹	70.9	134.5	217.1

Cost of electricity, COE	US\$ kWh⁻¹	0.031	0.049	0.089
Avoided cost, AC	US\$ tCO₂⁻¹	8.3	15.5	36.6

Once the reference plant is defined, a capture system of Fig. 1 can also be defined and referred to the production of 1kWhe of electricity. The system of Fig. 1 has three major components, and the same energy output as the reference system (1 kWhe adopted as reference). These include:

1. An existing power plant delivering a major fraction of the total power output, f_p . This should be the largest single component of the total system. The unit cost of producing power in this system is assumed identical to the reference system. This means that it is implicitly assumed that the scale of the existing power plant and the capture system are sufficiently large to be able to benefit from the same economies of scale that apply to the reference system defined in the upper part of Table 1. Therefore, all the economic factors (in particular the normalized capital cost) adopted for the reference case in Table 1 are still valid for the power plant of Fig. 1 delivering f_p kWhe of electricity. Standard equipment for flue gas clean-up in modern power plants is assumed to be included in this component as is the case in the reference system. This is a conservative assumption, as potential synergies (*i.e.*, cost savings) from integrating these components with the capture system (in particular referring to SO₂ and fly ash removal in the CaO loop) are ignored at this stage.

2. A circulating fluidized bed calciner operating as a circulating fluidized bed combustor burning coal in an atmosphere of O₂/CO₂. The oxygen comes from an air separation unit dimensioned to burn only the coal fed to the calciner. The heat requirement for the calciner determines the fraction of coal that is burned

in this unit respect to the total. This heat is used to drive the endothermic calcination reaction of CaCO₃ and raise all streams flowing to the calciner to the calcination temperature. The high enthalpy of the calcination reaction and the modest conversion of CaO to CaCO₃ that is expected in the carbonator, due to modest sorbent performance [3, 4], tend to increase the heat requirements in the calciner. As discussed in more detailed process simulation work [3-6], f_p should move between 0.5 and 0.6. This is a critical variable for cost estimates as will be shown below. As f_p becomes low, it is increasingly difficult to pursue a system as outlined in Fig. 1, because the same power output could be obtained with a stand-alone oxy-fired CFBC without the added cost of the carbonator described below. However, the fact that a large fraction of the power output in Fig. 1 comes from the existing (cheaper) power plant, is a critical factor in understanding the low cost figures that appear below. On the other hand, oxy-fired CFBC systems are being pursued by some major manufacturers of CFBC equipment [8], and although economic data are scarce, the data adopted in Table 1 are reasonably consistent (slightly more expensive than the expected cost for similar oxy-fired PF boilers) [1]. These figures include all the components required in the oxy fired power plant (CFB boiler, power island, air separation unit, CO₂ compression, *etc.*).

3. A circulating fluidized bed carbonator. This is a large reactor located between the two subsystems described above. It must be dimensioned to treat the combustion flue gases from the power plant, transform part of the CaO into CaCO₃ and deliver this solid stream to the calciner after separation from the flue gas in cyclones. It can be considered mechanically similar to existing CFB combustion chambers. This reactor is expected to operate at 600-700°C at velocities and solid circulation rates typical of CFBCs (see [3, 4, 5]). Since any equipment for heat recovery from the flue gases or solids in this system, and any gas purification equipment, have been implicitly accounted for in the existing power plant or in the oxy-fired calciner, the cost of this piece of equipment can be considered as a small fraction of the capital cost of the power plant described before.

Finally, any other equipment and components making up the capital cost of the full system can be related to the above main components. In particular, the CO₂ purification and conditioning equipment will include a compressor dimensioned to bring to supercritical conditions all the CO₂ flow leaving the calciner (that is the sum of the CO₂ released from the CaCO₃ formed in the carbonator and the CO₂ formed in the oxy-combustion of coal in the calciner plus a small fraction coming from the calcination of the CaCO₃ make up flow). Also, to estimate the cost of electricity, the maintenance costs (fixed and variable) must be defined. For simplicity and in the absence of more detailed information, the fixed costs have been assumed to be 4% of the capital cost, and the variable operating and maintenance costs (other than the fuel cost) have been assumed to be \$0.007/kWh, identical for all cases. As we can see for the reference set of assumptions in Table 1, the cost of electricity is ~\$0.039/kWh for the reference case, and reaches \$0.057/kWh when moving from the reference case to a capture system using oxy-fired circulating fluidized bed combustion. In both reference cases, there is a state-of-the-art steam cycle, delivering 43% LHV efficiency in the case without capture and 32% LHV efficiency in the oxy-fired case (~5% of the net efficiency drop comes from the compression of CO₂ to supercritical conditions and the CO₂ purification, while the other 6% net is due to the air separation unit). The COEs of both the reference case without capture and the case with oxy-fuel combustion are consistent with data collected in [1] and more specifically for CFBC oxy-fired systems in [8]. Capturing CO₂ under these conditions would generate costs between \$16-44/tonne CO₂ avoided, depending on the financial assumptions used in the two extreme (optimistic and pessimistic) cases in Table 1.

In order to estimate the COE of the capture system of Fig. 1 from the previous cost figures, we need to estimate the power generation efficiency of the new system, proportional to the share of the two major pieces of equipment in the generation of 1 kWh of electricity. We then discount the compression and purification penalty (assumed to be ~5 points of net efficiency) for the CO₂

captured in the carbonator (the penalty for compression of the CO₂ from the coal in the calciner is already included in the efficiency value of the oxy-fuel system). An additional point net efficiency penalty is added to account for purification. The result is:

$$\eta_{\text{capture}} = \eta_{\text{reference}} f_p + \eta_{\text{oxyfuel}}(1-f_p) - 0.05 f_p \quad (4)$$

With this equation, an intermediate efficiency is obtained for the proposed system, always higher than the efficiency of the equivalent oxy-fired boiler (that would be represented here with $f_p = 0$) and lower than the reference plant without capture (that would be represented here with $f_p = 1$). Efficiency penalties associated with the makeup flow of sorbent required to maintain a given activity in the capture loop [5] are not considered here, as it is argued that an equivalent energy credit would be obtained from a cement plant using deactivated CaO instead of CaCO₃ as cement feedstock [4].

In order to calculate the total capital requirement (TCR) of the new system (per kWh, in sufficiently large-scale systems), we use:

$$\text{TCR}_{\text{capture}} = \text{TCR}_{\text{reference}} f_p (1 + \delta_{\text{carb}}) + \text{TCR}_{\text{oxyfuel}} (1 - f_p) \quad (5)$$

This is a simple function of the TCR of the two main individual components (the power plant of reference and the oxy-fired CFBC power plant used as calciner), adding the carbonator cost (and the extra compression for the CO₂ from f_p) as an incremental fraction, δ_{carb} , of the TCR of the reference plant. This method to calculate the contribution of the carbonator to the TCR of the capture plant is only reasonable for central values of f_p (see Figure 2). If we maintain all the remaining “non technical” parameters of the cost equation (3) as indicated in Table 1, we obtain COEs for the new system that are again somewhere between the extremes for the reference plant and the reference oxy-fired system without carbonation. The avoided costs are calculated from the new emission factor of each system (see Table 1) and yield a central figure of \$15.5/tonne CO₂ avoided for the reference case and values below \$10/tonne CO₂ avoided for the optimistic case (see Table 1). Figure 2 represents the sensitivity of the cost of

electricity in the new capture system depending on the carbonator extra cost parameter and the fraction of total power generated in the power plant of reference.

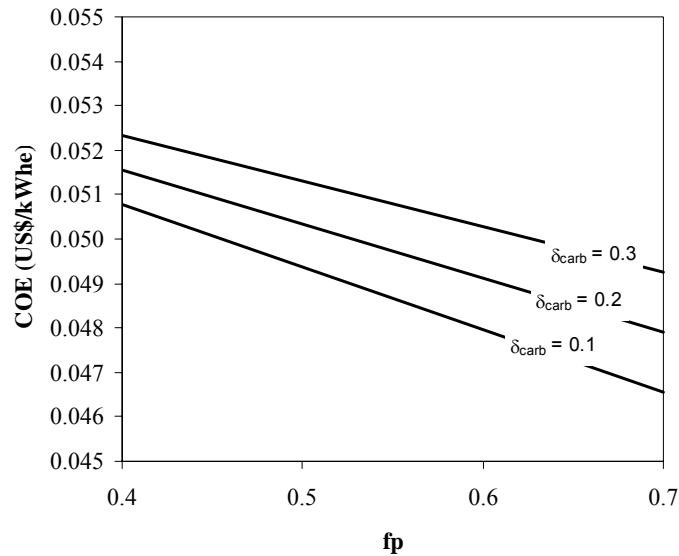


Figure 2. Sensitivity of COE to the fraction of total power output coming from the conventional plant for different carbonator capital cost.

DISCUSSION

The reduction in capture cost for the new system with respect to the oxy-fired reference case ($f_p = 0$) arises from the assumption that additional (new) power can be extracted from the capture components. Since the separation of CO₂ is carried out at the very high temperatures, all the energy fed to the calciner in the coal feed exits the system in high temperature streams, which are easy to recover (this includes the endothermic heat for calcination, that is recovered as carbonation heat in the carbonator at about 650°C). This makes the investment per kWh much lower than for an equivalent stand-alone oxy-fired system. Another way to look at this critical point (not detailed here because it yields similar quantitative results) is to take an oxy-fired CFBC system as the reference in the analysis and think of the carbonator as an interface between this oxy-fired capture system and an existing power plant. The inclusion of a

large fluidized bed carbonator in the system boundary of the oxy-fired system will increase (modestly) the capital cost and the COE from this system. But now, the oxy-fired CFBC is not only avoiding the CO₂ from its own coal combustion feed, but all the CO₂ coming from the flue gases of the neighbouring power plant, that has been captured as CaCO₃ in the carbonator. In other words, since the oxy-fired CFBC system is capturing about two times more CO₂ than it generates from the combustion of its own coal feed, the avoided CO₂ is higher thanks to the relatively low extra cost of the carbonator unit. This leads to very low avoided costs of capture respect to the stand alone oxyfired power plant.

The previous analysis is highly encouraging for the development of these carbonation-calcination systems. We are aware that the key point for the immediate future is to demonstrate the technical viability of the system operating at pilot scale in continuous mode. However, as indicated in the introduction, some key results have been completed already [5], and a large body of knowledge exists in the literature on fluidized bed technologies using limestone-derived solids for other purposes. We are, therefore, optimistic about the next steps and about the speed at which results can be escalated, since the key components are mechanically similar to existing large scale circulating fluidized bed combustors.

ACKNOWLEDGEMENTS

This work is partially funded by the European Commission (C3-Capture) and the Spanish Ministry of Education ("Juan de la Cierva" programme).

NOTATION

COE	levelized cost of electricity (US\$/kWh)
AC	cost of CO ₂ avoided by using a CO ₂ capture system with respect to a similar system without capture (equation 2)
CO ₂ kWh ⁻¹	CO ₂ emission factor of the system (kg CO ₂ emitted/kWh)
TCR	total capital requirement to build the power plant (US\$/kW)
FCF	fixed charge factor (fraction)

FOM	fixed operating costs (US\$/yr/kWh)
CF	capacity factor (fraction) and in a 8760 hours typical year
VOM	variable operating costs (US\$/kWh)
FC	unit fuel cost (US\$/kWh)
η	net plant efficiency (kWh _e / kWh)
f_p	fraction of power generated in the main power plant (assumed equal to the fraction of coal burned in the main power plant)
δ_{carb}	incremental carbonator cost (fraction)

REFERENCES

1. Metz, B.; Davidson, O.; de Coninck, H.; Loos, M.; Meyer, L. (Eds.). *Special Report on Carbon Dioxide Capture and Storage, Intergovernmental Panel on Climate Change*; Cambridge Univ. Press, 2005.
2. Thomas, D.C. (Editor). *Carbon Dioxide Capture for Storage in Deep Geological Formations-Results from the CO₂ Capture Project*; Elsevier, 2005.
3. Shimizu, T.; Hiramata, T.; Hosoda, H.; Kitani, K.; Inagaki, M.; Tejima, K. A twin fluid-bed reactor for removal of CO₂ from combustion processes. *Trans. IChemE* 1999, 77 (Part A), 62.
4. Abanades, J. C.; Anthony, E. J.; Wang, J.; Oakey, J. E. Fluidized Bed Combustion Systems Integrating CO₂ Capture with CaO. *Environ. Sci. Tech.* 2005, 39(8), 2861.
5. Abanades, J. C.; Anthony, E. J.; Alvarez, D.; Lu, D. Y.; Salvador, C. Capture of CO₂ from Combustion Gases in a Fluidized Bed of CaO. *AIChE Journal* 2004, 50(7), 1614-1622.
6. MacKenzie, A.; Granatstein, D. L.; Anthony, E. J.; Abanades, J. C. Economics of CO₂ Capture using the Calcium Cycle with a Pressurized Fluidized Bed Combustor. *Energy & Fuels* 2007, 21(2), 920-926
7. Romeo, L. M.; Abanades, J. C.; Ballesteros, J. C.; Valero, A.; Escosa, J. M.; Giménez, A.; Cortés, C.; Paño, J. Process Optimization in Postcombustion CO₂-Capture by means of Repowering and Reversible Carbonation/Calcination Cycle; 8th *International Congress on Greenhouse Gas Control Technologies-GHGT-8*, Trondheim, Norway, June 2006.

8. Nsakala, N.; Liljedahl, G.; Marion, J.; Bozzuto, C.; Andrus, H.; Chamberland, R. Greenhouse gas emissions control by oxygen firing in circulating fluidized bed boilers. *Second Annual National Conference on Carbon Sequestration*. Alexandria, VA, USA, May 5-8, 2003.

4 Experimental

Durante el tiempo de realización de esta Tesis en el INCAR-CSIC se diseñó y construyó una planta piloto de reactores de lecho fluidizado circulantes e interconectados para la realización de experimentos de captura de CO₂ con CaO. El diseño de la planta experimental se realizó con el objeto de demostrar a escala de prototipo de laboratorio la viabilidad de los distintos procesos de carbonatación-calcinación que se han descrito en el Capítulo 1. Se consideró objetivo prioritario de investigación para esta Tesis, el estudio del carbonatador como absorbedor de CO₂ de gases de postcombustión. Los experimentos realizados en la planta piloto tienen como objeto demostrar que la reacción de carbonatación tiene lugar de manera continua cuando un flujo de CaO, circulando entre el carbonatador y el calcinador, se pone en contacto con una mezcla sintética de gases que contienen CO₂. Así, el calcinador se considera un elemento secundario en esta etapa experimental, y en esta fase inicial de la investigación, la energía requerida para el proceso de calcinación será suministrada mediante la combustión de carbón con aire y/o a través de hornos eléctricos.

Como parte del contenido de esta Tesis se presenta la *Publicación IV* que se adjunta en la sección 4.3. Esta publicación resume los fundamentos del proceso de captura de CO₂ de gases de combustión con CaO y recoge las principales dificultades encontradas en la operación del sistema experimental. Además, se detallan algunos ejemplos de los resultados experimentales obtenidos.

4.1 Descripción de la Planta Piloto de Lechos Fluidizados Circulantes Interconectados

En la Figura 4.1 se muestra una fotografía de la instalación utilizada para la realización de los experimentos en estado estacionario de captura de CO₂ con CaO. Es una planta piloto compuesta por dos reactores de lecho fluidizado circulante, uno es el carbonatador y el otro el calcinador. Los reactores se encuentran interconectados de modo que la corriente de sólidos que abandona el reactor de calcinación se dirige al reactor de carbonatación a través de una tubería de reciclo, y los sólidos que abandonan el carbonatador se reciclan hacia el calcinador del mismo modo.

La planta piloto de 30 kW térmicos (se considera que el carbonatador está diseñado para tratar gases de combustión generados al quemar 30 kW de carbón) tiene una altura de 6,5 m. El sistema de reactores de carbonatación y calcinación está formado por dos *risers* de acero inoxidable refractario (AISI30) de 0,1 m de diámetro interior. Las tuberías de reciclo de sólidos conducen los sólidos de un reactor a otro gracias a las válvulas no mecánicas de tipo *loop-seal*. Su tamaño es de 200x100x400 mm, y funcionan fluidizando los sólidos con aire de modo que los descargan a través de una tubería hacia el reactor (ver Figura 4.2).

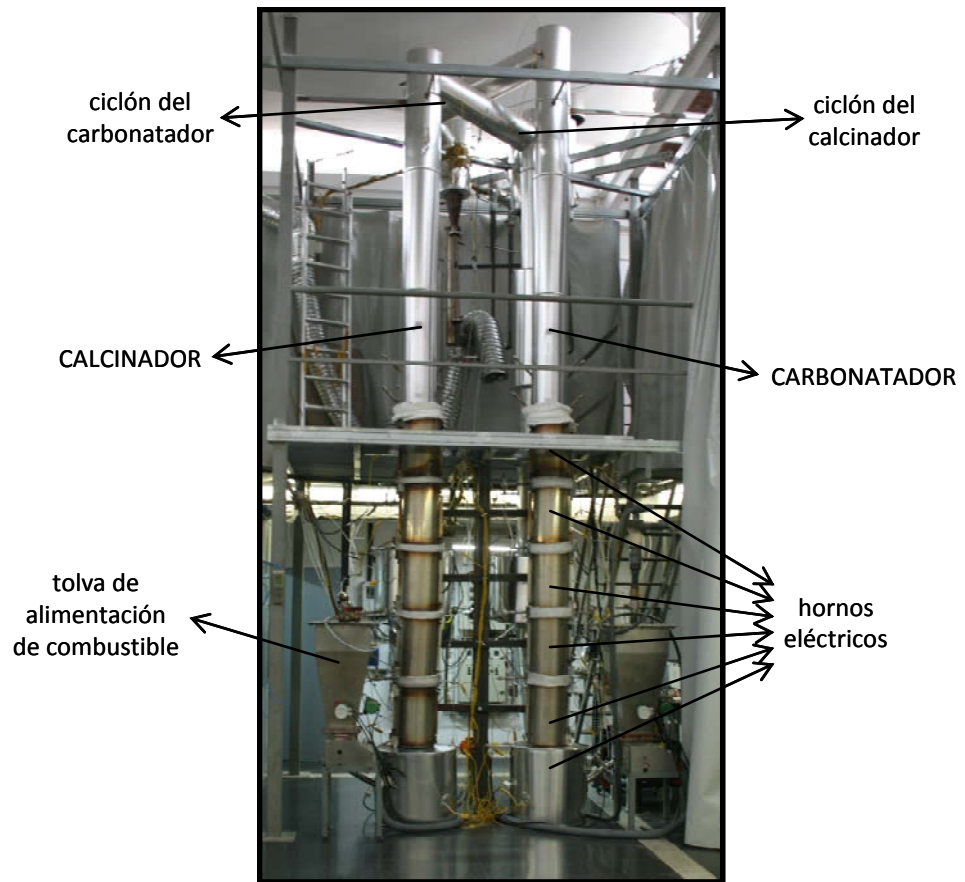


Figura 4.1. Fotografía de la planta piloto experimental de 30 kW instalada en el INCAR-CSIC.

La instalación dispone de seis hornos eléctricos en cada *riser*, además de un horno eléctrico en cada *loop-seal*. El calentamiento de las cámaras de reacción hasta el entorno de los 500°C se hace con ayuda de los hornos eléctricos. Para llevar la temperatura hasta las condiciones de calcinación (en torno a 800-900°C) se alimenta carbón a ambos reactores una vez que se han alcanzado los 500°C con los hornos.

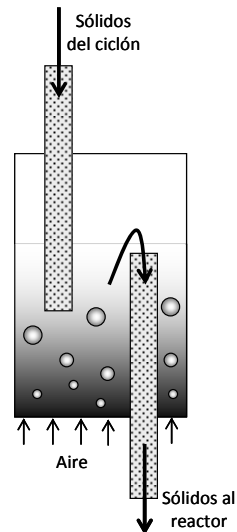


Figura 4.2. Detalle del funcionamiento de la válvula *loop-seal* que se sitúa en las tuberías de reciclo del carbonatador y calcinador.

En la instalación de la Figura 4.1 se dispone de un sistema discontinuo de alimentación de sólidos al sistema mediante el cual se pueden hacer inyecciones de caliza durante el transcurso de un ensayo. La alimentación de sólidos se hace a través de la *loop-seal* del calcinador. El objeto de hacer inyecciones de sólidos durante el experimento es aumentar el inventario y la circulación de sólidos del sistema. De este modo, y para hacer diferentes pruebas, se puede inyectar caliza fresca o parcialmente calcinada en cualquier momento.

En lo que se refiere a instrumentación y control, en la planta piloto se miden de forma continua:

- a) La temperatura en diferentes puntos de la instalación (40 puntos de medida) mediante termopares tipo K.
- b) La presión diferencial (40 puntos de medida) mediante transductores de presión.

- c) La concentración de O_2 en el lecho (tres sondas de zirconio en el reactor de carbonatación y una en el calcinador).
- d) Los caudales de aire y CO_2 a suministrar a los diferentes equipos y dispositivos, mediante cinco medidores controladores de flujo másico.
- e) La composición de los gases en continuo mediante dos analizadores de gases TESTO 360. Los analizadores permiten medir la concentración en continuo de gases: O_2 , CO y CO_2 . En la instalación se pueden tomar medidas de concentración de gases en cinco puntos diferentes: a la entrada del carbonatador, a la salida del carbonatador (antes y después del ciclón secundario) y a la salida del calcinador (antes y después del ciclón secundario).

Todos los datos medidos de forma continua quedan registrados en un sistema de adquisición de datos a través de un multímetro conectado a un ordenador.

Además, el sistema dispone de varios puntos de extracción de muestras sólidas. Es posible extraer muestras sólidas del carbonatador, del calcinador y de la tubería que recicla los sólidos desde la *loop-seal* al carbonatador. Las muestras sólidas obtenidas de los experimentos en la planta son analizadas en una termobalanza CSI Instruments, especialmente diseñada en el CSIC, con un sistema de dos hornos a distinta temperatura para estudiar el comportamiento del sorbente en este proceso (González et al. 2008).

Aunque todos los experimentos realizados en estado estacionario se realizaron en la planta piloto descrita en los párrafos anteriores, los primeros experimentos no estacionarios se realizaron en una planta piloto de similares características a la descrita pero con *risers* de menor altura (3,2 m). Los primeros ensayos realizados fueron de carácter muy dinámico y de menor calidad que los obtenidos en la instalación de la Figura 4.1. Estos experimentos fueron de gran utilidad para poner a punto y rediseñar el nuevo equipo de 6,5 m de altura, y fueron reportados en algunos de los informes realizados por el INCAR-CSIC para el módulo 3 del proyecto CENITCO2 y el contrato HUNOSA-

CSIC 23/02/07 (CENITCO2 diciembre 2007; HUNOSA-CSIC diciembre 2007; HUNOSA-CSIC diciembre 2008; CENITCO2 junio 2008; CENITCO2 mayo 2007), pero no se detallan en este trabajo.

4.2 *Metodología Experimental*

Se resume a continuación el protocolo experimental que es necesario desarrollar cada vez que se hace un ensayo de captura de CO₂ mediante ciclos de carbonatación-calcinación en la instalación descrita en el apartado anterior.

Se carga el sistema de sólidos, normalmente alrededor de 20 kg de caliza fresca o unos 15 kg de caliza calcinada de experimentos previos. Se encienden los hornos de la instalación y se empieza el calentamiento progresivo del equipo. Cuando la temperatura ronda aproximadamente los 400°C se comienza a introducir un caudal de aire que permite la circulación de los sólidos entre los reactores. Se aprovecha el tiempo de calentamiento de los reactores para hacer el calibrado del analizador de gases con botellas de gas patrón. Lo que se busca en las primeras horas del experimento es calcinar al máximo la carga de caliza fresca (o de sólidos parcialmente carbonatados de un experimento anterior) para tener cantidad abundante de óxido de calcio activo para hacer las pruebas de carbonatación. Por ello, en la mayoría de los experimentos realizados, una vez que la temperatura supera los 500°C a la salida de los *risers*, se comienza a alimentar carbón a ambos reactores para facilitar la calcinación. De este modo, se alcanzan rápidamente temperaturas cercanas a los 850°C, que garantizan una calcinación de la carga inicial de caliza fresca en pocas horas (aproximadamente 8 horas).

Una vez que se estima que la carga de caliza está suficientemente calcinada (se comprueba mediante la extracción ocasional de muestras sólidas), se extrae una muestra sólida del sistema para hacerle un posterior análisis en la termobalanza y comprobar la proporción de CaO/CaCO₃ de la muestra de

partida y su capacidad de captura de CO₂. A partir de ahí, se deja de alimentar combustible al reactor de carbonatación y se deja disminuir la temperatura, para poner el reactor en condiciones de carbonatación (temperatura alrededor de 650°C). Puesto que la reacción de carbonatación es exotérmica, en principio será necesario disminuir la temperatura del reactor por debajo de 600°C, ya que en el momento que empiece la reacción, la temperatura aumentará. Una vez que las condiciones son las adecuadas se empieza a alimentar CO₂ junto con el aire que entra al carbonatador. Se ajusta el caudal de CO₂ de manera que la concentración del mismo en el interior del carbonatador (teniendo en cuenta el aire que fluidiza las válvulas *loop-seals*) sea la deseada. Mientras, en el reactor de calcinación, se continúa quemando combustible para seguir la calcinación en continuo del carbonato que vaya llegando una vez formado en el carbonatador.

La experimentación en una instalación de estas características requiere la intervención de entre cuatro y cinco personas, que puede reducirse a dos cuando la operación es estable.

La información que se puede obtener durante un ensayo de la instalación experimental con la instrumentación antes detallada es la siguiente:

- Mediante los analizadores de gases se puede seguir la concentración de los gases a la entrada y salida del carbonatador, y a la salida del calcinador. Así, se puede comprobar en todo momento cómo se desarrolla la calcinación y la carbonatación y, en su caso, la combustión en el calcinador.
- Las sondas de zirconia para medir la concentración de oxígeno dentro de los reactores son útiles para contrastar con la señal del analizador y conocer la distribución del aire de las válvulas *loop-seal* en el sistema. La corriente de gas de entrada al carbonatador puede verse diluida por la corriente de aire que fluidiza la válvula *loop-seal* si este gas se dirige desde la *loop-seal* (que recoge los sólidos del ciclón primario del

calcinador) al propio carbonatador. Dependiendo de la fluidodinámica del sistema, este gas de aireación de la *loop-seal* puede también dirigirse hacia el ciclón primario.

- Con las sondas de presión distribuidas por toda la instalación se puede conocer el inventario total de sólidos en el sistema y su distribución en el mismo. En estos ensayos se ha prestado especial atención a las sondas de presión del carbonatador, para conocer el inventario de sólidos en el carbonatador.
- Con los termopares distribuidos por toda la instalación se conoce la temperatura en las diferentes partes de la instalación. Durante el transcurso del experimento, el análisis cualitativo de la distribución de temperaturas a lo largo de los *risers* da idea de la circulación de los sólidos en el interior. Se considera que la circulación de sólidos es buena cuando se observa igualdad de temperaturas en los cinco termopares del carbonatador.
- La circulación de sólidos en la instalación también puede ser medida cuantitativamente gracias a la instalación de una tubería con dos válvulas en la tubería de recirculación de los sólidos entre la válvula *loop-seal* y el calcinador. Con este sistema se pueden extraer sólidos circulantes del sistema. Conociendo la masa de sólidos extraída en un tiempo determinado se puede calcular la velocidad de circulación de los sólidos.
- Para obtener información de la fase sólida es necesario extraer muestras del reactor para posteriormente realizarles un tratamiento térmico en una mufla para conocer la proporción de CaO/CaCO_3 . Además, las muestras sólidas se analizan en una termobalanza para conocer la capacidad máxima de conversión a carbonato de las mismas. En la instalación es posible obtener muestras del calcinador y del

carbonatador en todo momento. Al medir la circulación en la tubería de reciclado entre la *loop-seal* y el carbonatador, se extraen sólidos del sistema. Las muestras sólidas de medir circulación también son tratadas posteriormente. Así, se puede conocer la composición de los sólidos antes de entrar al carbonatador.

Un experimento completo suele durar una media de 12 horas y se suelen extraer alrededor de 35 muestras sólidas. El tratamiento, tanto de las muestras sólidas recogidas como de los datos brutos registrados en el sistema de adquisición de datos por ensayo, requieren la intervención de varios de los miembros del grupo de investigación.

4.3 Publicaciones Relacionadas

4.3.1 Publicación IV

**CARBON DIOXIDE CAPTURE FROM
COMBUSTION FLUE GASES WITH A CALCIUM
OXIDE CHEMICAL LOOP. EXPERIMENTAL
RESULTS AND PROCESS DEVELOPMENT**

Publicado en:
International Journal of Greenhouse Gas Control
Volumen 4 (2)
Año 2009

CARBON DIOXIDE CAPTURE FROM COMBUSTION FLUE GASES WITH A CALCIUM OXIDE CHEMICAL LOOP. EXPERIMENTAL RESULTS AND PROCESS DEVELOPMENT

M Alonso^a, N Rodríguez^a, B González^a, G Grasa^b, R Murillo^b, J C
Abanades^a

^a *Instituto Nacional del Carbón, CSIC, Oviedo 33011, Spain*

^b *Instituto de Carboquímica, CSIC, Zaragoza 50015, Spain*

ABSTRACT

Post-combustion carbonate looping processes are based on the capture of carbon dioxide from the flue gases of an existing power plant in a circulating fluidized bed reactor (CFB) of calcium oxide (the carbonator) particles. The calcination of calcium carbonate in a new oxy-fired CFBC power plant regenerates the sorbent (calcium oxide particles) and obtains high purity carbon dioxide. This communication presents experimental results from a small test facility (30 kWt) operated in continuous mode using two interconnected CFB reactors as carbonator and calciner. Capture efficiencies between 70 and 97% have been obtained under realistic flue gas conditions in the carbonator reactor (temperatures around 650°C). The similarity between process conditions and those existing in CFBC power plants should allow a rapid scaling up of this technology. The next steps for this process development are also outlined.

Keywords: CO₂ capture, carbonate looping, carbonation, calcination, pilot testing

INTRODUCTION

Reducing the capture cost and the energy efficiency penalties are the primary driving forces that justify the development of new carbon dioxide capture systems. It is widely recognized that there is scope for large reductions in

capture costs by applying new concepts for separating carbon dioxide in the capture system (Metz 2005). Among the new concepts for carbon dioxide capture, it is important to distinguish between two categories. The first refers to totally new processes, with no analogous reactors of a sufficiently large scale in operation today. These technologies require a full scaling up from basic principles tested only in the laboratory or in the computer. The second category refers to new concepts that rely on the use of new functional materials in reactors already commercially established on a large scale (e.g., a new solvent for absorption columns or a new solid sorbent in a circulating fluidized bed system). The process discussed in this work falls into the second category.

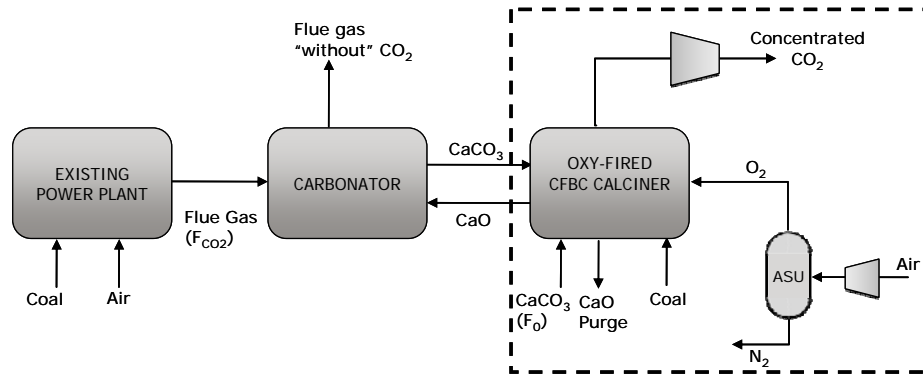


Figure 1. . Schematic of a carbonate looping system to capture CO₂ from an existing power plant, that generates more power when the oxyfired circulating fluidized bed combustor acts as calciner (area inside dotted line).

The carbon dioxide capture process discussed in this paper was originally proposed ten years ago (Shimizu 1999), and uses calcium oxide as a regenerable sorbent to capture carbon dioxide from combustion flue gases. Other regenerable processes using calcium oxide in gasification systems have been proposed as early as the XIX century (Squires 1967). Modern versions are still under development, and others have been proposed for natural gas reforming applications (Harrison 2008), but will not be discussed any further here. The current understanding of the sorbent fundamentals has also been reviewed recently (Anthony 2008; Harrison 2008). It is well known that CaO particles can react sufficiently fast with CO₂ only up to a certain level of conversion, marked by the formation of a product layer (Alvarez 2005) of

CaCO_3 on all free surfaces of CaO (including interior surfaces) . The sintering (loss interior surface) of CaO translates into rapid decay in the CO_2 capture capacity as the number of calcination-carbonation cycles increases (Curran 1967; Barker 1973), and this has been the subject of much concern about the viability of the reversible CO_2 capture process based on CaO (Anthony 2008). A substantial R&D effort is still devoted to better understand and reduce this decay and/or to formulate alternative methods for sorbent pretreatment and reactivation (Anthony 2008). However, it has also been recently established (Grasa 2006) that a residual activity exists (7-8% points of Ca conversion to CaCO_3) that remains stable after many hundred of carbonation calcination cycles, and that could be able to sustain the operation of the capture process if sufficiently large solid circulation rates are allowed between the carbonator and calcination units. This is another reason why circulating fluidized bed technology should be from now the main subject of application of these CaO looping concepts in postcombustion applications.

A schematic of overall CO_2 capture system as proposed by Shimizu et al. (Shimizu 1999) is presented in Fig. 1. Carbon dioxide is captured from the combustion flue gas of an existing power plant in a circulating fluidized bed carbonator operating between 600-700°C. The solids leaving the carbonator (with a certain conversion of calcium oxide to calcium carbonate) are directed to a second fluidized bed where calcination/regeneration takes place. Coal burns in the calciner in an atmosphere of oxygen/carbon-dioxide at temperatures over 900°C to produce the heat necessary to calcine the calcium carbonate back to calcium oxide and carbon dioxide. This second fluidized bed calciner operates with oxygen supplied by an air separation unit. The carbon dioxide captured from the flue gases as calcium carbonate, and the carbon dioxide resulting from the oxy-fired combustion of coal in the calciner, are recovered in concentrated form in the calciner gas and are suitable for final purification and compression. The calciner requires a relevant fraction (40-50%) of the total energy entering the system in order to heat the incoming gas and solids streams up to calciner temperatures and to provide the heat that

drives the endothermic calcination of calcium carbonate (Rodriguez 2008). However, this energy leaves the system in mass streams at high temperature (at $T > 900^\circ\text{C}$) or is recovered as carbonation heat in the carbonator (at around 650°C) in order to drive a high-efficiency steam cycle (Abanades 2004; Harrison 2008; Romeo 2008). This is a distinctive characteristic of this capture system with respect to any other carbon dioxide capture system: it is possible to generate additional power from the various high-temperature sources in the capture system. The calciner is in fact a new oxy-fired fluidized bed power plant (dotted boundary in Figure 1) that repowers the existing plant as well as capturing a large fraction of its carbon dioxide thanks to the carbonate loop. It has been shown (Anthony 2008; Romeo 2008) that the potential for high efficiencies exists in these combustion systems. Furthermore, a simple and transparent economic analysis using published cost data available on the main blocks of the system of Figure 1 (the existing combustion power plant, the new oxyfired power plant acting as calciner and the circulating fluidized bed reactor between them acting as carbonator) shows that there is clear scope for a breakthrough in capture cost to around 70% of the carbon dioxide avoided cost of the equivalent stand alone oxyfired system (Abanades 2007). As mentioned earlier, a serious drawback of the process is that for all these benefits to be realized, it is critical that sorbent cost (fresh limestone make up to maintain the activity of the sorbent in the carbonate loop) be negligible (Abanades 2004). The cost of the sorbent make up could be very high in some locations if the capture system generates a large purge of solids cannot be used. The purge will be made up of a mixture of ash from the fuel used in the calciner, deactivated CaO with a minor fraction of CaSO_4 if sulfur was present in the fuel used in the calciner and/or in the flue gas entering the carbonator. However, this cost should be affordable in many locations where cheap limestone is available (Rodriguez 2008) and/or there is an strong demand for calcium oxide for cement production. Also, it has recently been found (Grasa 2008) that the deactivated material resulting from the carbonation-calcination loop is a very effective sorbent of sulphur dioxide under CFBC conditions. Therefore, the purge of CaO solids from the carbonation loop (that in terms of mass flows is

comparable to the limestone requirements for desulphurization in CFBC boilers burning high sulfur fuels) could be fed to the boiler generating the flue gases (or to the flue gas desulfurization system associated with such a boiler) minimizing in this way the net consumption of limestone respect to the reference system without capture.

The ability of a fluidized bed reactor of CaO operating at 650°C to effectively capture CO₂ at typical concentrations of combustion flue gases at atmospheric pressure, has already been demonstrated in practice (Abanades 2004) in experiments in a batch fluidized bed of calcium oxide with reasonable gas residence times and bed inventories. These results have recently been validated in continuous mode, in a bubbling fluidized bed carbonator (Lu 2008) coupled with an oxyfired circulating fluidized bed calciner. Variations of this carbonation-calcination system are planned to be tested at small pilot scale (10s of kW) in ongoing projects in France, UK, Germany, Canada and Spain under the EU C3-capture project and other national projects. This paper presents the first experimental evidence of the full concept operating a circulating fluidized bed carbonator reactor absorbing CO₂ from flue gases in continuous mode.

EXPERIMENTAL

Experiments have been conducted in a 30kW test facility fully designed and built at CSIC, made up of two interconnected circulating fluidized bed reactors as shown in Figure 2. Both reactors have a 0.1 m internal diameter; the calciner is 6 m in height and the carbonator 6.5 m in height. Some experiments presented here were carried out in a previous rig set-up, similar to the current one, but with riser heights of 3.2 m. In both set ups, each riser is connected to a high efficiency primary cyclone. The solids fall from the cyclone through a vertical standpipe to a bubbling fluidized bed loop seal. Solids flow over the loop seals towards an inclined standpipe that directs them to the opposite reactor (ie solids captured in the primary cyclone of the carbonator are directed towards the calciner) at which point they have completed half of the

solid circulation loop. There is a bypass just below the loop seals to extract solid samples and to measure solid circulation rates (G_s , in $\text{kg}/\text{m}^2\text{s}$) by diverting solids to a dead volume for a certain period of time. Other solid samples can also be extracted directly from several riser ports for more detailed analysis. Two secondary cyclons and gas bypass with filters complete the gas flow paths of the carbonator and of the calciner.

A mixture of gas containing carbon dioxide (air from a blower and carbon dioxide from a Dewar) is fed into the carbonator simulating the flue gas. No air distributor is used for these small diameter risers, allowing the easy feed of solids when needed (screw feeders for solid fuels, in particular for the air-fired calciner, are not shown in the Figure 2 for simplicity). The loop seals are aerated with air. Electric ovens surround the first 2.5 m of the risers (six independently controlled heating elements in each) and also the loop seals. After start up, the ovens are switched off in the carbonator and even opened up slightly in order to release the excess heat generated in the carbonation reaction.

In the second circulating fluidized bed reactor, the calcium carbonate formed in the carbonator is regenerated under typical combustion conditions in a CFBC (800-900°C with 2-6% air excess). The calciner is air-fired in these particular experiments. It has been shown that by independent experiments in fluidized bed (Lu, Hughes et al. 2008) that oxygen/carbon dioxide calcination in CFB conditions is also feasible. There is strong evidence that typical calcination temperatures and atmospheres do not affect much the overall sorbent performance as long as temperatures are kept below 950°C (González 2008). This is also supported by early works conducted by (Curran 1967), conducted under very high temperatures (up to 1060°C) (in fluidized bed combustion) and yielding similar deactivation curves of the sorbent than at more moderate conditions.

Continuous analyses of gases (carbon dioxide, oxygen and carbon monoxide and others) can be carried out from different points in the installation. Zirconia oxygen probes are also present in the risers to measure local O_2 content, ensuring good quality of combustion in the calciner and adding confidence to

the gas composition measurements by the analyzer. This is particularly important in this small test rig because aeration in the loop seal can amount to 20% of the total flow of gas entering the risers and there is uncertainty about the path of this aeration gas. In normal circulation conditions, it should follow the circulating solids downwards towards the riser, and the oxygen probe should give the same average oxygen content as the gas analyzer. However, under some conditions of low solid circulation rates, a fraction of the air fed into the loop seal travels upwards towards the cyclone (lowering its solids capture efficiency). In these conditions, that were more common in the early test set-up with risers 3.2 m high, the oxygen content measured by the zirconia probe at the exit of the riser is smaller than measured by the gas analyzer (which samples gas after the secondary cyclone).

Finally, as can be seen in Figure 2 there are a number of ports for installing differential pressure transducers and thermocouples. All these signals, together with those from the oxygen probes, the mass flow controllers and the gas analysis system are collected in a computer.

All the solid samples taken from the calciner, the carbonator and the loop seals are analysed to determine total calcium oxide content and calcium conversion to calcium carbonate. Selected samples from the carbonator are taken to measure the carbonation reaction rate in a thermobalance specially designed for multi-cycle experiments (see (González 2008)). A typical high purity limestone (>98% calcium carbonate) was used in all the experiments, with a particle size range below 350 microns and with activity curves that have been reported elsewhere (González 2008).

In a characteristic run, a batch of 20 kg of limestone is loaded into the loop seals and the risers. Temperatures are allowed to rise up to around 600°C with electric heating and from that point fuel is fed into both risers in order to increase the temperature to calcination conditions. Due to the high heat losses from this small rig, several hours are necessary to complete calcination of the initial batch of solids. Furthermore, attrition during the first calcination of limestone is intense (in particular in the rig of Figure 2, which has high velocity sections because of the high efficiency cyclons). Therefore, batches of fresh

limestone had to be added occasionally to maintain the solids inventories and solids circulation rates, thereby increasing even further the total calcination time of the first batch of material. Future tests incorporating some suggested solutions to mitigate attrition losses (e.g. partial sulfation and/or controlled precalcination as proposed in (Jia 2007)) will be carried out in the future. But it is important to highlight that attrition losses are mainly relevant in the first calcination cycles and therefore, all the know-how and mechanical tests designed to make a suitable choice limestones for commercial CFBC boilers should be of application for carbonate looping cycles. Once the material had been calcined, solids in the circulation loop had a typical average particle size distribution below 100 microns with this particular limestone, and attrition was no longer a serious problem. Solids collected in the secondary cyclones were fed back to the main circulation loop. The bed inventory in each riser was calculated assuming that the ΔP measured in the riser is due to the bed inventory (W) as in minimum fluidization conditions ($\Delta P=W/A$).

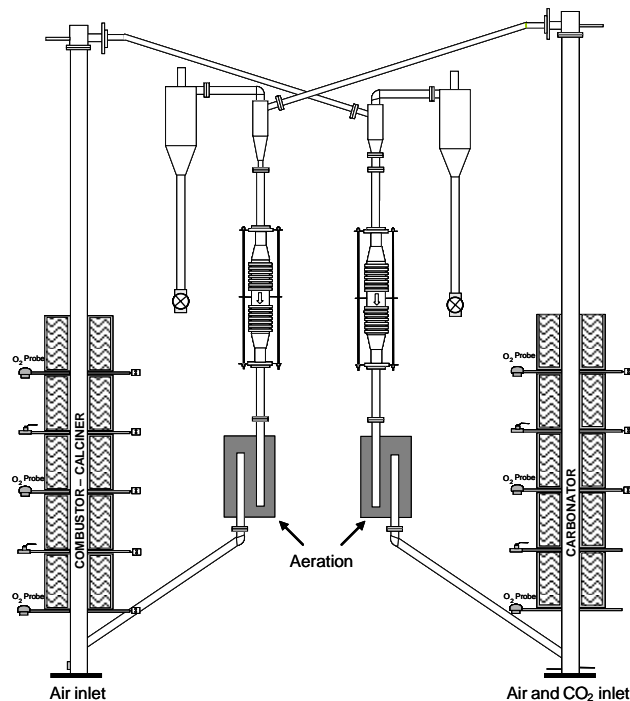


Figure 2. Schematic and overview of the interconnected circulating fluidized beds to test carbonate looping at INCAR-CSIC.

RESULTS AND DISCUSSION

Before discussing some of the results obtained during the carbonation-calcination test, it may be useful to report on the main problems and difficulties found before these tests were successfully completed. There were some fundamental problems associated with the initial rig design that had to be limited to a height of 3.2 m for space limitations in the building. In addition, the original cyclones were not operating with sufficient efficiency (92-97%), and as a result, the total solids inventory in the main circulation loop could only be maintained for relatively short periods of time. This was compensated for by re-injecting frequently to the circulation loop the solids collected from the secondary cyclone. In these conditions, a dynamic type of operation was attained. An example of the type of information obtained from a typical test in the 3.2 m installation is shown in Figure 3. The plot at the top includes the temperatures along the riser height of the carbonator. The plot in the centre shows the carbon dioxide concentration (black line) measured at the exit of the secondary cyclone, with occasional measurements also taken from the gas inlet entering the carbonator. The light and dark grey lines are oxygen measurements from the zirconia oxygen probe and from the analyzer. The plot at the bottom of the Figure shows the continuous recording of the pressure drop in the carbonator risers with some points indicating the solids circulation measurements. This particular experiment was carried out with partially deactivated sorbent material from previous experiments. As can be seen, the carbonator retained good axial isothermicity ($\pm 20^\circ\text{C}$) at any particular time when circulation rates were above $1\text{kg}/\text{m}^2\text{s}$. Superficial gas velocities were varied between 1.5 and 3 m/s. As discussed above, this particular rig (risers of only 3.2 m height and low efficiency primary cyclones) only retains relatively low stable solids circulation rates and bed inventories ($0.5\text{ kg}/\text{m}^2\text{s}$ and ΔP between 5-10 cm H_2O). The addition of batches of solids to the carbonator (see for example at 13:35) translates into a rapid increase of the solids inventory in

the riser, a rapid drop in the carbon dioxide concentration of the gas coming from the carbonator and a sharp increase in the solids circulation rates (see also the perfect isothermity of the riser under these conditions). These situations occur when capture efficiencies are well over 95%, close to the maximum allowed by the equilibrium of carbon dioxide on calcium oxide at the average temperature of the carbonator reactor. Unfortunately, as discussed above, it was not possible to maintain this situation for more than a few minutes in the 3.2 m height rig, and as the solids abandoned the primary circulation loop, carbon dioxide capture efficiency decreased rapidly. Many experiments like this one were carried out using different starting materials (different activities), different gas velocities in the carbonator (between 1.5 and 3.5 m/s) and with different carbon dioxide contents in the gas that entered the carbonator. These conditions provided a good base for the development and validation of a model and for the practical design of the modified rig in Figure 2.

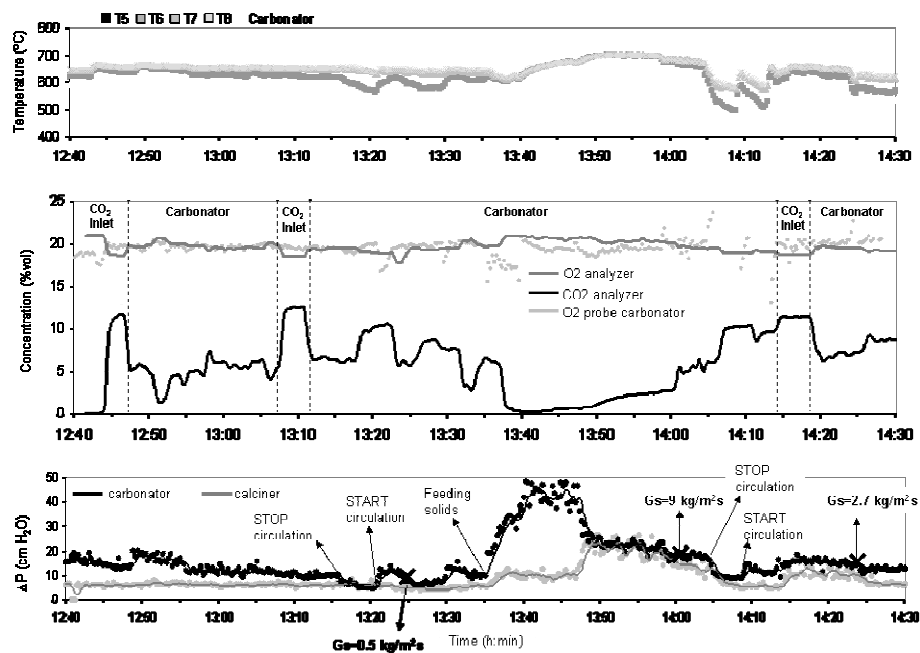


Figure 3. Example of experimental results from the carbonate looping test rig.

Although these were non-stationary conditions respect to the solid circulation and inventories, it is important to highlight that the gas residence time in the 3.2 m carbonator was only 1-2 seconds in all experiments. Therefore, the experimental CO₂ capture efficiencies measured in the gas phase from the CO₂ flow fed into the carbonator and the CO₂ measured at in the flue gas at the exit of the carbonator, are established "instantly" for a given value of bed inventory and average activity of the solids in the bed. This was already discussed in (Abanades 2004), where it was possible to fit with an stationary state bubbling model for the gas phase the experimental efficiencies measured with a batch of solids of changing composition with time. The key variable introduced to allow the interpretation of results with this approach was the fraction of active CaO reacting in the fast reaction regime (f_a) at any time, that was defined as the difference between the maximum carbonation conversion achievable by the solids in the bed (X_{max}) and the actual carbonation conversion of the solids in the bed (X_{carb}). Therefore, it is also possible to assume here that for any time during the experiment, the perfectly mixed bed of solids in the carbonator contains (in the absence of sulphur and ash) three types of solids: a fraction of inactive CaO from previous carbonation-calcination cycles ($1-X_{max}$), a fraction of CaCO₃ given by the carbonation conversion (X_{carb}), and a fraction of active CaO, f_a , that is the only responsible of the effective absorption of CO₂ from the gas phase. Using this concept, combined with submodels for reaction rates of this active fraction of CaO and assumptions of ideal reactor for the CFB carbonator and calciner, full reactor models have recently been formulated (Hawthorne 2008; Alonso 2009) for the carbonator. These models provide a great source of information for gaining confidence in the process. However, from a practical point of view, it is very important to demonstrate the possibility of operating the system in continuous mode respect to the solid circulation between carbonator and calciner. It was clear from the test in the experimental set up with risers heights of only 3.2 m, that gas velocities in the CFB carbonator higher than 2 m/s and lime particle sizes around 100 microns, only allowed for very modest solid inventories in the carbonator. Stable efficiencies associated with these modest inventories where typically below 30%. Efficiencies higher

than 95% where only possible for short periods of time (5-10 minutes) soon after injection of batches of material to the circulation loop (see example of Figure 3).

Figure 4 presents some results for the same rig after the extension of the riser heights (carbonator height up to 6.5 m and calciner height up to 6 m) and reconstruction of high efficiency cyclones. The results are qualitatively identical to the previous ones, but much more stable in terms of solids circulation rates and the bed inventory in the carbonator. For the sake of simplicity, the experimental information on gas compositions has been plotted as instant capture efficiency (black dotted lines) calculated from the experimental concentration of CO₂ at the exit of the carbonator. These capture efficiencies are compared with the maximum efficiency allowed by the equilibrium at the average temperature in the carbonator reactor at that particular time. As can be seen in the Figure on the left hand side, carbon dioxide capture efficiencies are consistent and stable to over 70% and close to 90% (superficial gas velocities between 2.0-2.1 m/s, solids circulation rates of 0.8-2.3 kg/m²s, average temperature 650°C). However, there are three events in this figure that show a much lower capture efficiency, illustrating once again the importance of a good solids circulation and sufficient solids inventory in the riser. The second event (at around 22:15) corresponds to the deliberate switching off of the aeration of the loop seal, which interrupted the solids circulation to the carbonator. As a result, efficiency dropped to zero as due to the lack of solids reacting in the carbonator. In addition, in the absence of the exothermic carbonation reaction and a continuous supply of solids from the loop seal, the temperature dropped in the carbonator reactor, as indicated by the sharp increase in theoretical capture efficiency allowed by the equilibrium. The third low efficiency peak in the same figure at around 22:40 corresponds to a measurement of the solids circulation rate (when solids were diverted to a container for a certain period of time) that translates into a rapid reduction of the solids inventory in the carbonator and an associated reduction in capture efficiency.

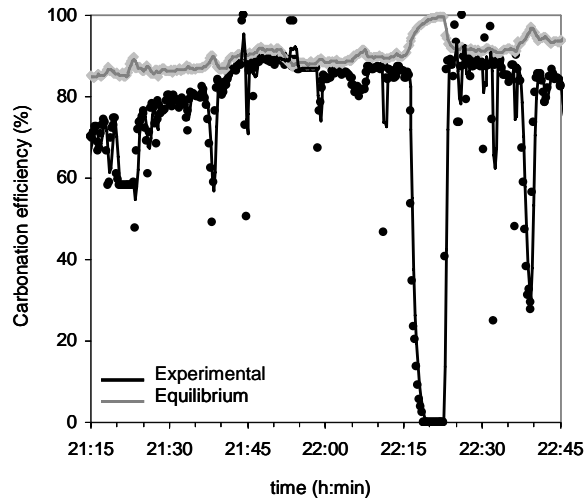


Figure 4. Example of experimental results for the rig of Fig. 2 which operates with continuous carbonations and calcinations.

Fig. 5 corresponds to an experimental period conducted under similar conditions but with calcium oxide particles highly deactivated and close to the residual activity of the limestones (0.07–0.12) after hundreds of carbonation–calcination cycles (Grasa and Abanades, 2006). This particular experiment ran for more than 8 h under stable conditions, with carbon dioxide capture efficiencies between 65 and 75%, with relatively modest circulation rates (1–1.8 kg/m² s) and solids inventories. Higher efficiencies would be feasible in taller risers and/or with fluid dynamic improvement in order to sustain higher circulation rates and higher solids inventories in the carbonator. The low efficiencies measured on the left hand side of the figure correspond to a period when the ovens of the calciner were switched off. This caused the temperatures in the calciner to drop below 750 °C and calcination intensity to fall. In addition, progressive carbonation of the material in the system led to low (eventually zero) capture efficiencies. When the ovens were switched on at 17:15, calcination intensity was restored and capture efficiencies recovered in less than 1 h to a stable value of between 70 and 75%. Since the activity of the sorbent was close to its residual value and did not change with time, it was

possible to restore these conditions and efficiency values after 6 h of continuous operation under other conditions.

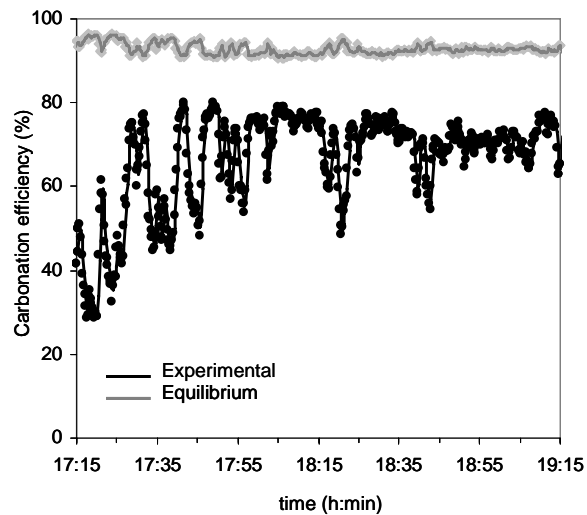


Figure 5. Example of experimental results using calcium oxide particles highly deactivated.

FUTURE WORK

The results presented above, together with the increasing number of new information published by other authors (see Hawthorne et al., 2008, and previous papers reviewed in Anthony, 2008; Harrison, 2008) from laboratory and bench scale results, supports the technical and economic viability of carbonate looping cycles, as represented in Fig. 2. The focus of ongoing work at CSIC is on the development of the carbonator reactor, assuming that technology for oxy-fired circulating fluidized bed combustion will be available to serve as calciner (Fig. 2). As the results have shown, it is feasible to design a CFB carbonator as a very effective carbon dioxide absorber as long as this reactor is supplied with a continuous flow of calcium oxide to match the carbon dioxide flow to be captured. High calcium conversions of the solids to calcium carbonate are not required, because gas densities are three orders of magnitude lower than solid densities and even with carbonation conversions as low as 5% it is possible to capture the carbon dioxide using solid/gas mass ratios below

20, typically used in existing large scale CFB boilers. Only heat balance considerations (Rodriguez et al., 2008a) prevent lower carbonation conversions to be used. However, research on how to improve sorbent performance can only lead to higher benefits and cost savings for this technology (Anthony, 2008).

As regards to the oxy-fired calciner, one can anticipate that the introduction of an endothermic reaction (continuous calcination) to the oxy-fired combustor will only bring benefits in terms of heat management and temperature control in the highly exothermic combustion reaction that takes place in an oxy-fired CFB combustor. The link of carbonate looping processes with oxy-fired CFB technology is not only one of the strengths of the process of Fig. 2 but also the source of the weakest point with respect to more exotic emerging carbon dioxide capture systems: the need for an air separation unit to drive the calciner of Fig. 2, still entails a substantial energy and cost penalty. However, we are pursuing advanced carbonate looping processes where there is no need for an oxygen fired calciner because part of the heat generated in the main combustion chamber of the power plant is transferred (by circulating calcium oxide particles and refractory ash) to a calciner operating at as low temperature as possible thanks to the dilution of carbon dioxide with steam. Aspen Hysys simulations have proven that the combustor and the calciner in this configuration can be designed as adiabatic reactors, and it is possible to recover the energy produced in the carbonator to produce overheated steam. These theoretical calculations (Murillo et al., 2009) have shown that when a sub-critical Rankine cycle is used and a moderate thermal integration is performed, there is very low energy penalty other than the penalty associated to carbon dioxide purification and compression. Tests conducted at small laboratory scale (Gonza'lez et al., 2008) have shown that the calcium oxide particles may maintain sufficient activity under the typical high-temperature conditions (around 1000 8C) and atmosphere of such a system.

The test facility used in this work (Fig. 2) will continue to be used to obtain more data on the behavior of different limestones in the system, the effect of sulfur and ash contents on the fuels used, etc. Plans for a 1-MW scaling up in a

real industrial environment (the 50-MWe CFB power plant of Hunosa in La Pereda, Asturias, Spain) have already been initiated, with an aggressive schedule in order that the first experimental campaigns starts in the 1-MW rig by the end of 2010. The successful tests conducted so far make us feel optimistic about the next steps and about the speed at which results can be escalated, because the key components for carbonate looping post-combustion systems are mechanically similar to already existing large scale circulating fluidized bed combustors and their emerging oxy-fired counterparts.

CONCLUSION

Carbonate looping cycles are very promising concepts for postcombustion carbon dioxide capture applications. This work has shown that the new key piece of equipment, the CFB carbonator, works as an effective carbon dioxide absorber when supplied with a sufficient flow of active calcium oxide. Temperatures, solid circulation rates and bed inventories associated to the operation of the carbonator are relatively mild, compared to the established operating conditions for large scale CFBC boilers. Furthermore, since the carbonation is a fast exothermic reaction that takes place between 600 and 700 °C, the large amount of energy supplied to the calciner to regenerate calcium carbonate back to calcium oxide and carbon dioxide can be recovered from the carbonation heat output. The carbonator can be designed as an interface between an existing power plant and a new oxy-fired CFB power plant that is acting as calciner. The oxy-fired CFBC is not only avoiding the carbon dioxide from its own coal combustion feed, but also all the carbon dioxide coming from the flue gases of the neighbouring power plant, that have been captured as calcium carbonate in the carbonator. Future designs of carbonate looping cycles may even lead to further savings in energy and costs by integrating the combustion chamber with the calciner. Experimental results from a 30-kW test facility designed, constructed and operated by CSIC (Spain) have demonstrated the essential viability of the process. The results were using a rig configuration that included different riser heights and cyclone designs and allowed obtained longer periods of stable solids circulation rates and bed inventories. Attrition of

the limestone was very intense in the first calcinations but the remaining solids showed little tendency to further attrition. The carbonator reactor functions as an effective absorber of carbon dioxide (efficiency higher than 70%) as long as there is a sufficient bed inventory and solids circulation rate, even with highly deactivated calcium oxide (activity lower than 0.3 and even close to the residual activity below the typical 0.1 of sorbents cycled hundreds of times). Plans have already been made to extend the experimental database and gain experience and design data for the next 1-MW scale pilot.

ACKNOWLEDGEMENT

This work has been carried out thanks to the financial support from the Spanish companies Hunosa and Endesa. Experimental help provided by F Fuentes and I Rodríguez is also acknowledged.

REFERENCES

- Abanades, J. C., Anthony, E. J., Lu, D. Y., Salvador, C., Alvarez, D. (2004). "Capture of CO₂ from combustion gases in a fluidized bed of CaO." *Aiche Journal* **50**(7): 1614-1622.
- Abanades, J. C., Grasa, G., Alonso, M., Rodriguez, N., Anthony, E. J., Romeo, L. M. (2007). "Cost structure of a postcombustion CO₂ capture system using CaO." *Environmental Science & Technology* **41**(15): 5523-5527.
- Abanades, J. C., Rubin, E. S., Anthony, E. J. (2004). "Sorbent cost and performance in CO₂ capture systems." *Industrial & Engineering Chemistry Research* **43**(13): 3462-3466.
- Alonso, M., Rodríguez, N., Grasa, G., Abanades, J. C. (2009). "Modelling of a fluidized bed carbonator reactor to capture CO₂ from a combustion flue gas." *Chemical Engineering Science* **64**(5): 883-891.
- Alvarez, D., Abanades, J. C. (2005). "Determination of the critical product layer thickness in the reaction of CaO with CO₂." *Industrial & Engineering Chemistry Research* **44**(15): 5608-5615.
- Anthony, E. J. (2008). Solid Looping Cycles: A New Technology for Coal Conversion. **47**: 1747-1754.

- Barker, R. (1973). "Reversibility of the reaction $\text{CaCO}_3 = \text{CaO} + \text{CO}_2$." *J Appl Chem Biotechnol* **23**(10): 733-742.
- Curran, G. P., Fink, C. E., Gorin, E. (1967). "CO₂ acceptor gasification process. Studies of acceptor properties." *Adv. Chem. Ser.* **69**: 141-161.
- González, B., Grasa, G. S., Alonso, M., Abanades, J. C. (2008). "Modeling of the deactivation of CaO in a carbonate loop at high temperatures of calcination." *Industrial and Engineering Chemistry Research* **47**(23): 9256-9262.
- Grasa, G. S., Abanades, J. C. (2006). "CO₂ capture capacity of CaO in long series of carbonation/calcination cycles." *Industrial & Engineering Chemistry Research* **45**(26): 8846-8851.
- Grasa, G. S., Alonso, M., Abanades, J. C. (2008). Sulfation of CaO Particles in a Carbonation/Calcination Loop to Capture CO₂. **47**: 1630-1635.
- Harrison, D. P. (2008). "Sorption-Enhanced Hydrogen Production: A Review." *Industrial & Engineering Chemistry Research* **47**(17): 6486-6501.
- Hawthorne, C., Charitos, A., Perez-Pulido, C.A., Bing, Z., Scheffknecht, G. (2008). *Design of a dual fluidised bed system for the post-combustion removal of CO₂ using CaO. Part I: CFB carbonator reactor model.* 9th International Conference on Circulating Fluidized Beds, Hamburg, Germany.
- Jia, L., Hughes, R., Lu, D., Anthony, E. J., Lau, I. (2007). "Attrition of calcining limestones in circulating fluidized-bed systems." *Industrial & Engineering Chemistry Research* **46**(15): 5199-5209.
- Lu, D. Y., R. W. Hughes, et al. (2008). "Ca-based sorbent looping combustion for CO₂ capture in pilot-scale dual fluidized beds." *Fuel Processing Technology* **89**(12): 1386-1395.
- Lu, D. Y., Hughes, R. W., Anthony, E. J. (2008). "Ca-based sorbent looping combustion for CO₂ capture in pilot-scale dual fluidized beds." *Fuel Processing Technology* **89**(12): 1386-1395.
- Metz, B., Davidson, O., Coninck, H. de, Loos, M., Meyer, L. (Eds.) (2005). "Special Report on Carbon Dioxide Capture and Storage." *Intergovernmental Panel on Climate Change (IPCC)*(Cambridge Univ. Press).
- Murillo, R., Grasa, G., Martínez, I., Rodríguez, N., Abanades, J. C. (2009). Conceptual design of a three bed fluidized bed combustion system capturing

CO₂ with CaO. 5th Trondheim Conference on CO₂ Capture, Transport and Storage. Trondheim.

Rodriguez, N., Alonso, M., Grasa, G., Abanades, J. C. (2008). "Heat requirements in a calciner of CaCO₃ integrated in a CO₂ capture system using CaO." Chemical Engineering Journal **138**(1-3): 148-154.

Rodriguez, N., Alonso, M., Grasa, G., Abanades, J. C. (2008). "Process for Capturing CO₂ Arising from the Calcination of the CaCO₃ Used in Cement Manufacture." Environmental Science & Technology **42**(18): 6980-6984.

Romeo, L. M., Abanades, J. Carlos, Escosa, J. M., Paño, J., Giménez, A., Sánchez-Biezma, A., Ballesteros, J. C. (2008). "Oxyfuel carbonation/calcination cycle for low cost CO₂ capture in existing power plants." Energy Conversion and Management **49**(10): 2809-2814.

Shimizu, T., Hirama, T., Hosoda, H., Kitano, K., Inagaki, M., Tejima, K. (1999). "A Twin Fluid-Bed Reactor for Removal of CO₂ from Combustion Processes." Chemical Engineering Research and Design **77**(1): 62-68.

Squires, A. M. (1967). "Cyclic Use of Calcined Dolomite to Desulfurize Fuels Undergoing Gasification." Advances in Chemistry Series(69): 205-&.

5 *Modelo de Reactor de Carbonatación*

El trabajo experimental realizado en la planta piloto de la Figura 4.1 que tiene que ver con esta Tesis se ha centrado en observar la extensión de la reacción de carbonatación en un lecho fluidizado circulante bajo diferentes condiciones de operación. El trabajo teórico se ha basado en la realización de una primera aproximación al modelado de un carbonatador de lecho fluidizado circulante. Se ha propuesto un modelo de reactor basado en simples suposiciones fluido-dinámicas, integrando además el conocimiento sobre la capacidad de captura del sorbente y su reactividad en función de la distribución del tiempo de residencia de las partículas circulando entre carbonatador y calcinador. En este aspecto se ha realizado un artículo que ha sido publicado, y que se adjunta en el apartado 5.4.1 (ver *Publicación V*).

Uno de los aspectos clave para realizar el modelado del reactor de carbonatación es la definición de la actividad media máxima (capacidad de carbonatación o conversión máxima) de los sólidos que llegan al reactor de carbonatación. Con un modelo de mezcla de sólidos en sistemas de reactores de lecho fluidizado circulantes e interconectados, y otro para la desactivación del CaO con el número de ciclos de calcinación-carbonatación, se había calculado la conversión media máxima de las partículas en el sistema suponiendo conversión completa (Abanades 2002). Como parte de esta Tesis, se ha desarrollado un modelo más general para el cálculo de la actividad media de los sólidos que llegan al reactor de carbonatación, en el que se tiene en cuenta la

extensión de la reacción de carbonatación y de calcinación en el cálculo de la conversión media máxima. Es decir, se contempla en el cálculo la posibilidad de alcanzar la conversión parcial en los respectivos reactores. Este trabajo ha sido recientemente publicado, y se adjunta en el apartado 4.3 (*Publicación VI*).

Por último, a partir de los ensayos realizados en la planta piloto, con el protocolo experimental detallado en la sección 3, se ha obtenido un gran abanico de datos experimentales bajo diferentes condiciones de operación. Con un modelo de carbonatador sencillo, basado en el de la *Publicación V*, se ha estudiado la tendencia que sigue la eficacia de captura de CO_2 ante diferentes parámetros. Este modelo se ha validado con los datos experimentales obtenidos y ha sido enviado para su publicación. En el momento de la impresión de esta Tesis el artículo se encuentra pendiente de aceptación tras realizar los cambios sugeridos por los revisores. Este trabajo se adjunta en la sección 5.4.2 como la *Publicación VII* y se presenta como parte del contenido de esta Tesis.

5.1 Descripción del Modelo del Carbonatador

Durante el desarrollo de esta Tesis se ha realizado un modelo del reactor de carbonatación. El objetivo del modelo es calcular la eficacia de captura de CO_2 en el carbonatador a partir de los datos de entrada de flujo de CO_2 (F_{CO_2}), flujos de sólidos (F_0 y F_R) e inventario de sólidos en el carbonatador (W_{CaO}).

Con el modelo se calcula el valor de eficacia de carbonatación, por un lado, igualando el CO_2 que desaparece de la fase gas con el CaCO_3 que aparece en la corriente de circulación de sólidos; y por otro lado, igualando el CO_2 desaparecido de la fase gas con el CaO que reacciona en el reactor.

$$\left(\begin{array}{c} \text{CO}_2 \text{ que desaparece} \\ \text{de la fase gas} \end{array} \right) = \left(\begin{array}{c} \text{CaCO}_3 \text{ que se forma en la} \\ \text{corriente de circulación} \end{array} \right) = \left(\begin{array}{c} \text{CaO reacciona con} \\ \text{CO}_2 \text{ en el carbonatador} \end{array} \right) \quad (1)$$

Para definir el modelo se han establecido una serie de suposiciones, de las cuales, las principales se resumen a continuación:

- Mezcla perfecta e instantánea de los sólidos en los reactores de carbonatación y calcinación.
- Flujo pistón para la fase gas del reactor de carbonatación.
- Se considera que la reacción de calcinación se da de forma completa e instantánea en el calcinador.
- Es conocido que la reacción de carbonatación tiene dos etapas, una rápida y otra lenta controlada por la difusión del CO_2 a través de la capa de producto de CaCO_3 (Bhatia y Perlmutter 1983). Además, se sabe que la conversión máxima del CaO a CaCO_3 decrece con el número de calcinaciones y carbonataciones (Curran et al. 1967). Para simplificar el modelo de reacción del CaO con el CO_2 , se ha definido un tiempo de reacción característico denominado t^* . Este tiempo marca el fin de la etapa de reacción rápida y el comienzo de la etapa lenta. Se considera que las partículas de CaO que lleven en el sistema un tiempo igual o inferior a t^* , alcanzan su conversión máxima a una velocidad de reacción constante. Las partículas de CaO que tengan un tiempo de residencia mayor de t^* , se considera que ya no reaccionan.
- La conversión de carbonatación media máxima se calcula suponiendo que es la media de las conversiones de las fracciones individuales de partículas, tal y como se definió en (Abanades 2002).
- Se define una fracción de partículas, f_a , que tienen un tiempo de residencia en el carbonatador inferior a t^* . Esta fracción de partículas de CaO es clave para cerrar el modelo. Se ha de tener en cuenta que las partículas que lleven en el carbonatador un tiempo inferior a t^* están reaccionando cuando abandonan el carbonatador, por tanto se ha de calcular cuál es la conversión media de esa fracción de partículas teniendo en cuenta su distribución de tiempos de residencia.

Con estas suposiciones, queda definida la primera parte del balance. Es decir, conociendo los flujos de gas y sólidos del sistema, se puede suponer un valor de la fracción de CaO que está reaccionando en el régimen de reacción rápido, f_a , e inmediatamente se obtiene la eficacia de captura o de carbonatación, E_{carb} . Para validar el valor de f_a supuesto, y por consiguiente el valor obtenido de eficacia de captura se ha de atender a la segunda parte del balance. Las suposiciones realizadas para definir la parte del modelo que tiene que ver con la reacción en el carbonatador, y que se suman a las suposiciones anteriores, son:

- Durante el régimen de reacción rápido se supone que el control de la reacción de CaO con CO₂ es cinético de primer orden. Se supone que no hay ninguna otra resistencia al progreso de la reacción que no sea la reacción cinética (Grasa y Abanades 2006).
- Para la constante intrínseca de la reacción de carbonatación se supone un valor de $4 \cdot 10^{-10} \text{ m}^4 (\text{mol s})^{-1}$. Este valor se considera conservador atendiendo a distintos valores obtenidos para la carbonatación de CaO tras una calcinación, (Bhatia y Perlmutter 1983; Grasa y Abanades 2006) y ofrecidos en la literatura para CaO derivado de ensayos multiciclo (Grasa y Abanades 2006).
- La superficie específica media de CaO disponible para la reacción con CO₂ se calcula teniendo en cuenta que cuando se forma una capa de carbonato de 50 nm sobre la pared del poro de CaO, se ha alcanzado la conversión máxima de las partículas (Alvarez y Abanades 2005).

Con estas suposiciones para la velocidad de reacción de las partículas, se puede formular el balance de materia en la fase gas en un elemento diferencial del reactor de carbonatación. La fracción de partículas, f_a , que tienen un tiempo de residencia inferior a t^* son las que reaccionan en el carbonatador a la velocidad de reacción definida anteriormente. Por tanto, con el valor de f_a supuesto para calcular la eficacia de carbonatación según la fase gas, es posible ahora calcular la eficacia de carbonatación, E_{carb} , según la reacción del CaO con CO₂ en el

reactor. La comparación de las eficacias de carbonatación obtenidas determinará la bondad de la f_a supuesta.

Para resolver el modelo mas fácilmente para diferentes condiciones de entrada, se creó un código en el programa MatLab con el que se obtiene una fracción de fase activa, f_a , que iguala la eficacia de carbonatación definida por ambas fases con un error menor del 1%.

Los detalles de la definición de este modelo y la discusión de los resultados obtenidos con el mismo se encuentran publicados en un artículo que se adjunta en la sección 5.4.1 (ver la *Publicación V*).

5.2 *Estimación de la Actividad Media de las Partículas del Sorbente*

Como se ha comentado anteriormente, una de las suposiciones realizadas para definir el modelo del carbonatador tiene que ver con la conversión de carbonatación media máxima que alcanzan las partículas en el sistema, X_{ave} . Las partículas de CaO circulando entre reactores pierden capacidad para capturar CO_2 con el número de carbonataciones y calcinaciones (número de ciclos, N). La fracción activa de CaO en una partícula es definida como la conversión de carbonatación, X_N , que está relacionada con la conversión alcanzada cuando acaba la fase rápida de reacción (Abanades y Alvarez 2003).

En el sistema de reactores de lecho fluidizado interconectados se considera que los sólidos están perfectamente mezclados. Teniendo en cuenta el flujo de caliza fresca que se alimenta (F_0) y el flujo de sólidos que circula entre reactores (F_R), en el sistema existirán diferentes fracciones de partículas (r_N) con diferentes números de ciclo (N). Cada fracción de estas partículas tiene capacidad para alcanzar una conversión de carbonatación, X_N , según su número de ciclo. Para

calcular X_{ave} en el modelo descrito anteriormente se supone que cada vez que las partículas pasan por el calcinador se calcinan totalmente de manera efectiva, y cada vez que las partículas pasan por el carbonatador alcanzan la conversión de carbonatación, X_N , que les corresponde a cada ciclo. Por tanto, se puede calcular la conversión de carbonatación media máxima como el sumatorio del producto de cada fracción de partículas en un ciclo N , r_N , por la conversión alcanzada en dicho ciclo, X_N . Estos balances para el cálculo de la conversión de carbonatación media de una mezcla de partículas con diferente tiempo de vida en el sistema, fueron desarrollados por (Abanades 2002) y fueron utilizados para la definición de la conversión de carbonatación en el modelo del carbonatador introducido anteriormente.

Esta formulación de los balances de población es válida siempre y cuando las condiciones de operación y el diseño del reactor permitan la calcinación completa y la máxima conversión de los sólidos durante la carbonatación. Los tiempos de residencia habituales en los *risers* de reactores de lecho fluidizado circulante son de 3-5 s. Con estos tiempos de residencia es posible que no se consiga la carbonatación total de las partículas. De hecho, en estado estacionario, es necesario que en el carbonatador haya en todo momento una cierta cantidad de CaO activo que todavía no haya reaccionado. Este requisito es fundamental para que el carbonatador funcione como un absorbedor de CO_2 . En estos casos de carbonatación y/o calcinación parcial, la actividad media del CaO será diferente de aquella calculada bajo las suposiciones de carbonatación y calcinación total. Por tanto, es posible formular una nueva expresión para la actividad media máxima del sorbente incluyendo dos nuevos parámetros: la fracción de carbonatación (f_{carb}) y la fracción de calcinación (f_{calc}) de todas las partículas del sistema. La entrada en juego de estos dos nuevos parámetros obliga a la distinción entre número de ciclos, N , y número de carbonataciones y calcinaciones totales. Cuando las reacciones de carbonatación y de calcinación son totales, el número de ciclos (N) o número de calcinaciones y carbonataciones completas coincide con el número de veces que las partículas circulan entre el carbonatador y el calcinador. Sin embargo, cuando la

carbonatación y/o la calcinación no se dan completamente, las partículas habrán de circular más veces entre reactores (N mayor) para conseguir el mismo número equivalente de carbonataciones y calcinaciones completas (N_{age}). Esto lleva a que para alcanzar la misma eficacia de carbonatación (transportar una misma cantidad de CO_2) se requiera un mayor flujo de sólidos circulando en el sistema, con todas las implicaciones que conlleva esto en cuanto a los límites impuestos por el diseño del equipo y al incremento de la demanda de calor por parte del calcinador (ver *Publicación I*).

La consideración de la fracción de carbonatación y de calcinación, además de los flujos de sólidos (F_0 y F_R) en los balances de población llevó a la realización de la *Publicación VI* (adjunta en la sección 5.4.2). En ella se explica en detalle cómo llegar a la ecuación final que define la conversión media máxima de las partículas de sorbente en sistemas de sólidos circulantes e interconectados con alimentación de sorbente fresco. Esta ecuación puede ser aplicada para otro tipo reacciones y de sorbentes con diferente curva de desactivación cuyo principio sea el de captura y regeneración en dos pasos diferenciados (por ejemplo, procesos de chemical looping para captura de CO_2). En la *Publicación VI* se hace además un análisis del efecto de los flujos de sólidos (F_0 y F_R) sobre la conversión media máxima (X_{ave}) y sobre la eficacia de captura (E_{carb}) cuando la carbonatación y la calcinación son parciales.

5.3 Validación y Análisis de Tendencias de Datos Experimentales

En el capítulo 4 se presentó la planta piloto para captura de CO_2 mediante ciclos de carbonatación y calcinación, y se detalló la metodología experimental llevada a cabo para desarrollar un experimento completo. Además, en la *Publicación IV* (sección 4.3) se presentaron algunos ejemplos de los resultados experimentales obtenidos en la planta piloto. Se han contabilizado más de 450

horas de operación en la planta piloto, de éstas, unas 140 han sido de funcionamiento en condiciones estacionarias. Durante estas horas de operación en estado estacionario se han extraído alrededor de 200 muestras de sólidos de los reactores (100 muestras extraídas del carbonatador y 100 muestras del calcinador), lo que constituye unos 100 puntos experimentales.

Un punto experimental queda definido cuando se conocen, en condiciones estacionarias, los siguientes datos de operación:

- a) velocidad superficial del gas en el carbonatador
- b) velocidad superficial del gas en el calcinador
- c) temperatura media del carbonatador
- d) temperatura media del calcinador
- e) flujo de CO_2 alimentado al carbonatador
- f) flujo de CO_2 a la salida del carbonatador
- g) flujo de combustible al calcinador
- h) flujo de CO_2 a la salida del calcinador
- i) inventario del lecho de sólidos en el carbonatador
- j) conversión media máxima de carbonatación de las partículas del sistema
- k) conversión de carbonatación alcanzada en el carbonatador
- l) contenido en CaCO_3 de las partículas que abandonan el calcinador

Con la instrumentación disponible en la planta piloto (detallada en el apartado 4.1) es posible tener medidas continuas e instantáneas de los datos (a)-(i). Con el análisis en termobalanza de las muestras de sólidos extraídas de la planta se conocen los datos (j)-(l). Por tanto, con la extracción y el posterior análisis de las muestras quedan definidos los puntos experimentales.

Se han obtenido puntos experimentales en diferentes condiciones de operación. Principalmente se ha variado la velocidad del gas en el carbonatador, la concentración de CO_2 alimentado, la temperatura del carbonatador, la

velocidad de circulación de sólidos, la actividad del sorbente y el inventario de sólidos en el lecho.

Se ha llevado a cabo un ejercicio de validación y tendencias seguidas por los datos experimentales obtenidos de los ensayos en la planta piloto. El modelo del carbonatador utilizado, en general, sigue los mismos principios que el modelo definido en la *Publicación V*, se basa en el balance al carbonatador expresado por la ecuación (1).

En primer lugar, el ejercicio llevado a cabo con cada uno de los datos experimentales se basa en la comparación de los términos del balance al carbonatador de la ecuación (1) (el CO_2 desaparecido de la fase gas con el CaCO_3 formado en la corriente de circulación de sólidos; y el CO_2 desaparecido de la fase gas con el CO_2 reaccionando con el CaO en el carbonatador).

A continuación se hace un análisis de la evolución de la eficacia de captura de CO_2 (Ecarb) ante la variación de diferentes parámetros, como son el inventario de sólidos en el carbonatador, el inventario de sólidos activos para capturar CO_2 o la actividad del flujo de sólidos circulantes. Además, los puntos experimentales se agrupan según las condiciones de operación en las que fueron obtenidos y se sitúan en las correspondientes gráficas de tendencias de la eficacia de captura de CO_2 . De esta manera se puede comprobar si los puntos experimentales siguen la tendencia esperada según la definición del modelo del carbonatador.

Con este trabajo se ha realizado una publicación, adjunta en la sección 5.4.3 con el nombre de *Publicación VII*.

5.4 *Publicaciones Relacionadas*

5.4.1 *Publicación V*

**MODELLING OF A FLUIDIZED BED
CARBONATOR REACTOR TO CAPTURE CO₂
FROM A COMBUSTION FLUE GAS**

Publicado en:
Chemical Engineering Science
Volumen 64
Año 2009

MODELLING OF A FLUIDIZED BED CARBONATOR REACTOR TO CAPTURE CO₂ FROM A COMBUSTION FLUE GAS

M Alonso^a, N Rodríguez^a, G Grasa^b, J C Abanades^a

^a *Instituto Nacional del Carbón, CSIC, Oviedo 33011, Spain*

^b *Instituto de Carboquímica, CSIC, Zaragoza 50015, Spain*

ABSTRACT

In recent years several processes incorporating a carbonation–calcination loop in an interconnected fluidized bed reactor have been proposed as a way to capture CO₂ from flue gases. This paper is a first approximation to the modelling of a fluidized bed carbonator reactor. In this reactor the flue gas comes into contact with an active bed composed of particles with very different activities, depending on their residence time in the bed and in the carbonation–calcination loop. The model combines the residence time distribution functions with existing knowledge about sorbent deactivation rates and sorbent reactivity. The fluid dynamics of the solids (CSTR) and gases (PF) in the carbonator are based on simple assumptions. The carbonation rates are modelled defining a characteristic time for the transition between a fast reaction regime to a regime with a zero reaction rate. On the basis of these assumptions the model is able to predict the CO₂ capture efficiency for the flue gas depending on the operating and design conditions. Operating windows with high capture efficiencies are discussed, as well as those conditions where only modest capture efficiencies are possible.

INTRODUCTION

The UN Intergovernmental Panel for Climate Change (IPCC), Nobel Prize laureate for Peace in 2007, has already established that CO₂ capture and storage “would be an option in the portfolio of actions for stabilization of greenhouse gas concentrations while allowing for the continued use of fossil fuels” [1]. Large scale “capture systems” are already operating in the gas, oil and

chemical industries, where CO₂ and other key gases (H₂ or O₂) are routinely separated from different process streams. Such existing technologies could be adapted for the capture of CO₂ in flue gases from fossil fuel power plants at an acceptable cost (30–50 \$/t CO₂ avoided) compared to other methods of large scale power production with near-zero CO₂ emissions. Despite the maturity of several of these existing capture systems, it is widely recognised that there is need for large reductions in the CO₂ capture costs and energy efficiency penalties. Indeed lower costs and lower energy penalties are currently the driving forces behind all R&D in this emerging area.

One promising means of CO₂ capture for coal based power plants is to use a lime carbonation–calcination cycle (or “carbonate looping”) which is illustrated in Fig. 1. This process was originally proposed by Shimizu et al. (1999), and uses CaO as a regenerable sorbent to capture CO₂ from combustion flue gases. Other processes that use CaO in combustion systems have been proposed (Wang et al., 2004; Abanades et al., 2005) while others have also been considered for H₂ production routes (Yi and Harrison, 2005; Ochoa-Fernandez et al., 2007; Pfeifer et al., 2007; Sun et al., 2007; Weimer et al., 2008).

In the basic system of Fig. 1 CO₂ is captured from the combustion flue gas of a power plant in a circulating fluidized bed carbonator operating between 600 and 700 °C. When the solids leave the carbonator (with some of the CaO being converted to CaCO₃) they are directed to a second fluidized bed where calcination/regeneration takes place. Coal burns in the calciner in an atmosphere of O₂/CO₂ at temperatures over 900 °C, thus producing the heat necessary to calcine the CaCO₃ back to CaO and CO₂. It is assumed that this second fluidized bed calciner operates with oxygen supplied by an air separation unit, but other sources of heat for calcination may be used in the future (Abanades et al., 2005). The CO₂ captured from the flue gases as CaCO₃, and the CO₂ produced by the oxy-fired combustion of coal in the calciner, are recovered in concentrated form from the calciner gas, which is now suitable for final purification and compression, and subsequently for transport and safe storage in a deep geological formation. The calciner employs a considerable

fraction (35–50%) of the total energy entering the system to heat the incoming gas and solid streams up to the calciner temperatures and in order to provide the heat necessary for the endothermic calcination of CaCO_3 (Rodríguez et al., 2008). However this energy leaves the system in mass streams at high temperature (at $T > 900^\circ\text{C}$) or is recovered as carbonation heat in the carbonator (at around 650°C). Thus the large energy input into the calciner comes out of the system as high quality heat that can be recycled in a highly efficient steam cycle (Shimizu et al., 1999; Abanades et al., 2005; Romeo et al., 2008). The calciner functions in fact like a new oxyfired fluidized bed power plant. But in this new power plant it may be possible to almost double the amount of CO_2 output thanks to the CO_2 captured in the carbonator as CaCO_3 and regenerated back to CaO and CO_2 in the oxyfired calciner.

The carbonator reactor depicted on the left hand side of Fig. 1 is therefore a key process unit that must be designed and operated in such a way as to achieve high capture efficiencies of CO_2 from the flue gas. The flow rates of flue gases from a typical 1000 MWt power plant are about $300 \text{ Nm}^3/\text{s}$. Bringing this huge flow of gas into contact with CaO particles is only possible with reactors of a very high gas throughput per unit area such as circulating fluidised bed reactors. In addition, we may take advantage of the mechanical similarities between the carbonator and the currently employed large scale circulating fluidised bed combustors that operate with gas velocities, solid circulation rates and types of solid similar to those required to implement the carbonation–calcination loop.

Despite the increasing number of published works that deal with different aspects of such systems (sorbent performance and reactivation studies, batch experiments and modelling, process simulation work etc) there is a lack of information about the role of the fluidized bed carbonator reactor in systems such as that depicted in Fig. 1. The purpose of this study is to fill this knowledge gap by proposing a model based on simple assumptions about the fluid-dynamics of the reactors involved and by integrating existing knowledge about sorbent capture capacity and reactivity to the residence time distribution functions of the particles cycling between the carbonator and calciner reactors

in the loop of Fig. 1. The results of this work will help to gain insight into the operating modes of these reactors when they are employed at large scale. They may also be helpful for designing of pilot plants in which the process can be tested in continuous mode or for interpreting the results obtained from small pilot plants (10–70 kW thermal) like those entering operation in Canada, Germany, Spain, France and the UK under the C3 Capture project of the EU and other projects.

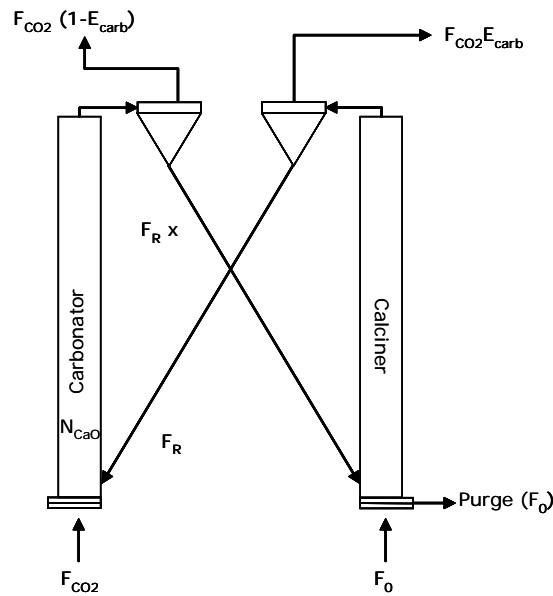


Figure 1: Scheme of the process for CO₂ capture using the lime carbonation-calcination loop.

MODEL DESCRIPTION

As mentioned above, the main objective of the model is to estimate CO₂ capture efficiency, E_{carb} , in the carbonator, where

$$E_{carb} = \frac{\text{CO}_2 \text{ reacting with CaO in the bed}}{\text{CO}_2 \text{ entering the bed in the flue gas}} \quad (1)$$

The overall mass balances in the system can be written as:

$$\left(\begin{array}{l} \text{CO}_2 \text{ reacting with} \\ \text{CaO in the bed} \end{array} \right) = \left(\begin{array}{l} \text{CO}_2 \text{ removed from} \\ \text{the gas phase} \end{array} \right) = \left(\begin{array}{l} \text{CaCO}_3 \text{ formed in the} \\ \text{circulating stream of CaO} \end{array} \right) \quad (2)$$

The model is solved when all the terms in the previous equation are calculated for a given set of input operating and design conditions. The first assumptions to set up equations for the different terms are: instantaneous and perfect mixing of solids in the carbonator and in the calciner, plug flow for the gas phase in the carbonator, instantaneous and complete calcination of particles in the calciner.

$$\left(\begin{array}{l} \text{CO}_2 \text{ removed from} \\ \text{the gas phase} \end{array} \right) = F_{\text{CO}_2} \times E_{\text{carb}} \quad (3)$$

$$\left(\begin{array}{l} \text{CaCO}_3 \text{ formed in the} \\ \text{circulating stream of CaO} \end{array} \right) = F_R \times X \quad (4)$$

$$\left(\begin{array}{l} \text{CO}_2 \text{ reacting with} \\ \text{CaO in the bed} \end{array} \right) = N_{\text{Ca}} \times f_a \times r_{\text{ave}} \quad (5)$$

The concept of f_a was already introduced in a previous work modelling batch carbonation experiments (Abanades et al., 2004). To explain the meaning of f_a in this work we must first review what is known about the reaction mechanism and reaction rates of the carbonation reaction. It is well known that the carbonation reaction has a fast reaction regime followed by a slow reaction regime controlled by CO_2 diffusion through the product layer of CaCO_3 formed on the free CaO surfaces (Deadman and Owens, 1962; Bhatia and Perlmutter, 1983; Mess et al., 1999). Furthermore, it is also well established that the maximum conversion of CaO (that marks the end of the fast carbonation period) decreases rapidly as the number of carbonation calcinations cycles increases (Curran et al., 1967; Barker, 1973; Abanades and Alvarez, 2003; Grasa and Abanades, 2006). In order to model these key sorbent features, and to facilitate the integration of the rate and the residence time distributions it is assumed that the CaO particles attain the maximum conversion, X_N , at a

constant rate, in a characteristic time t^* , and after that the reaction rate becomes zero.

$$r_{\text{CaO}} = \begin{cases} \frac{X_N}{t^*} & \text{if } t < t^* \\ 0 & \text{for } t > t^* \end{cases} \quad (6)$$

Fig. 2 illustrates this reaction model. For illustrative purposes, several series of experimental data from Grasa et al. (2008) are also included. More elaborate models for the kinetics of the carbonation reaction are likely to appear in the future, but we believe the model of Eq. (6) is sufficient at this stage as long as the characteristic t^* is consistent with the experimental measurements. This equation implies that particles with a residence time higher than t^* , reach their maximum average conversion, X_N , and that their reaction rate is zero from that point onwards. Particles with a residence time lower than t^* approach their maximum conversion at a reaction rate that is constant for a given cycle number. As will be shown below, setting the rate of reaction and the fraction of active particles of the bed as functions of t^* greatly facilitates the resolution of the model.

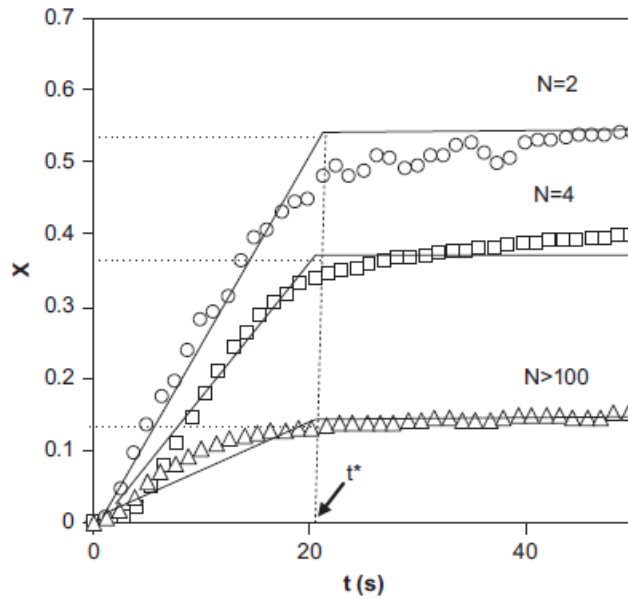


Figure 2. Scheme of the kinetic model adopted to describe the progress of the carbonation reaction with time for different cycle numbers

The maximum conversion, X_N in Eq. (6) is the conversion that the particles reach at the end of the fast carbonation period, which depends on the number of calcination-carbonation cycles in accordance with the following equation (Grasa and Abanades, 2006):

$$X_N = \frac{1}{\frac{1}{(1-X_r)} + Nk} + X_r \quad (7)$$

where typical values of $k=0.52$ and $X_r=0.075$ (Grasa and Abanades, 2006). Therefore, Eq. (6) allows the calculation of the rate of carbonation of a particle that is progressing towards its maximum allowable carbonation conversion X_N , given by Eq. (7) as a function of the number of cycles, N . However, with the continuous feed of fresh particles and the purging of solids from the perfectly mixed beds of Fig. 1, there will be a large population of particles in the system with different cycle numbers, different capacities for CO_2 capture (depending

on N) and different reactivities (also depending on N). Particle size did not influence the sorption capacity of the sorbent that remains determined only by the number of calcination/carbonation cycles (N) (Grasa and Abanades, 2006). The mass balance to estimate the fraction of particles that have been cycling in the system N times was solved in a previous work (Abanades, 2002) for a carbonation–calcination loop with full maximum carbonation conversion (represented by Eq. (7)) and total calcination. This mass balance may be refined for conditions where these reactions are incomplete, but for the sake of simplicity it is retained here.

The average maximum carbonation conversion that can be achieved by the particles in the carbonator is the average of the individual conversions:

$$X_{ave} = \sum_{N=1}^{N=\infty} r_N X_N \quad (8)$$

where (Abanades, 2002):

$$r_N = \frac{F_0 F_F^{N-1}}{(F_0 + F_R)^N} \quad (9)$$

Taking into account the kinetic model for an individual particle represented by Eq. (6), and assuming that the solids are perfectly mixed, it is possible to calculate the average reactivity of the CaO particle in the bed, r_{ave} , by replacing the subscript “ N ” in Eq. (6) by the subscript “ ave ” as calculated in Eq. (8). This means that Eqs. (6), (7), (8) and (9) allow the calculation of the rate at which the bed is capturing CO₂ (Eq. (5)) when the average concentration of CO₂ and the inventory of active calcium particles in the bed are known ($N_{Ca} \times f_a$). As will be shown below, the most important variable to be taken into account when estimating the average concentration of CO₂ in the bed is also the fraction of active particles that is reacting in the fast reaction regime, f_a .

As shown in Fig. 2, the fraction of active particles, f_a , corresponds to the particles that have not yet fully reached their maximum possible conversion or,

in other words, f_a is the fraction of particles with a residence time in the carbonator below t^* . Therefore, for a perfect mixed model, f_a is defined as:

$$f_a = (1 - e^{-t^*/\tau}) \quad (10)$$

where τ is the average particle residence time in the carbonator which is defined as:

$$\tau = \frac{N_{Ca}}{F_R} = \frac{W}{40F_R} \quad (11)$$

Thus taking into account the simple reaction model adopted in Fig. 2, it can be seen that the CaCO_3 leaving the carbonator reactor is the sum of two contributions: carbonate in particles converted to their maximum level of conversion (with a residence time higher than t^*) depending on their individual cycle number, and particles with a residence time lower than t^* , which abandon the carbonator when they are still reacting at the rate given by Eq. (6):

$$\left(\text{CaCO}_3 \text{ formed in the circulating stream of CaO} \right) = F_R \times X = F_R (f_a X|_{<t^*} + (1-f_a) X|_{>t^*}) \quad (12)$$

The average conversion of particles when $t > t^*$ is:

$$X|_{>t^*} = X_{ave} \quad (13)$$

Since r_{ave} is constant between 0 and t^* , $X|_{<t^*}$ can be calculated as follows:

$$X|_{<t^*} = \frac{\int_0^{t^*} (r_{ave} \times t) \frac{1}{\tau} e^{-t/\tau} dt}{f_a} r_{ave} \tau \frac{\left[1 - e^{-t^*/\tau} \left(\frac{t^*}{\tau} + 1 \right) \right]}{(1 - e^{-t^*/\tau})} \quad (14)$$

Using Eq. (12) for r_{ave} , and incorporating Eqs. (13) and (14) into Eq. (12), the following expression for the average carbonate conversion of the solids leaving the carbonator reactor is obtained:

$$X = X_{ave} \frac{\tau}{t^*} (1 - e^{-t^*/\tau}) \quad (15)$$

or substituting Eq. (13) to express X in terms of f_a :

$$X = X_{ave} \frac{f_a}{\ln(1/(1-f_a))} \quad (16)$$

The difference between the maximum conversion achievable by the solids in the carbonator, X_{ave} , and the actual conversion of the solids leaving the reactor, X represents the fraction of CaO that was originally active in the calcined solid stream entering the carbonator and that has not yet been converted to CaCO₃. The difference between this fraction of active CaO, defined as $(X_{ave}-X)$, and the fraction of active CaO, f_a , defined previously as the fraction of CaO particles reacting in the fast reaction regime (i.e. with residence times lower than t^*) is worth noting. Because of the simple kinetic model adopted (constant carbonation rate from $t=0$ to t^* irrespective of conversion) the fraction f_a contains a certain fraction of CaCO₃ (given by Eq. (14)), and therefore $f_a > (X_{ave}-X)$.

Substituting the result of Eq. (16) into Eq. (4):

$$\left(\text{CaCO}_3 \text{ formed in the} \right. \\ \left. \text{circulating stream of CaO} \right) = F_R \times X = F_R X_{ave} \frac{f_a}{\ln(1/(1-f_a))} \quad (17)$$

So the carbonation efficiency in the carbonator reactor can be defined as a simple function of f_v as:

$$E_{carb} = \frac{F_R}{F_{CO_2}} X_{ave} \frac{f_a}{\ln(1/(1-f_a))} \quad (18)$$

As stated in Eq. (2), the carbon balance in the reactor demands identical carbonation efficiency to account for the disappearance of CO₂ from the gas phase and to account for the reaction of CO₂ with the active CaO in the bed (also depending of f_a according to Eq. (5)). For a given set of input data F_R, F_0, F_{CO_2} ,

W_{CaO} (or N_{Ca}), and for a given sorbent defined by its deactivation and reactivity constants, there is only one value of f_a that provides an identical value of E_{carb} when this is calculated from Eq. (18) or from Eq. (5). Therefore, in order to close the mass balance and solve the model, we need to develop Eq. (5) to find an equation for the reaction rate, r_{ave} , as a function of process conditions.

The first step is to define a rate expression for the carbonation reaction of the solids entering the carbonator consistent with the kinetic model adopted in previous paragraphs and represented in Fig. 2. In accordance with Eq. (8) the calcined particles of CaO are entering the carbonator with a maximum capacity to carbonate up to X_{ave} . It has also been established in a previous work (Alvarez and Abanades, 2005) that for most limestones and cycle numbers, the maximum conversion of a particle is attained when there is a carbonate layer of 50 nm thickness on the pore wall (Alvarez and Abanades, 2005). So, the specific reaction surface at the beginning of the N cycle, S_N , and the maximum conversion X_N can be related as follows:

$$X_N = \frac{e_{max} S_N \frac{\rho_{CaCO_3}}{PM_{CaCO_3}}}{\frac{\rho_{CaO}}{PM_{CaO}}} \quad (19)$$

Eq. (19) allows the estimation of the average reaction surface available for the CaO particles entering the carbonator as:

$$S_{ave} = \frac{X_{ave} \frac{\rho_{CaO}}{PM_{CaO}}}{e_{max} \frac{\rho_{CaCO_3}}{PM_{CaCO_3}}} \quad (20)$$

Once reaction surface has been calculated and assuming kinetic control in the reaction of CaO with CO₂ during the fast reaction regime:

$$r_{ave} = k_s S_{ave} (C_{CO_2} - C_{e,CO_2}) \quad (21)$$

This rate expression is similar to the one used in previous works (Abanades et al., 2004, Grasa and Abanades, 2006), but without the term $(1 - X)^{2/3}$, which is

characteristic of grain models. This modification is a minor one in quantitative terms, considering that conversions are typically low except in the first few cycles and that there will be few particles of this type in the continuous process of Fig. 1 (see below). Bhatia and Perlmutter (1983) also used a similar first order expression and found that the intrinsic carbonation rate constant was around $5.95 \times 10^{-10} \text{ m}^4 (\text{mol s})^{-1}$. The rate constant for highly cycled particles has recently been determined by Grasa and Abanades (2006) and it is consistently within a range of 3.2×10^{-10} to $8.9 \times 10^{-10} \text{ m}^4 (\text{mol s})^{-1}$. Unless stated otherwise, in this work we adopt a conservative value of $4 \times 10^{-10} \text{ m}^4 (\text{mol s})^{-1}$. With the rate of reaction of the active particles in the bed defined by Eq. (21), it is possible to formulate the carbon mass balance in the gas phase in a differential element of the carbonator reactor. Assuming that the gas passes in plug flow through a bed of perfectly mixed solids, the balance for a differential element is:

$$F_{\text{CO}_2} \frac{dE_{\text{carb}}}{dz} = Af_a \frac{\rho_{\text{CaO}}}{PM_{\text{CaO}}} r_{\text{ave}} = Af_a \frac{\rho_{\text{CaO}}}{PM_{\text{CaO}}} k_S S_{\text{ave}} \rho_{\text{M.g}} \left[\frac{(f_0 - f_e) + (f_0 f_e - f_0) E_{\text{carb}}}{(1 - f_0 E_{\text{carb}})} \right] \quad (22)$$

Using a dimensionless variable for height, the integrated form of this equation is:

$$f_e = \frac{10^{\left(7.079 - \frac{8308}{T}\right)}}{P_{\text{total}}} \quad (23)$$

where the equilibrium molar fraction of CO_2 is calculated from the expression (Barker, 1973):

$$\frac{F_{\text{CO}_2} PM_{\text{CaO}}}{W k_S S_{\text{ave}} \rho_{\text{M.g}} f_a} \left[\frac{-f_0}{(f_0 f_e - f_0)} E_{\text{carb}} + \frac{f_0 (f_0 - 1)}{(f_0 f_e - f_0)^2} \ln \left(\frac{(f_0 - f_e) + (f_0 f_e - f_0) E_{\text{carb}}}{(f_0 - f_e)} \right) \right] = z' \quad (24)$$

where T is the operation temperature (K) and P the total system pressure (atm).

By means of this implicit equation, it is possible to determine the CO_2 concentration profile along the carbonator when z' takes values between 0 and 1. At the exit of the carbonator ($z'=1$), the carbonation efficiency calculated from Eq. (23) needs to be equal to the carbonation efficiency calculated from Eq. (18). In fact, the model is solved when there is a solution of f_a that yields identical carbonation efficiencies in the gas and solid material balances.

A matlab code was developed to solve the model and the sequence of calculations used by the programme is shown in Fig. 3 and briefly outlined here.

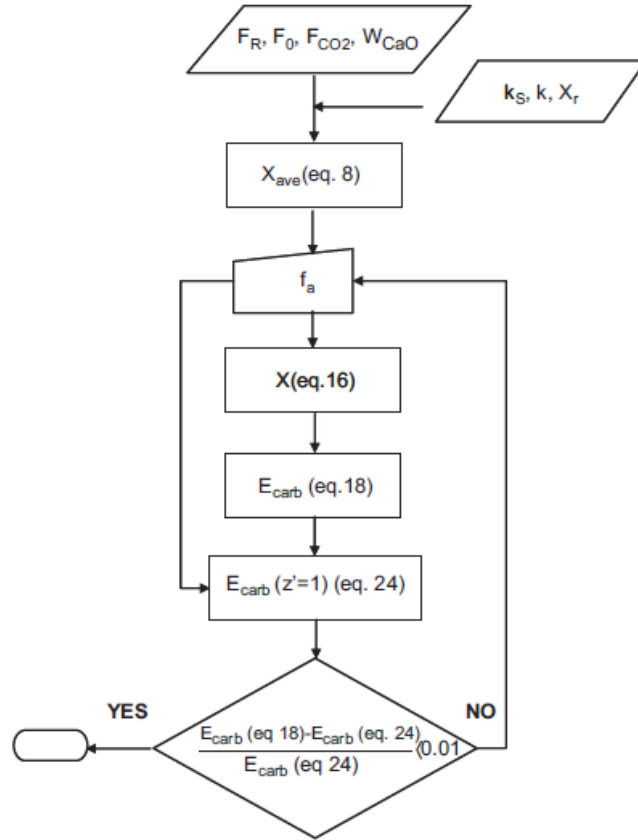


Figure 3. Sequence of calculations used to solve the proposed model.

There is a set of input conditions ($F_R, F_0, F_{CO_2}, W_{CaO}$) and a set of constant values characteristic of the sorbent (k_s, k, X_r). The average activity of the sorbent, or the maximum allowable conversions, X_{ave} , can be calculated using Eq. (8). Although there are simpler expressions for X_N that allow an analytical solution of this infinite sum (Abanades, 2002), this is not possible if Eq. (7) is used, and therefore the summing of Eq. (8) is carried out numerically with sufficient cycle numbers (N) as to guarantee that the sum of the volume fractions given by Eq. (9) is higher than 0.99.

Assuming from this point the presence of a volumetric fraction of active CaO in the bed, f_a the carbonation efficiency is calculated by two parallel routes, iterating the value of f_a until both routes yield the same efficiency (allowing

for an error of 1%). Whereas the first calculation route uses Eq. (18), the second route uses the same f_a . In this case the carbonation efficiency is calculated at the carbonator exit ($z' = 1$) and solving for the implicit Eq. (23).

Finally, to facilitate the Discussion section that follows, we must define an average CO₂ concentration in the gas phase, that will allow an estimation of the average reaction rate from Eq. (21) which, when applied to Eq. (5), will also yield the overall carbonation efficiency. This is similar to the concept of the mean logarithmic concentration widely used in plug flow reactors. In this case, from the design equations for a CSTR and a PFR assuming a first order of kinetic reaction:

$$k\tau = \frac{\rho_{M,g} f_0 E_{carb}}{(f_{CO_2} - f_e)} \quad (25)$$

$$k\tau = \int_0^{E_{carb}} \frac{f_0 \rho_{M,g} (1 - f_0 x) dX}{[(f_0 - f_e) + (f_0 f_e - f_0) X]} \quad (26)$$

Solving the integral and making both equations equal, we get:

$$\overline{(f_{CO_2} - f_e)} = \frac{E_{carb}}{\left[-\frac{f_0}{(f_0 f_e - f_0)} E_{carb} + \left(\frac{(f_0 f_e - f_0) + (f_0 - f_e) f_0}{(f_0 f_e - f_0)^2} \right) \ln \left(\frac{(f_0 - f_e) + (f_0 f_e - f_0) E_{carb}}{(f_0 f_e - f_0)^2} \right) \right]} \quad (27)$$

Applying this average concentration to the bed, the average reactivity of the active particles in the bed (f_a) is:

$$r_{ave} = \frac{\rho_{CaO} k_s S_{ave} \rho_{M,g} \overline{(f_{CO_2} - f_e)}}{PM_{CaO}} \quad (28)$$

Applying this equation with N_{Ca} and the solution of f_a from the model yields the same capture efficiency as the one obtained from Eq. (18) or (23).

DISCUSSION

The model has been applied to conditions representative of a real case (a power plant delivering a given flow rate of CO_2 , F_{CO_2} , in the flue gases fed to the capture system via the carbonator). The objective of the model is to achieve a reasonable estimate of the capture efficiency. The model described in the previous paragraphs is able to calculate this efficiency when the different parameters in Eqs. (2), (4) and (5) can be estimated from the operating conditions and the sorbent deactivation and reactivity parameters can be obtained from the laboratory experiments. As in the case of any fluidized bed reactor (Kunii and Levenspiel, 1990; Levenspiel, 2005) there is a need for a good knowledge of the fluid-dynamics of the circulating fluidized bed carbonator to determine the solid circulation rate (F_R) the inventory of CaO in the riser (W_{CaO}) and the gas–solid contact quality. However, it is beyond the scope of this work to incorporate a fluidynamic submodel to the carbonator reactor model. Instead, we will show that the carbonator reactor can operate at a reasonable set of values for the key fluidynamic variables (F_R and W_{CaO}) in circulating fluidized bed systems. What might be considered “reasonable” for a new process like the one being considered in this work is open to discussion, but it is clear that the process will be more credible and ready for scaling up if the typical values of the solid circulation rates and solid inventories are within the range of values characteristic of similar systems such as circulating fluidized bed combustors, CFBC. Assuming that this is the case, the mechanical design of the twin reactor system in Fig. 1 and the choice of sorbent particle size distribution and operation conditions (surface gas velocities in the risers) should be such as to ensure the circulation of solids between the reactors (F_R) and the presence of solids inventory in the carbonator reactor (N_{Ca} or W_{CaO}) which, according to the model, is necessary to achieve a high CO_2 capture efficiency. CFBC power plants can operate with solid circulation rates between 1 and 45 $\text{kg/m}^2 \text{ s}$, whereas solids inventories could in principle range from a few thousand Pa to the 0.02–0.03 MPa characteristic of dense bubbling fluidized beds. High solids inventories in a fluidized bed reactor increase the residence time of the circulating solids and maximise their conversion but, at

the same time, they cause a high pressure drop that in turn leads to a higher power consumption by fans.

In the following paragraphs we will use the model to discuss the performance of the carbonator reactor over a wide range of reasonable values for the key operating parameters F_R and W_{CaO} . The choice of parameters to solve the model was justified in the description of the model. All the calculations shown below are referred per MW calculated for a typical coal combustion power plant (0.15 volumetric fraction of CO_2 and 0.1 kg CO_2/s). To translate the results to per m^2 of cross-sectional area of the carbonator, one has to bear in mind that a typical heat duty in a commercial CFBC is around 5 MW/ m^2 .

Fig. 4 shows the CO_2 capture efficiency as a function of the solids inventory (W_{CaO}) at different F_R/F_{CO_2} ratios and for two different F_0/F_{CO_2} ratios. The interval chosen for F_R/F_{CO_2} (between 1 and 20) is consistent with CaO solid circulation rates between 0.6 and 12.3 kg/ m^2 s. Two values of F_0/F_{CO_2} were chosen to illustrate the impact of the make up flow of fresh limestone on the system (around 0.5 kg of limestone per kg of coal when F_0/F_{CO_2} is 0.1 as in Fig. 4a, and around 0.05 kg/kg of coal when this is 0.01 as in Fig. 4b). Both figures show that CO_2 capture efficiency rises rapidly for low values of W_{CaO} until it reaches asymptotically a certain limit. It can be seen that there is an upper limit for all the curves representing the equilibrium (a thick dotted horizontal line in each figure). The predicted CO_2 capture efficiencies approach this equilibrium limit when the flow of active CaO ($F_R * X_{ave}$) is higher than the flow of CO_2 , F_{CO_2} , and there is a sufficient bed inventory to ensure that most CaO particles entering the carbonator in F_R reach a conversion close to their maximum (given by Eq. (8)). When this is not the case and $F_R * X_{ave} < F_{CO_2}$, the carbonation capacity of the solids entering the carbonator is not sufficient to capture all the CO_2 being fed into the carbonator. Hence, the CO_2 carbonation efficiency is limited by the F_R/F_{CO_2} ratio. Again, the upper limit of efficiency (indicated by thin dashed lines in Fig. 4) is only reached when the solids inventory is sufficiently high to ensure that most of the solids achieve their maximum carbonation conversion. In view of this, one might be inclined to favour system

operation modes with the highest possible solid circulation rates, F_R . However, as F_R increases, the solids inventory required to achieve a certain level of solid conversion also increases (so that the same solids residence time is maintained). Furthermore, the heat balance between the calciner and carbonator also imposes certain limits: since it is important to minimise the heat requirements in the calciner it is necessary to reduce the heat required to heat up the solids circulating from the carbonator to the calciner at a lower temperature. This makes it necessary to operate the system with moderate solid circulation rates, ideally no higher than $20 \text{ kgCaO/m}^2 \text{ s}$ (Rodriguez et al., 2008).

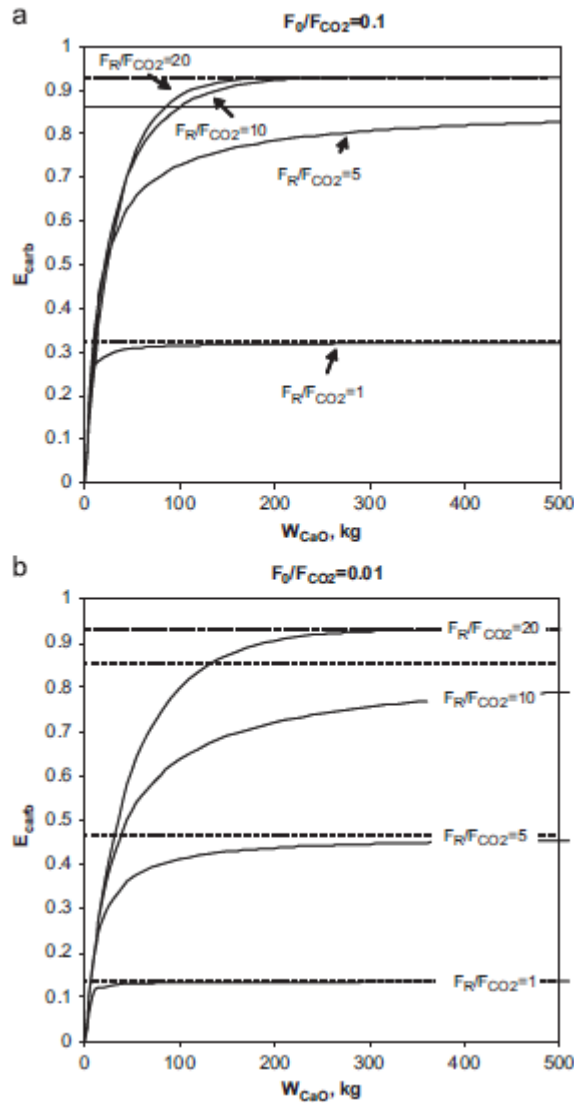


Figure 4. Carbonation efficiency as a function of the solids inventory in the carbonator at different F_R/F_{CO_2} and (a) F_0/F_{CO_2} ratio of 0.1 and (b) F_0/F_{CO_2} ratio of 0.01.

The effect of F_0/F_{CO_2} on the predicted CO_2 capture efficiencies in Fig. 4b can also be explained by similar arguments. When the make up flow of fresh limestone is low, the average activity, X_{ave} , of the solids arriving at the carbonator is low (it would equal X_r for $F_0/F_{CO_2}=0$). The low value of X_{ave}

would require higher values of solid circulation, F_R between the reactors, for $F_R \cdot X_{ave}$ to match the value of F_{CO_2} . Fig. 5 plots the effect of the F_0/F_{CO_2} ratio on CO_2 capture efficiency for two examples of F_R/F_{CO_2} ratios of 20 and 5 and two examples of solid inventories of 50 and 200 kg/MW. Theoretically, when there is no make up flow of fresh limestone, there is no loss of sorbent in the system and the average activity of the sorbent particles in stationary state is the residual activity given by Eq. (7), $X_{ave} = X_r$. In these conditions, the maximum CO_2 capture efficiency for very large values of W_{CaO} is only proportional to the solid circulation rate. Thus it may be possible to attain capture efficiencies close to 90% with no make up flow of sorbent, given sufficiently large solid inventories (over 200 kg/MW) and sufficiently large solid circulating rates (higher than 12 kgCaO/m²s). Of course this is a theoretical limit that cannot be attained in practise because the losses of sorbent from attrition and the need to purge solids to extract ashes and $CaSO_4$, require a continuous make up flow of fresh limestone. However, despite the strong deactivation of CaO with respect to the carbonation reaction after several carbonation–calcination cycles (Eq. (7)), it is theoretically feasible to compensate for the low residual capture capacity by using a higher solid circulation rate, which is within the limits acceptable for similar CFBC units. As can be seen in Fig. 5, high capture efficiencies are also possible for a much wider range of solid circulation rates and solids inventories when there is a make up flow of fresh limestone that improves the average activity or carbonation capacity of the material circulating between the reactors. It should also be noted that for a low F_R/F_{CO_2} , CO_2 capture efficiency is more sensitive to changes in the F_0/F_{CO_2} ratio for both solids inventories. This is not surprising considering that for moderate and low solid circulation rates, only highly active solids (a high X_{ave} due to a high F_0/F_{CO_2}) can achieve high levels of capture efficiency. Fig. 5 shows that there is a range of design choices to be made in order to attain high solid capture efficiencies. The model proposed will be a valuable tool for understanding the trade off between high capture efficiency and minimising the make up flow of

fresh limestone, while at the same time maintaining reasonable solid circulation rates and a sufficient solids inventory in the carbonator.

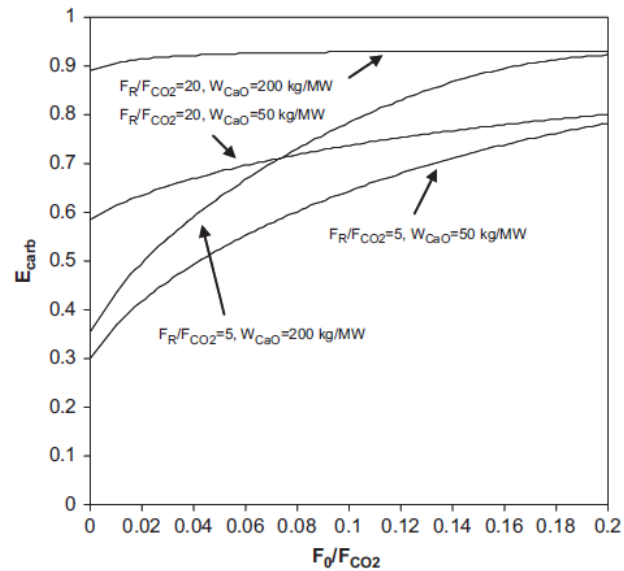


Figure 5. Carbonation efficiency vs F_0/F_{CO_2} ratio at two different F_R/F_{CO_2} ratios and solids inventories.

The CO_2 concentration profiles in the carbonator are also a function of F_R/F_{CO_2} and F_0/F_{CO_2} and the average activity of the sorbent (Eq. (23)). Fig. 6 exemplifies the CO_2 volume fraction axial profiles in the carbonator for different situations. Assuming that the gas in the carbonator reactor is in plug flow, the bed height can be normalised between 0 and 1 for any cross-section of the bed. The equilibrium limit is again represented by a dotted line. Three types of characteristic curves represent the situations already discussed in the previous paragraphs for CO_2 capture efficiency. In Fig. 6, the make up flow of limestone is 0.02 kg/s and the average activity of the sorbent circulating in the system is 0.32, 0.17, 0.11, for the three F_R/F_{CO_2} chosen. There is a sharp drop in CO_2 concentration in the bed in the case of the high solid circulation rate, because of the low carbonation conversion achieved by the sorbent arriving from the calciner. Consequently, the fraction of active solids in the bed (f_a) is

higher (Eq. (16)). In these conditions, the first quarter of the bed is sufficient to absorb most of the CO_2 fed into the reactor. Although this scenario yields very high capture efficiencies, it should be avoided in practise because most of the bed is not effectively capturing CO_2 and therefore, there is an unnecessarily high value of solid circulation rates and solids inventories. In contrast there is a curve corresponding to a very low value of solid circulation rates ($F_R/F_{\text{CO}_2}=1$) that yields a CO_2 concentration profile associated to a low capture efficiency at the exit of the reactor ($E_{\text{carb}}=0.32$). The residence time of the solids is 20 times higher than in the previous case, and they achieve a conversion very close to their maximum at these conditions ($X_{\text{ave}}=0.32$). However it leads to a very ineffective bed (which is full of deactivated CaO and CaCO_3) where few particles are reacting with the gas ($f_a=0.022$). The scenario that offers the optimum combination of conditions is the one represented by the curve for $F_R/F_{\text{CO}_2}=5$. The CO_2 capture efficiency is sufficiently large (in this case $E_{\text{carb}}=0.78$) and this is achieved with a reasonably low value of solid circulation rates, bed inventory and make up flow ratio.

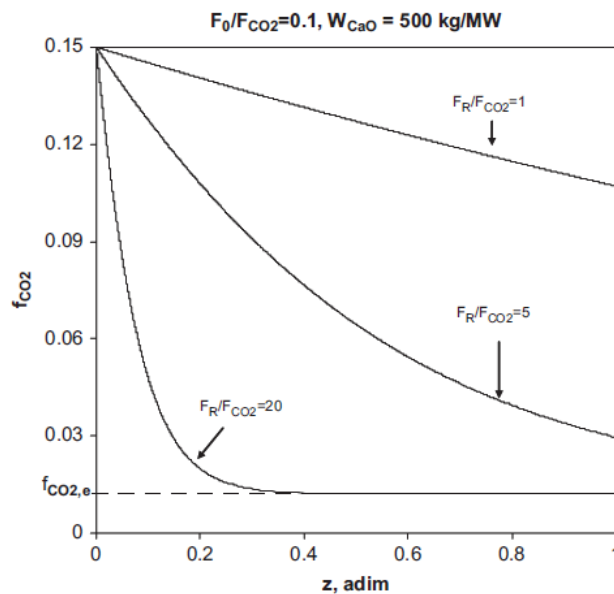


Figure 6. CO₂ profiles along the carbonator for a solid inventory of 500kg/MW and a F_0/F_{CO_2} ratio of 0.1 as a function of the F_R/F_{CO_2} ratio.

All the calculations discussed in the previous paragraphs have been performed assuming that there is no other resistance to the progress of the carbonation reaction than the kinetic reaction. This assumption has been confirmed by recent kinetic studies on the carbonation reaction (Grasa and Abanades, 2006) which show that the typically large pores present in deactivated particles of CaO do not introduce a relevant resistance to the progress of the reaction for typical particle size ranges in CFBs (70–400 μm). However, any deviation from the ideal plug flow model adopted for the gas phase or any other mechanism of deactivation of the CaO surface (e.g. partial sulfation) may reduce the carbonation rates represented by Eq. (21). For this reason, we carried out a sensitivity analysis to estimate the impact of a reduction of the rate parameter on the predicted carbonation efficiencies. The results are represented in Fig. 7 for an effective kinetic constant 5 and 10 times lower than the intrinsic kinetic constant for typical F_0/F_{CO_2} and F_R/F_{CO_2} ratios (0.1 and 10 respectively). As expected, a reduction in the rate of reaction causes a substantial drop in the CO₂ capture efficiencies when the other parameters are kept constant. If the sorbent shows a lower reactivity towards carbonation, CO₂ capture efficiency decreases sharply, in particular for the lower range of solids inventories, when the solid residence times are lower and their conversion is mainly limited by the rate of the carbonation reaction. In contrast, the predicted capture efficiency tends to converge to the same value at high values of bed inventory, because with sufficiently large solids residence times, all particles would achieve their maximum carbonation conversions given by Eq. (8).

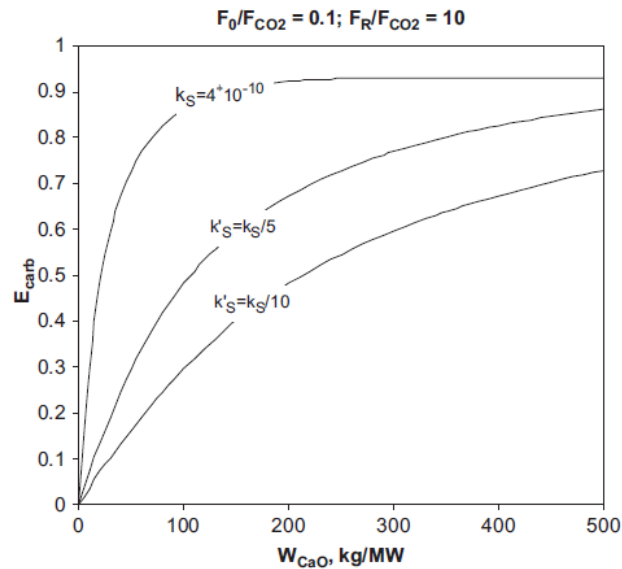


Figure 7. Carbonation efficiency vs solid inventory as a function of the kinetic constant at a F_0/F_{CO_2} ratio of 0.1 and a F_R/F_{CO_2} ratio of 10.

CONCLUSIONS

The results obtained with the model presented in this work show that given a wide range of reasonable conditions for solid circulation rates, solids inventory and typical CaO reactivity parameters, a high CO₂ capture efficiency can be expected from a carbonate looping system when it is applied to combustion flue gases. The model also reveals many conditions in which the capture of CO₂ from the flue gas cannot be effective. This may be due to an insufficient solid circulation rate or solids inventory or to insufficient sorbent activity. The proposed model is based on very simple assumptions about the fluid dynamics of the gas (plug flow) and solids (instant and perfect mixing), but it can integrate in a transparent way the information available about sorbent reactivity and deactivation during cycling. CO₂ capture efficiencies of over 80% are feasible when bed inventories are higher than 200 kg/MW and solid circulation rates are higher than 3 kg/m² s for a typical reaction performance of CaO particles from natural sorbents and make up flows of around 0.5 kg of limestone per kg of coal. Moreover capture efficiencies of over 90% are achievable in a wide range of conditions when solid circulation rates are

increased (up to 6 kg/m² s). Thus the model presented in this work may serve as a valuable tool for designing and optimising postcombustion carbonate looping systems.

NOTATION

A → carbonator section, m²

C_{CO_2} → inlet concentration of CO₂, mol/m³

$C_{\text{CO}_2,e}$ → the CO₂ equilibrium concentration at reaction conditions, mol/m³

e_{max} → maximum thickness of the layer of CaCO₃ on the pore wall, 50nm

E_{carb} → CO₂ capture efficiency in the carbonator

f_0 → inlet molar fraction of CO₂

f_a → volumetric fraction of CaO that reacts in the carbonator in the fast reaction regime

f_e → molar fraction of CO₂ at the point of equilibrium in the reaction conditions

F_0 → molar flow rate of fresh limestone, mol/s

F_{CO_2} → CO₂ molar flow rate at the inlet of the carbonator, mol/s

F_R → molar flow rate of CaO coming from the calciner, mol/s

k_S → kinetic constant, m⁴ mol/s

N_{Ca} → mol of Ca in the carbonator including CaO and CaCO₃, mol

$\text{PM}_{\text{CaCO}_3}$ → molecular weight of CaCO₃, g/mol

PM_{CaO} → molecular weight of CaO, g/mol

r_{ave} → average reaction rate of the active material, s⁻¹

r_N → particle fraction in the N cycle

S_{ave} → maximum average reaction surface, m⁻¹

S_N → reaction surface in the N cycle, m⁻¹

t^* → characteristic time at which the reaction rate becomes zero, s

W_{CaO} → solid inventory in the carbonator, kg

X → solid conversion at the exit of the carbonator

X_{ave} → maximum average conversion of solids

X_N → maximum conversion of particles in the N cycle

$X|<t^*$ → conversion of particles with a residence time lower than t^*

$X|>t^*$ → conversion of particles with a residence time higher than t^*

Greek letters

ρ_{CaCO_3} → CaCO₃ density, g/m³

ρ_{CaO} → CaO density, g/m³

$\rho_{\text{M,g}}$ → molar density of the gas, mol/m³

τ → average residence time in the carbonator, s

ACKNOWLEDGEMENTS

Alonso M. and Rodriguez N. acknowledge the grants received from the JAE-Doc Programme from CSIC and FICYT.

REFERENCES

J.C. Abanades, The maximum capture efficiency of CO₂ using a carbonation/calcination cycle of CaO/CaCO₃, *Chemical Engineering Journal* **90** (2002), pp. 303–306.

J.C. Abanades and D. Alvarez, Conversion limits in the reaction of CO₂ with lime, *Energy and Fuels* **17** (2003), pp. 308–315.

J.C. Abanades, E.J. Anthony, D.Y. Lu, C. Salvador and D. Alvarez, Capture of CO₂ from combustion gases in a fluidized bed of CaO, *A.I.Ch.E. Journal* **50** (2004), pp. 1614–1622.

J.C. Abanades, E.J. Anthony, J.S. Wang and J.E. Oakey, Fluidized bed combustion systems integrating CO₂ capture with CaO, *Environmental Science and Technology* **39** (2005), pp. 2861–2866.

D. Alvarez and J.C. Abanades, Determination of the critical product layer thickness in the reaction of CaO with CO₂, *Industrial and Engineering Chemistry Research* **44** (2005), pp. 5608–5615.

R. Barker, Reversibility of the reaction CaCO₃ ↔ CaO + CO₂, *Journal of Applied Chemistry & Biotechnology* **23** (1973), pp. 733–742.

S.K. Bhatia and D.D. Perlmutter, Effect of the product layer on the kinetics of the CO₂-lime reaction, *A.I.Ch.E. Journal* **29** (1983), pp. 79–86

- G.P. Curran, C.E. Fink and E. Gorin, CO₂ acceptor gasification process. Studies of acceptor properties, *Advanced in Chemistry Series* **69** (1967), pp. 141–161.
- A.J. Deadman and A.J. Owens, Calcium cyanamide synthesis. Part 4-The reaction $\text{CaO} + \text{CO}_2 = \text{CaCO}_3$, *Transactions of the Faraday Society* **58** (1962), pp. 2027–2035.
- G.S. Grasa and J.C. Abanades, CO₂ capture capacity of CaO in long series of carbonation/calcination cycles, *Industrial and Engineering Chemistry Research* **45** (2006), pp. 8846–8851.
- G.S. Grasa, J.C. Abanades, M. Alonso and B. Gonzalez, Reactivity of highly cycled particles of CaO in a carbonation/calcination loop, *Chemical Engineering Journal* **137** (2008), pp. 561–567.
- D. Kunii and O. Levenspiel, *Fluidization Engineering*, Butterworth-Heinemann, Stoneham, MA (1990).
- O. Levenspiel, What will come after petroleum?, *Industrial & Engineering Chemistry Research* **44** (2005), pp. 5073–5078.
- D. Mess, A.F. Sarofim and J.P. Longwell, Product layer diffusion during the reaction of calcium oxide with carbon dioxide, *Energy and Fuels* **13** (1999), pp. 999–1005.
- Metz, B., Davidson, O., Coninck, H.D., Loos, M., Meyer, L., 2005. Special Report on Carbon Dioxide Capture and Storage. Intergovernmental Panel on Climate Change (IPCC), New York, NY, USA.
- E. Ochoa-Fernandez, G. Haugen, T. Zhao, M. Ronning, I. Aartun, B. Borresen, E. Rytter, M. Ronnekleiv and D. Chen, Process design simulation of H₂ production by sorption enhanced steam methane reforming: evaluation of potential CO₂ acceptors, *Green Chemistry* **9** (2007), pp. 654–662.
- C. Pfeifer, B. Puchner and H. Hofbauer, In-situ CO₂-absorption in a dual fluidized bed biomass steam gasifier to produce a hydrogen rich syngas, *International Journal of Chemical Reactor Engineering* **5** (2007).

- N. Rodriguez, M. Alonso, G. Grasa and J.C. Abanades, Heat requirements in a calciner of CaCO_3 integrated in a CO_2 capture system using CaO , *Chemical Engineering Journal* **138** (2008), pp. 148–154.
- L.M. Romeo, J.C. Abanades, J.M. Escosa, J. Paño, A. Giménez, A. Sánchez-Biezma and J.C. Ballesteros, Oxyfuel carbonation/calcination cycle for low cost CO_2 capture in existing power plants, *Energy Conversion and Management* **49** (2008), pp. 2809–2814.
- T. Shimizu, T. Hirama, H. Hosoda, K. Kitano, M. Inagaki and K. Tejima, A twin fluid-bed reactor for removal of CO_2 from combustion processes, *Chemical Engineering Research and Design* **77** (1999), pp. 62–68.
- P. Sun, J.R. Grace, C.J. Lim and E.J. Anthony, The effect of CaO sintering on cyclic CO_2 capture in energy systems, *A.I.Ch.E. Journal* **53** (2007), pp. 2432–2442.
- J.S. Wang, E.J. Anthony and J.C. Abanades, Clean and efficient use of petroleum coke for combustion and power generation, *Fuel* **83** (2004), pp. 1341–1348
- T. Weimer, R. Berger, C. Hawthorne and J.C. Abanades, Lime enhanced gasification of solid fuels: examination of a process for simultaneous hydrogen production and CO_2 capture, *Fuel* **87** (2008), pp. 1678–1686.
- K.B. Yi and D.P. Harrison, Low-pressure sorption-enhanced hydrogen production, *Industrial & Engineering Chemistry Research* **44** (2005), pp. 1665–1669

5.4.2 *Publicación VI*

**AVERAGE ACTIVITY OF CAO PARTICLES IN A
CALCIUM LOOPING SYSTEM**

Publicado en:
Chemical Engineering Journal
Volumen 156 (2)
Año 2010

AVERAGE ACTIVITY OF CaO PARTICLES IN A CARBONATE LOOPING SYSTEM

N. Rodríguez¹, M. Alonso¹, J. C. Abanades¹

¹ *Instituto Nacional del Carbón, CSIC, Oviedo 33011, Spain*

ABSTRACT

Carbonate looping cycles for capturing CO₂ from large emissions sources will most likely use interconnected circulating fluidized bed reactors. The mass balances that govern the mixed solids in the main reactors of these systems, combined with a description of sorbent reaction and decay in activity, are used in this work to define the average activity of the material as a function of the sorbent recycling and make up flow ratios. The new formulation of the mass balances takes into account the fact that particles during carbonation and/or calcination achieve partial conversion in the respective reactors. In these conditions, average activity is shown to be not only a function of sorbent properties and make up flow ratios, but also of the internal solid circulation rates between the reactors. Explicit equations are obtained for the average activity of the circulating materials. These equations are used to discuss the effect of the key operating variables on CO₂ capture efficiency. The equations proposed here for the CaCO₃/CaO system may also be valid for other chemical reactor systems that use interconnected circulating fluidized beds.

Keywords: CO₂ capture, carbonation, deactivation

INTRODUCTION

In order to mitigate the effects of climate change over the next few decades it will be necessary to find a way to balance the use of cheap and widely available fossil fuels, coal in particular, with the ambitious goal of drastically reducing global emissions of CO₂ before 2050 [1]. When the mitigation options take into account the need to ensure the minimum cost of this mitigation, CO₂ capture and storage (CCS) emerges as one of the main options for combating climate change [2]. The devices necessary to deploy CCS on a large scale already exist in the oil, natural gas and chemical industries, and only minor additional investment is required for them to be applied at an even larger scale in the power generation sector. CO₂ capture is known to be the most costly and energy consuming step in the CCS chain. Therefore the goal of many ongoing projects is to develop more energy and cost effective capture methods. One growing area of investigation is that of chemical looping processes. These operate at high temperatures and can theoretically capture CO₂ with minimum energy penalties. Anthony [3] has recently reviewed the development of these processes. From this review it can be seen that they have already entered experimental validation in small pilot plants. The use of the carbonation reaction of CaO with CO₂ and the subsequent calcination of CaCO₃ into CaO and CO₂ is one of these promising chemical looping concepts [3]. A schematic of the carbonation calcination loop is represented in Fig. 1 to illustrating the key gas and sorbent mass streams.

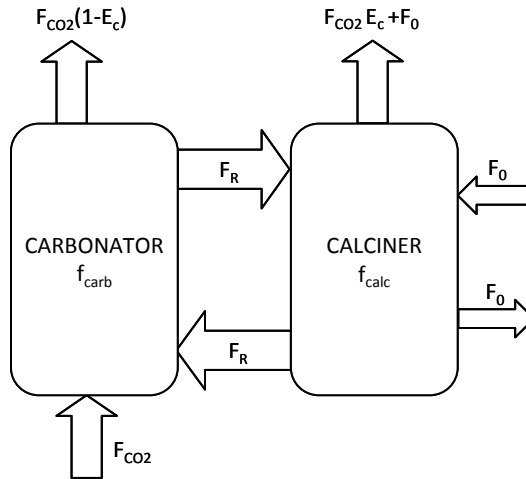


Fig. 1. Schematic of a carbonate looping system to capture CO_2 and main gas and solid streams.

In postcombustion applications, a flue gas containing diluted CO_2 (F_{CO_2} in mol of CO_2/s) is brought in contact with CaO particles to form CaCO_3 in the carbonator reactor up to a certain level of conversion. The CaO particles are continuously coming into the carbonator from the calciner in the solids stream, F_R . A make up flow of limestone (F_0) is introduced into the calciner (or at any other point in the system) and this is balanced in stationary state by an identical flow of CaO (mixed with ashes and other solids if present) leaving the system. The resulting carbonation reaction takes place at temperatures of around 650°C . Over 900°C the reverse calcination reaction takes place in the calciner, as a result of which the CaO is regenerated and a concentrated CO_2 stream is obtained.

The material (CaO particles) cycling in the carbonation-calcination loop is known to become deactivated (loss of CO_2 capture capacity) with the number of carbonation and calcination cycles [4-9]. After each cycle, the fraction of active CaO in a particle is usually defined as the carbonation conversion, X_N , which is reached at the end of the rapid carbonation stage. A general equation

for this deactivation has been proven to be valid for many limestones up to 500 cycles [8, 10]:

$$X_N = \frac{1}{\frac{1}{(1-X_r)} + kN} + X_r \quad (1)$$

where k is the deactivation constant (this has a value of 0.52 for many limestones and under many conditions), X_r is the residual conversion of CaO after an infinite number of cycles ($X_r=0.075$) and N is the number of full carbonation and calcination cycles. Recent works have proposed simple measures to reduce the tendency of deactivation of natural sorbents expressed by Eq. (1) (whereby the effective deactivation constant is reduced and/or the value of the residual activity is increased). Examples of such measures are reactivation methods [11], hydration [12] or treatment of the limestone with doping agents [13]. However for the purpose of our analysis, we have assumed that the decay in conversion is only dependent on the number of cycles as described by Eq. (1).

In a continuous system involving interconnected circulating fluidized beds such as that in Fig. 1, the particles in the fluidized bed reactors are ideally mixed with respect to solid residence time distributions. There is therefore a wide range of particles, with different cycle numbers, constantly present in the system. A mass balance of the carbonate loop of Fig. 1 was carried out in an earlier work [14] to estimate the fraction of particles that have cycled the system N times, r_N , as a function of the circulation rates, F_R , and make up flow ratio, F_0 :

$$r_N = \frac{F_0 F_R^{N-1}}{(F_0 + F_R)^N} \quad (2)$$

The average activity, X_{ave} , or maximum carbonation conversion of a sample of solids from the system, was calculated assuming complete calcination of the

sorbent and the total completion of the fast carbonation stage (up to the level given by Eq. (1)) in the reactors of Fig. 1. N would then represent both the number of times that a particle cycles between each reactor and the number of total carbonation-calcination cycles it experiences when the average activity of the solids in the system is defined as:

$$X_{\text{ave}} = \sum_{N=1}^{N=\infty} r_N X_N \quad (3)$$

This equation generates explicit equations for X_{ave} (depending on the choice of deactivation curve for X_N), and have been used for reactor designs and systems analysis in previous works (see [15-19]). The equations for X_{ave} are valid as long as the operating conditions and reactor designs allow the maximum conversion of solids during carbonation and calcination. This is most likely to occur in the precombustion applications of the carbonation-calcination loop, because the high temperature and high partial pressures of CO_2 guarantee a very fast carbonation reaction, which was demonstrated experimentally by Curran et al. [9] when developing the CO_2 acceptor process. However, recent indications from modelling and experimental results [17, 20-22] suggest that the total carbonation conversion of solids may not be feasible with the typical residence times of particles in a circulating fluidized bed carbonator. This is because the application of carbonate looping cycles to large flow rates of characteristic flue gases in postcombustion CO_2 capture systems would require very compact reactor designs (short gas-solid contact times). In these conditions, the carbonator reactor would have to operate at low partial pressures of CO_2 and which would not allow the particles to undergo their maximum conversion. Furthermore, for the system to operate at a reasonable capture efficiency, a certain amount of active material must be present in the carbonator reactor in stationary state [17, 20, 21, 23], which means that it is necessary a certain amount of CaO with capacity to react with CO_2 . This

requisite implies that partial carbonation of the solids is necessary for the carbonator reactor to be able to operate as an absorber of CO_2 .

On the other hand, the need to keep calcination temperatures down in the calciner, in order to avoid materials and ash related problems, means that calcination temperatures should exceed the equilibrium calcination temperature of CaCO_3 as little as possible. Therefore, although the conditions for a very fast carbonation (up to the limit given by Eq. (1)) and a very fast calcination (up to complete calcination) can be expected given the high rates of carbonation and calcinations reactions, these conditions are in fact likely to be somewhat different from what one would expect for an optimum reactor design. In other words, the search for carbonator reactors of minimum size and with small bed inventories that are able to operate at minimum calcination temperatures will inevitably lead to conditions in which carbonation and calcination cannot be completed. The average activity of the sorbent material flowing into the carbonator will be different from that predicted for these conditions of partial solid conversions. And yet an accurate estimation of this average activity is essential for the design of the carbonator reactor. Thus, the objective of this work is to find a general and simple function that expresses the average activity of the sorbent in the carbonate loop of Fig. 1 when only partial carbonation and calcination conversions take place in the reactors.

MASS BALANCES WITH INCOMPLETE PARTICLE CONVERSION

As mentioned above, Eq. (1) represents the capture capacity of a sorbent after N complete carbonation and calcination cycles and Eq. (2) is the equation used to estimate the fraction of particles that have cycled N times between the carbonator and calciner. However, if the carbonation and calcination reactions are not completed, the two “ N ” mentioned in the previous sentences are no longer the same. For the purpose of this work, however, we retain the meaning of N as being the number of times that a particle has cycled between the carbonator and calciner. As recently discussed elsewhere [24], since Eq. (1) establishes a link between the total carbonation conversion, and the number of

complete carbonation/calcination cycles, we can define a cycle number from the maximum conversion attainable by the sorbent, X_{ave} , which represents the 'reaction age' of the particles, or the cycle number associated to such particles, irrespective of their previous history of partial or complete carbonation/calcination cycles:

$$N_{age} = \frac{1}{k} \left(\frac{1}{X_{ave} - X_r} - \frac{1}{1 - X_r} \right) \quad (4)$$

Furthermore, it is possible to define in the system of interconnected reactors illustrated in Fig. 1 two characteristic conversions of the solids that leave the carbonator (X_{carb}) and the calciner (X_{calc}), and the characteristic changes in carbonation conversion of the solids entering and leaving each reactor. Fig. 2 shows the notation employed for these conversions. Since full conversions are not achieved in the carbonator or in the calciner, it is possible to define the extent or fraction of calcination or carbonation in each reactor, which is as follows:

$$f_{carb} = \frac{X_{carb} - X_{calc}}{X_{ave} - X_{calc}} \quad (5)$$

$$f_{calc} = \frac{X_{carb} - X_{calc}}{X_{carb}} \quad (6)$$

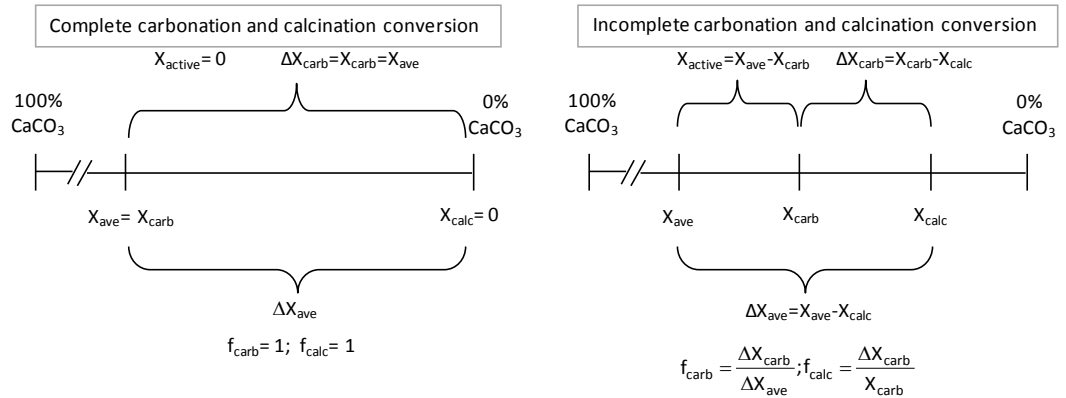


Fig. 2. Definition of the main carbonation conversions involved in the mass balances.

It should be emphasized here that X_{ave} in Eq. (5) is still the average of the maximum carbonation conversion of the family of all particles of the CaO fractions arriving at the carbonator (Eq. (3)). In the carbonator reactor, there will be a certain amount of active solids that have not yet been carbonated and that are responsible for the absorption of CO₂ from the gas phase [17, 20, 21, 23] defined here as X_{active} (see Fig. 2). It is also important to note that the fraction of carbonation and calcination defined above are assumed to apply to all the particles in the system, irrespective of their individual activity or capture capacity. In perfectly mixed reactors, this will not be the case because the large residence time distribution of particles in the bed makes it possible for fully converted particles (long individual residence times) to coexist with particles of low conversion (short residence times). However, it is possible to assume an average conversion that applies to all the particles looping in the system and with this assumption subsequent analysis is greatly simplified. Furthermore, it is also assumed that individual fractions of CaO change their actual age (by Eq. (4)) in discrete mode, by completing a new calcination cycle after their carbonation. In other words, we assume here that partial conversion does not affect the mechanism of decay that leads to Eq. (1) and that a given volume of CaO changes its activity after each calcination cycle.

Following the schematic representations of Fig. 1 and 2 and the previous set of assumptions, the target in this section is to obtain an explicit expression for the average activity, X_{ave} (or maximum carbonation conversion) of the solids entering the carbonator reactor as a function of the solids circulation flows (F_R and F_0) and assumed fractional carbonation and calcination conversions, f_{calc} and f_{carb} .

According to our previous analysis, a certain mass of CaO (particles or fraction of CaO in these particles) has a discrete value of activity that is associated to a specific maximum conversion capability ($X_{N_{age}}$). A certain fraction of CaO, $r_{N_{age}}$, that has experienced N_{age} full carbonations and calcinations in the loop, enters the carbonator in the solid stream (F_R). If total carbonation has occurred after complete calcination, $X_{N_{age}}=X_N$ (Eq. (1)) and $r_{N_{age}}=r_N$ (Eq. (2)). When the carbonation and/or calcination are not completed, the fraction of CaO, $r_{N_{age}}$, together with activity $X_{N_{age}}$, can be calculated from a succession of mass balances by incorporating the fraction of calcination and the fraction of carbonation (f_{calc} and f_{carb}). The first mass balance applies to r_0 , which represents the mol fraction of CaO circulating through the loop that has not experienced any calcination (i.e. is still in the same form of fresh $CaCO_3$ as when it comes from the make up flow). The total flow of solids leaving, or entering, the calciner is the sum of F_0 and F_R . There will be an uncalcined flow of fresh limestone from the make up flow leaving the calciner, $F_0(1-f_{calc})$, and an uncalcined flow of fresh limestone arriving from the carbonator and leaving the calciner, $F_R r_0(1-f_{calc})$. Therefore, the fraction of calcium in the system that has never been calcined is:

$$r_0 = \frac{F_0(1-f_{calc}) + F_R r_0(1-f_{calc})}{F_0 + F_R} \quad (7)$$

Or in explicit form:

$$r_0 = \frac{F_0(1-f_{\text{calc}})}{F_0 + F_R f_{\text{calc}}} \quad (8)$$

Note that the absorption capacity of this fraction of CaO is zero ($X_{N_{\text{age}}}$ or X_N are equal to zero when N_{age} or N are zero because not even the first calcination has yet taken place). In contrast, the next fraction of CaO, r_1 represents the mol fraction of CaO or CaCO_3 that has experienced just one calcination, i.e., the fraction r_1 is made up of CaO and CaCO_3 with an equivalent cycle number $N_{\text{age}}=1$. r_1 is obtained from a mass balance around the calciner. The mass balance is made up of four terms (all with a CO_2 capture capability or capacity equal to X_1 in Eq. (1)): flow of calcium oxide leaving the calciner resulting from the calcination for the first time of the fresh limestone fed into the calciner ($F_0 f_{\text{calc}}$), flow of calcium oxide cycling in the loop (and therefore arriving from the carbonator) that has never been calcined and are calcined now for the first time ($F_R r_0 f_{\text{calc}}$), flow of calcium oxide cycling in the loop that belongs to cycle number 1 but has never been carbonated in the carbonator reactor, and for that reason they still keep on the same capture capacity of cycle number 1 ($F_R r_1 (1-f_{\text{carb}})$) and flow of calcium carbonate cycling in the loop that has been calcined once, it has also been carbonated once, but it is not calcined again when it leaves the calciner ($F_R r_1 f_{\text{carb}} (1-f_{\text{calc}})$). Thus, r_1 is expressed by:

$$r_1 = \frac{F_0 f_{\text{calc}} + F_R (r_0 f_{\text{calc}} + r_1 (1-f_{\text{carb}}) + r_1 f_{\text{carb}} (1-f_{\text{calc}}))}{F_0 + F_R} \quad (9)$$

In a similar mass balance, we define r_2 as the mol fraction of CaO with a carbonation conversion that corresponds to cycle number two (X_2 in Eq. (1)). The mass fraction of CaO in the system that belongs to r_2 is made up of: flow of calcium that changes from cycle number 1 to number 2 after being calcined and carbonated for the second time ($F_R r_1 f_{\text{carb}} f_{\text{calc}}$), flow of calcium that has been calcined twice but it has been carbonated only once, thus its capture capacity is kept on the cycle number 2 ($F_R r_2 (1-f_{\text{carb}})$) and flow of calcium that has been

calcined and carbonated twice, thus it is already part of the fraction of calcium of cycle number 2, but in their third chance to be calcined in the calciner, they are not calcined ($F_R r_2 f_{\text{carb}} (1-f_{\text{calc}})$).

$$r_2 = F_R \frac{r_1 f_{\text{carb}} f_{\text{calc}} + r_2 (1 - f_{\text{carb}}) + r_2 f_{\text{carb}} (1 - f_{\text{calc}})}{F_0 + F_R} \quad (10)$$

It can be seen that the general term for the fraction of CaO in the cycle N_{age} is given by Eq. (11).

$$r_{N_{\text{age}}} = \frac{\left(r_0 + \frac{F_0}{F_R} \right) f_{\text{carb}}^{N_{\text{age}}-1} f_{\text{calc}}^{N_{\text{age}}}}{\left(\frac{F_0}{F_R} + f_{\text{carb}} f_{\text{calc}} \right)^{N_{\text{age}}}} \quad (11)$$

Note here that the Eq. (1), which represents how any fraction of calcium (originally as CaCO_3 in the fresh limestone) decreases the capacity to react with CO_2 with the number of cycles, is still valid for this system. It is assumed what when the carbonation and calcination reactions are not completed, particles will end up with a variety of Ca fractions ($r_0, r_1, r_2 \dots r_{N_{\text{age}}}$) within the particle, but the evolution of the activity in each of these fractions of CaO will still be governed by equation (1). Eq (2) is also valid for this system, but the physical meaning of r_N is different from the physical meaning of $r_{N_{\text{age}}}$ above. In the first case, r_N is the fraction of CaO that has cycled N times between carbonator and calciner. In Eq. (11) $r_{N_{\text{age}}}$ is the fraction of CaO and CaCO_3 that has been fully calcined N_{age} times after $N_{\text{age}}-1$ complete carbonations. Complete carbonation and complete calcination can take place in many partial steps, so that N is always larger than N_{age} except when $f_{\text{calc}}=f_{\text{carb}}=1$ (Eq. (11) becomes Eq. (2) when this happens). However, when it is a question of defining the average activity of the material, we can still define this as an infinite sum of small

contributions from each fraction of material with an activity X_{Nage} . Therefore, we can rewrite Eq. (3) as:

$$X_{ave} = \sum_{Nage=1}^{Nage=\infty} r_{Nage} X_{Nage} \quad (12)$$

We have not been able to find an explicit expression for this sum when using Eq. (1) for X_{Nage} and Eq. (11) for r_{Nage} . But the solution is straightforward when deactivation of CaO (Eq. (1)) is approached as a geometric progression [14]. However, to retain the quality of the fit provided by Eq. (1) for the real deactivation curves, it is convenient to put this equation into the form recently proposed by Li et al. [17]:

$$X_{Nage} = a_1 f_1^{Nage+1} + a_2 f_2^{Nage+1} + b \quad (13)$$

where the fitting constants, $a_1=0.1045$, $f_1=0.9822$, $a_2=0.7786$, $f_2=0.7905$ and $b=0.07709$, fit the data of Eq. (1) with a regression square coefficient higher than 0.99, which means that X_{Nage} in Eq. (13), represents virtually the same deactivation curve as the one expressed by Eq. (1). The advantage of approximating Eq. (13) to Eq. (1) is that when substituting Eq. (13) into Eq. (12) it is then possible to calculate the limit of the infinite sum of the geometric series and calculate the maximum average conversion by means of the following equation:

$$X_{ave} = (F_0 + F_R r_0) f_{calc} \left[\frac{a_1 f_1^2}{F_0 + F_R f_{carb} f_{calc} (1 - f_1)} + \frac{a_2 f_2^2}{F_0 + F_R f_{carb} f_{calc} (1 - f_2)} + \frac{b}{F_0} \right] \quad (14)$$

This is a key purpose designed equation for carbonate looping systems because it links the key sorbent performance parameters with the main solid circulation flows and reactor performance indicators (f_{carb} and f_{calc}) providing a way to estimate the average activity of the material circulating between the reactors.

It is now possible to analyze the impact of partial carbonation and calcination on systems where the same CO₂ capture parameters are maintained constant. For this purpose, we define here the molar flow of the CO₂ captured as:

$$F_c = E_c F_{CO_2} \quad (15)$$

The mass balance in Fig. 1 also defines CO₂ capture efficiency as:

$$E_c = \frac{F_R \Delta X_{carb}}{F_{CO_2}} \quad (16)$$

Carbonation conversion of solids in the carbonator reactor ($\Delta X_{carb} = X_{carb} - X_{calc}$) is maximum when the carbonation and calcination reactions are completed, since X_{carb} will be equal to X_{ave} and X_{calc} will be equal to zero. When the reactions are not completed, the carbonation conversion can be expressed as function of the partial carbonation and calcination as follows:

$$\Delta X_{carb} = f_{carb} f_{calc} X_{ave} \quad (17)$$

Thus, the sorbent molar flow circulating between the reactors (F_R) can be expressed as a function of the CO₂ molar flow captured (F_c), the partial carbonation and calcination fractions (f_{carb} , f_{calc}), and the maximum average conversion attained in the carbonator (X_{ave}):

$$F_R = \frac{F_c}{f_{carb} f_{calc} X_{ave}} \quad (18)$$

Hence, in the next sections we will discuss the effect of f_{carb} and f_{calc} on the average capture capacity of the material circulating in the system for different ratios of characteristic flows of material in the capture system.

EFFECT OF SOLIDS CIRCULATION RATES ON AVERAGE ACTIVITY

In order to discuss the effect of the main solids circulation rates on the average activity of the sorbent we shall begin with a case where complete calcination is achieved in the calciner ($f_{\text{calc}}=1$), where Eq. (14) becomes:

$$X_{\text{ave}} = \frac{a_1 f_1^2 F_0}{F_0 + F_R f_{\text{carb}} (1 - f_1)} + \frac{a_2 f_2^2 F_0}{F_0 + F_R f_{\text{carb}} (1 - f_2)} + b \quad (19)$$

Eq. (19) is represented in Fig. 3 to show how the maximum average conversion (continuous lines) increases for the same molar ratio F_0/F_R , at different values of f_{carb} and when capture efficiency is set to 0.9. The carbonation conversion (X_{carb}) reached in the reactor is indicated by dotted lines for each carbonation fraction (Fig. 3). As can be seen from this figure, the effect of incomplete carbonation in the system for any value of F_0 and F_R is an increment of X_{ave} for decreasing numbers of the partial carbonation fraction. This seems a radical improvement with respect to full carbonation conditions because the active phase (X_{active}) in the carbonator reactor increases as X_{ave} increases and X_{carb} decreases. However, this apparently positive result is misleading because the improvements are at the expense of the increase in the solids circulation rates F_R necessary for the same flow of carbonate to be transported between reactors when the carbonation conversions decrease (see Eq. (16)). Furthermore, since Fig. 3 represents the results as a function of F_0/F_R , the necessary increase in F_R to compensate for lower X_{carb} under partial carbonation conditions also entails an increment of F_0 to maintain the F_0/F_R ratios constant, thereby causing a further increase in the average activity of the materials as a result of the increase in the make up flow of limestone.

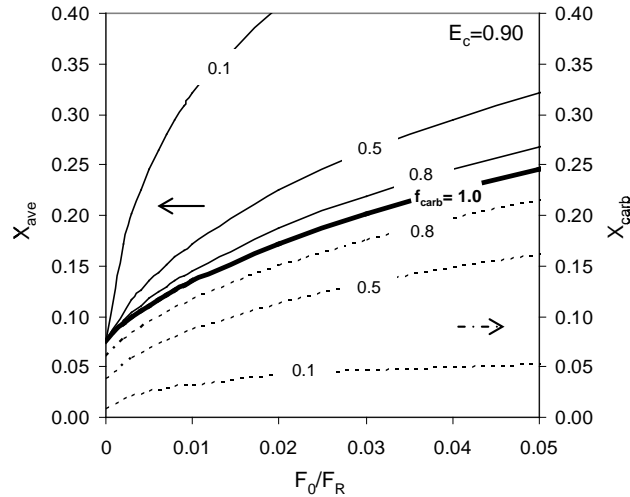


Fig. 3. Maximum average conversion and carbonation conversion attained as a function of the molar flow relation F_0/F_R for different partial carbonation conversions. ($f_{\text{calc}}=1$, $E_c=0.9$).

As pointed out above, once the CO_2 capture parameters (E_c and F_{CO_2}) are fixed, the flow ratios F_0/F_{CO_2} and F_R/F_{CO_2} are connected by the mass balance (Eq. (14) and (16)). In order to clarify this point, Fig. 4 represents the relationship between the make up and recycle flow ratios for different values of f_{carb} . This is a critical point in design choice for achieving the desired capture efficiency: high values of make up flow (which will increase the operational cost of the capture system of Fig. 1 if no use is found for the solids purged from the deactivated CaO) or high values of internal solid circulation rates (which will increase heating requirements in the calciner among other problems). In principle, any one of the points on the solid lines indicates a set of conditions under which it would be possible to capture 90% of the CO_2 fed into the carbonator. Points on the left hand side of the curve represent systems with circulating solids of high average activity because of the large value of the F_0/F_{CO_2} make up flow. These systems require the lowest solids circulation values between reactors, F_R/F_{CO_2} . The partial carbonation of the solids requires a higher value of F_R/F_{CO_2} and therefore all solid lines move to the right. As discussed in previous paragraphs, this means that the average activity of the material increases since partial carbonation is achieved at the expense of an

increase in internal solids circulation. Thus, both increasing the make up flow and increasing the partial carbonation has the same effect of increasing the average activity of the material. In summary one might argue from Fig. 3 that partial carbonation introduces a net benefit into the design at no apparent extra cost. However, Fig. 4 highlights the opposite effect of partial carbonation on the other key parameter in the reactor design: the solids circulation rate increases proportionally as the value of partial carbonation decreases provided that the make up flow is kept constant. Therefore, the apparent benefit of partial carbonation (increasing the average activity of the circulating material) has to be weighed against its negative effect on the increase in solids circulation.

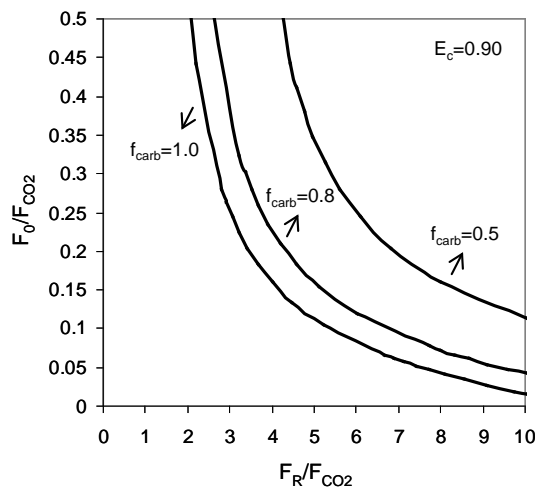


Fig. 4. Relationship between the make up and recycled flow ratios in order to achieve a target capture efficiency of CO₂ for different fractions of carbonation reaction.

Another way to analyze in more detail the effect of partial carbonation on maximum average conversion once capture efficiency is set to a certain value, is by substituting F_R (Eq. (19)) into r_{Nage} (Eq. (11)) when $f_{calc}=1$. The following expression for r_{Nage} is thus obtained:

$$r_{\text{Nage}} = \frac{\frac{F_0}{F_C} X_{\text{ave}}}{\left(\frac{F_0}{F_C} X_{\text{ave}} + 1 \right)^{\text{Nage}}} \quad (20)$$

It can be seen from this implicit equation that the maximum average conversion of any type of CaO in the system is actually independent of the fraction of carbonation (f_{carb}) as long as full calcination takes place after carbonation. Then, under full calcination conditions, the average activity of the solids in the loop is only determined by the flow of fresh make-up limestone to the system. The flow of solids cycling affects the solids conversion in the carbonator. For a given flow of CO₂ capture, higher solid circulation flows lead to partial carbonation conversion and in addition, this will improve the average activity of the circulating solids according to equation (20)..

The question now arises as to what happens when calcination is not completed in the calciner ($f_{\text{calc}} < 1$). The first thing to note is that r_0 (Eq. (7)), or the fraction of calcium from the make up flow that have never been calcined, is greater than zero. These particles therefore do not have the capacity to capture CO₂. Their activity is considered to be zero despite their potential to yield particles with the highest possible capture capacity after the first calcination. By substituting F_R (Eq. (20)) into r_{Nage} (Eq. (11)) when f_{calc} and f_{carb} are not equal to one, the following general equation is obtained for the fraction of CaO in the N_{age} cycle:

$$r_{\text{Nage}} = \frac{\frac{(F_0/F_C)(1-f_{\text{calc}})X_{\text{ave}}}{(F_0/F_C)f_{\text{carb}}X_{\text{ave}} + 1} + (F_0/F_C)f_{\text{calc}}X_{\text{ave}}}{\left(\frac{F_0}{F_C} X_{\text{ave}} + 1 \right)^{\text{Nage}}} \quad (21)$$

Unlike Eq. (20), Eq. (21) shows that, in this case, the maximum average conversion of particles in the system is indeed affected by the fraction of partial calcination (f_{calc}) and the fraction of partial carbonation (f_{carb}) when complete

calcination is not achieved. Thus, the activity of the solids in the loop (represented by Eq. (12)) is not only determined by the flow of fresh make-up limestone (as in the case of complete calcination) but also by f_{carb} and f_{calc} .

Fig. 5 shows the maximum average carbonation conversion as a function of the F_0/F_{CO_2} ratio when f_{calc} takes on different values. For the sake of simplicity f_{carb} is considered to be equal to one in the figure). Once the capture efficiency is set to a certain value, the figure shows that the effect of the partial calcination and/or carbonation becomes significant when the make up flow of fresh limestone, F_0 , is high. The decrease in X_{ave} with lower values of f_{calc} , is more pronounced when F_0/F_{CO_2} has values higher than 0.2. However, it must be emphasized that the looping system for capturing CO_2 is unlikely to work with such a large flow of fresh limestone ($F_0/F_{CO_2}=0.2$ would entail make up flows of limestone of about 1 kg limestone/kg of coal). The grey area in the figure shows a more feasible operating window.

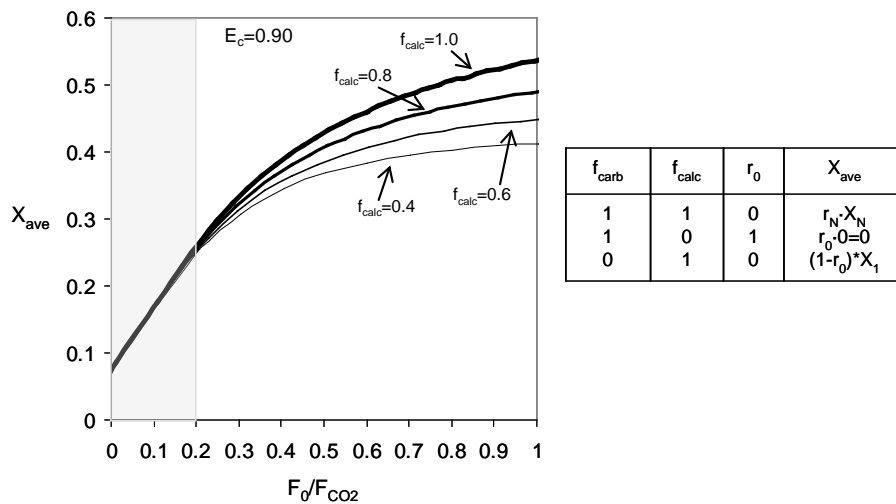


Fig. 5. Maximum average conversion attainable in the carbonator as a function of the F_0/F_{CO_2} ratio for different fractions of calcination ($f_{carb}=1.0$)

The decrease in X_{ave} as f_{calc} decreases is due to the increase in the fraction of calcium that have never been calcined, r_0 . When calcination is incomplete and

F_0 increases, there will be an increasing amount of fresh CaCO_3 entering the carbonator reactor. r_0 is always lower than f_{calc} because, as Eq. (7) shows, r_0 depends on both the make up flow and the recycled flow ratio. For instance, the fraction of r_0 is 19% of the total amount of solids in the system when f_{calc} is 0.4 and the ratio F_0/F_{CO_2} is 1. This means that only 19% of the particles have not yet been calcined despite the low value of f_{calc} . This is because the circulation system offers the particles more than one opportunity to calcine even when the calciner is operating at low values of f_{calc} .

It can be concluded from the previous analysis that, once the capture efficiency is fixed, and given a feasible operating window of make up flows ($F_0/F_{\text{CO}_2} < 0.2$) partial calcination does not significantly affect the average maximum conversion provided that there is no limit to the flow of CaO being recycled. Of course, this is not a realistic supposition because there are well established limits to the solid circulation flows between reactors, as discussed with reference to Fig. 4. It will always be necessary to take into account the F_R/F_{CO_2} ratio.

Fig. 6 shows the capture efficiency attained in the carbonator reactor as a function of the F_0/F_{CO_2} ratio and for two different values of recycled flow. As shown in the figure, the increase in the activity of the solids inside the reactor due to partial carbonation (e.g. of $f_{\text{carb}}=0.8$ and $f_{\text{calc}}=1$), does not benefit the capture efficiency unlike complete carbonation and calcination ($f_{\text{carb}}=f_{\text{cal}}=1$) when the recycled flow of CaO is fixed. As discussed in previous paragraphs, higher values of carbonation and calcination (f_{carb} and f_{calc} close to 1) lead to higher capture efficiencies for the same solid circulation rates. However, in these conditions, the active fraction of calcium ($X_{\text{ave}}-X_{\text{carb}}$) will be low and a very high amount of solids will be needed for the bed inventory to achieve a good capture efficiency. There is then a clear tradeoff between these two effects, and the equations proposed in this work could be very useful for optimizing the design of the system.

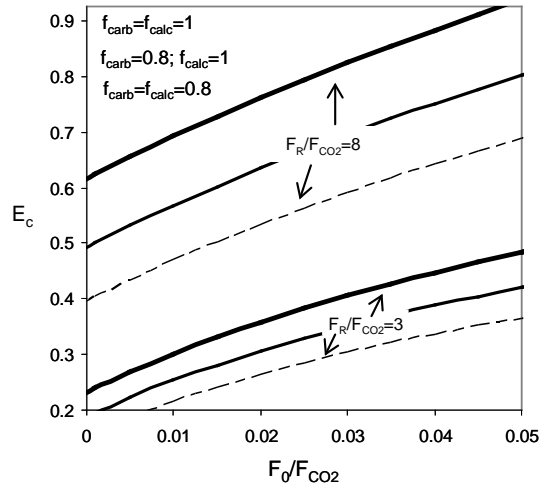


Fig. 6. CO₂ capture efficiency in the loop using different flow ratios.

CONCLUSIONS

CaO looping system can be designed to capture CO₂ from flue gases by means of cycling carbonation and calcination reactions. Large solid flows between reactors will lead to limited residence times of particles in each of their pass through the carbonator or calciner reactors. Complete carbonation and calcination conversion may not take place and particles will have to cycle between carbonation and calcination reactors a higher number of times in order to transport the same amount of CO₂. For a fixed value of capture efficiency the effect of incomplete carbonation and calcination will translate an increase in the average capture capacity of the circulating material. However, the active phase in the circulating solids will increase at the expense of an increase in solid circulation rates. Therefore, the relative benefit achieved from incomplete particle conversions will be the lower solid inventory required in the carbonator reactor thanks to the increase in the active fraction of calcium. However this advantage needs to be offset against the limitations on the reactor

design imposed by the increment of the solids circulation rates, that tend to increase the heat requirements in the calciner.

NOTATION

E_c	CO ₂ capture efficiency in the carbonator reactor.
f_{calc}	Fraction of calcination of all the particles in the system.
f_{carb}	Fraction of carbonation of all the particles in the system.
F_0	Molar flow of fresh make-up limestone fed into the system (mol/s).
F_C	Molar flow of CO ₂ captured (mol/s).
F_{CO_2}	Molar flow of CO ₂ that enters the carbonator reactor (mol/s).
F_R	Molar flow of recycled solids inside the loop (mol/s).
k	General deactivation constant for limestones.
N	Number of calcination and full carbonation cycles
N_{age}	Equivalent number of full carbonation and calcination cycles for a sorbent to reach its current maximum conversion potential (measured as XN_{age}).
r_0	Fraction of calcium in the system as CaCO ₃ that has never been calcined.
r_N	Fraction of calcium that have cycled between carbonator and calciner N times.
$r_{N_{age}}$	Fraction of calcium that have been fully calcined N_{age} times after at least N_{age-1} complete carbonations.
X	Molar conversion of CaO to CaCO ₃ .
X_{active}	CaO reacting in the fast reaction regime in the carbonator.
X_{ave}	Maximum average carbonation conversion attainable by the solids in the system.
X_{calc}	Conversion to CaCO ₃ of solids leaving the calciner.
X_{carb}	Conversion to CaCO ₃ of solids leaving the carbonator.
XN	Maximum carbonation conversion achieved after N calcination and full carbonation cycles

X_{Nage} Maximum carbonation conversion achieved in a full carbonation cycle irrespective of the history of the sorbent in terms of previous calcination-carbonation cycles

X_r General residual conversion of limestones after an infinite number of cycles.

ΔX_{carb} Carbonation conversion of solids in the carbonator reactor.

ΔX_{ave} Maximum possible carbonation conversion possible in the carbonator reactor.

ACKNOWLEDGEMENTS

N. Rodríguez acknowledges a fellowship grant awarded by FICYT (Asturias-Spain). Funding supplied by Endesa and Hunosa is also acknowledged.

REFERENCES

1. IPCC. Intergovernmental Panel on Climate Change, Climate Change 2007. Mitigation. Fourth Assessment Report, Cambridge University Press, 2007.
2. IPCC. Intergovernmental Panel on Climate Change, Special Report on Carbon Dioxide Capture and Storage, Cambridge University Press, 2005.
3. E. J. Anthony, Solid Looping Cycles: A New Technology for Coal Conversion, *Ind. Eng. Chem. Res.* 47 (2008) 1747-1754.
4. A. Silaban and D. P. Harrison, High temperature capture of carbon dioxide: Characteristics of the reversible reaction between CaO(s) and CO₂(g), *Chem Eng Commun.* 137 (1995) 177-190.
5. R. Barker, Reversibility of the reaction CaCO₃ = CaO + CO₂, *J. Appl. Chem. Biotechnol.* 23 (1973) 733-742.
6. T. Shimizu, T. Hiram, H. Hosoda, K. Kitano, M. Inagaki and K. Tejima, A Twin Fluid-Bed Reactor for Removal of CO₂ from Combustion Processes, *Trans. Inst. Chem. Eng.* 77 (1999) 62-68.
7. J. C. Abanades and D. Alvarez, Conversion limits in the reaction of CO₂ with lime, *Energy Fuels.* 17 (2003) 308-315.
8. G. S. Grasa and J. C. Abanades, CO₂ capture capacity of CaO in long series of carbonation/calcination cycles, *Ind. Eng. Chem. Res.* 45 (2006) 8846-8851.
9. G. P. Curran, C. E. Fink and E. Gorin, CO₂ acceptor gasification process. Studies of acceptor properties, *Adv. Chem. Ser.* 69 (1967) 141-161.
10. G. S. Grasa, J. C. Abanades, M. Alonso and B. Gonzalez, Reactivity of highly cycled particles of CaO in a carbonation/calcination loop, *Chem Eng J.* 137 (2008) 561-567.
11. V. Manovic and E. J. Anthony, Steam reactivation of spent CaO-based sorbent for multiple CO₂ capture cycles, *Environ Sci Technol.* 41 (2007) 1420-1425.
12. P. S. Fennell, J. F. Davidson, J. S. Dennis and A. N. Hayhurst, Regeneration of sintered limestone sorbents for the sequestration of CO₂ from combustion and other systems, *J. Energy Inst.* 80 (2007) 116-119.

13. C. Salvador, Lu, D., Anthony, E. J., Abanades, J. C., Enhancement of CaO for CO₂ capture in an FBC environment, *Chem Eng J.* 96 (2003) 187-195.
14. J. C. Abanades, The maximum capture efficiency of CO₂ using a carbonation/calcination cycle of CaO/CaCO₃, *Chem Eng J.* 90 (2002) 303-306.
15. J. C. Abanades, E. S. Rubin and E. J. Anthony, Sorbent cost and performance in CO₂ capture systems, *Ind. Eng. Chem. Res.* 43 (2004) 3462-3466.
16. T. Weimer, R. Berger, C. Hawthorne and J. C. Abanades, Lime enhanced gasification of solid fuels: Examination of a process for simultaneous hydrogen production and CO₂ capture, *Fuel.* 87 (2008) 1678-1686.
17. Z. S. Li, N. S. Cai and E. Croiset, Process analysis of CO₂ capture from flue gas using carbonation/calcination cycles, *AIChE J.* 54 (2008) 1912-1925.
18. N. Rodríguez, M. Alonso, G. Grasa and J. C. Abanades, Heat requirements in a calciner of CaCO₃ integrated in a CO₂ capture system using CaO, *Chem Eng J.* 138 (2008) 148-154.
19. L. M. Romeo, J. C. Abanades, J. M. Escosa, J. Paño, A. Giménez, A. Sánchez-Biezma and J. C. Ballesteros, Oxyfuel carbonation/calcination cycle for low cost CO₂ capture in existing power plants, *Energy Convers Manage.* 49 (2008) 2809-2814.
20. M. Alonso, N. Rodríguez, G. Grasa and J. C. Abanades, Modelling of a fluidized bed carbonator reactor to capture CO₂ from a combustion flue gas, *Chem Eng Sci.* 64 (2009) 883-891.
21. C. Hawthorne, A. Charitos, C. A. Perez-Pulido, Z. Bing and G. Scheffknecht, Proceedings of the 9th International Conference on Circulating Fluidized Beds, Hamburg, Germany, 2008.
22. J. C. Abanades, M. Alonso, N. Rodríguez, B. González, G. Grasa and R. Murillo, Proceedings of the 9th International Conference on Greenhouse Gas Control Technologies (GHGT-9), Washington DC, USA 2008.
23. J. C. Abanades, E. J. Anthony, D. Y. Lu, C. Salvador and D. Alvarez, Capture of CO₂ from combustion gases in a fluidized bed of CaO, *AIChE J.* 50 (2004) 1614-1622.

24. G. Grasa, J. C. Abanades and E. J. Anthony, Effect of Partial Carbonation on the Cyclic CaO Carbonation Reaction, *Ind. Eng. Chem. Res.* 48 (2009) 9090-9096.

6 Conclusiones

Esta memoria, y los artículos presentados en ella, muestran los resultados del análisis teórico de tecnologías de captura de CO₂ en las que interviene el CaO, bien como sorbente, o bien como producto objetivo del proceso (caso de cementeras). Además recoge la experiencia adquirida en planta piloto sobre el proceso de captura de CO₂ con CaO mediante un proceso en ciclos de carbonatación y calcinación. Por último se ha definido un modelo del carbonatador y se ha validado el mismo con los resultados experimentales obtenidos. Las conclusiones extraídas de este trabajo se presentan a continuación:

Análisis de procesos de captura de CO₂ por carbonatación

- ⊙ La rápida desactivación del CaO para el ciclo de captura de CO₂ por carbonatación-calcinación puede compensarse con un flujo continuo suficientemente alto de caliza fresca al sistema, en torno a 0.5 kg por kg de carbón.
- ⊙ Con combustibles de bajo contenido en azufre (o gases de combustión ya desulfurados) la necesidad de caliza fresca puede ser menor, o

incluso nula si se confirma la posibilidad de trabajar con conversiones de carbonatación bajas pero muy estables con el número de ciclos.

- ⊙ Con carbones de alto contenido en azufre y cenizas, es necesario aumentar la purga del sistema. En estas condiciones, el sistema de captura debería destinar los sólidos purgados a una cementera, recuperando de esta forma el crédito asociado a la emisión del CO₂ procedente de la caliza fresca alimentada y la energía asociada a dicha calcinación.
- ⊙ La mínima demanda de calor por parte del calcinador en un sistema de carbonatación-calcinación con eficacias de captura superiores al 70% se sitúa por encima del 30% del total de la potencia térmica que entra a la central.
- ⊙ La demanda de calor del calcinador tiene una compleja relación con los caudales de sólidos en el sistema y con la actividad del CaO como sorbente de CO₂, alcanzando unos mínimos que deben ser objetivo de diseño básico.
- ⊙ La implementación en cementeras de un sistema de pre-calcinación con un flujo de CaO sobrecalentado llevaría a un aumento de la demanda de energía entre 0.8-1.5 GJ/t cemento fabricado. Sin embargo conduciría a evitar en torno a un 55% de las emisiones de CO₂ a la atmósfera respecto del proceso convencional de fabricación de cemento.
- ⊙ El análisis preliminar de costes de CO₂ evitado para el proceso de captura de CO₂ por carbonatación-calcinación de gases de combustión indica costes muy competitivos respecto a otras tecnologías de captura (entre el 20 y 40% inferiores a los de tecnologías dominantes de captura de CO₂ cuando se aplica la misma metodología de estimación

de costes). Parte de estos competitivos costes se debe a que el calcinador es en realidad una nueva central de oxidación, que con una misma unidad de separación de aire está evitando a la atmósfera además del CO_2 de su propia combustión, el CO_2 de los gases de combustión de la central existente que han sido capturados en forma de CaCO_3 en el carbonatador.

- ⊙ El análisis preliminar de costes de CO_2 evitado para el sistema de pre-calcinación de caliza con captura de CO_2 aplicable a cementeras también indica costes muy competitivos. Esto se debe principalmente a que la fabricación de cemento es un proceso energético muy intensivo, con altas emisiones de CO_2 , tanto del consumo de combustible como de la calcinación de la piedra caliza, que conllevan relaciones de CO_2/GJ de más del doble que para una central térmica convencional.

Modelo del carbonatador

- ⊙ Una vez conocido el comportamiento del CaO como sorbente de CO_2 , la eficacia de captura de CO_2 por carbonatación-calcinación en el sistema de reactores de lecho fluidizado circulante interconectados queda caracterizada principalmente por tres variables: F_{CO_2} (flujo de alimentación de dióxido de carbono), F_0 (flujo de alimentación de caliza fresca al sistema) y F_R (flujo de sólidos entrando al carbonatador).
- ⊙ Disponiendo de la curva de desactivación del sorbente, con el flujo de alimentación de caliza fresca (F_0) y el flujo de CaO recirculados (F_R) queda definida la conversión máxima a carbonato (X_{ave}) que las partículas de CaO pueden alcanzar en el reactor de carbonatación, siempre y cuando las reacciones de carbonatación y calcinación se den completamente (f_{carb} y f_{calc} igual a uno).

- ⊙ Para capturar un determinado flujo de CO_2 , es condición necesaria el mismo flujo molar de óxido de calcio activo entrando al reactor de carbonatación ($F_R \cdot X_{\text{ave}}$). Además, las partículas de CaO han de permanecer en el reactor un tiempo de residencia suficientemente alto como para alcanzar su conversión máxima.

- ⊙ Maximizar el flujo de sólidos en el reciclo, para garantizar suficiente flujo de CaO activo para capturar el CO_2 , implicará por un lado, un aumento del inventario de sólidos requerido en el carbonatador para mantener el mismo tiempo de residencia de los sólidos en el reactor y garantizar la máxima conversión a carbonato; por otro lado, un incremento de la demanda de calor del calcinador debido al gran flujo de sólidos circulando entre reactores.

- ⊙ Cuando no se alimenta caliza fresca al sistema ($F_0=0$) e idealmente no se producen pérdidas de sorbente, la actividad media máxima de las partículas en estado estacionario es la actividad residual (X_r) de la caliza utilizada. En este caso, se puede capturar un flujo de CO_2 alto a costa de incrementar el flujo de sólidos circulando (F_R) hasta que los límites del balance de calor y del diseño del equipo lo permitan.

- ⊙ Cuando las reacciones de carbonatación y calcinación no se dan completamente, las partículas de CaO tendrán que circular entre carbonatador y calcinador más veces para transportar la misma cantidad de CO_2 .

- ⊙ Sin cambiar las condiciones de alimentación de caliza fresca, la carbonatación y calcinación parcial implicará una necesidad de mayor flujo de circulación de sólidos para una misma eficacia de captura de CO_2 . Así mismo, la cantidad de sorbente requerida en el carbonatador

podría ser menor debido a que el inventario del sistema presenta una mayor proporción de fase activa disponible para reaccionar.

- ⊙ Además, para una misma eficacia de captura de CO₂ y mismo flujo de alimentación de caliza fresca, el efecto de una calcinación incompleta se traduce en una disminución de la capacidad media máxima de captura de CO₂ de las partículas en el sistema. Esto es debido a la aparición de la fracción de partículas nunca calcinadas (r_0), que no suman capacidad de captura al cálculo de conversión media. La importancia de este efecto se ve disminuida puesto que la disminución de la capacidad de captura máxima, X_{ave} , empieza a ser notable a partir de valores de alimentación de caliza fresca altos (relaciones mayores de 1 kg CaCO₃/1 kg carbón) que están fuera de la ventana de operación óptima del proceso.

Desarrollo del proceso y validación de resultados experimentales

- ⊙ La experiencia obtenida del trabajo experimental en la planta piloto ha demostrado la viabilidad de este proceso. Tanto las temperaturas de los reactores, los valores de flujos de circulación de sólidos y los inventarios de sólidos requeridos para la óptima operación del proceso están dentro de los intervalos de operación asociados a los actuales equipos circulantes que funcionan a gran escala, como son los combustores de lecho fluidizado circulantes.
- ⊙ Los ensayos en la planta piloto de 30 kW han demostrado que el carbonatador CFB funciona como un absorbedor efectivo de CO₂ con CaO con diferentes grados de actividad (con eficacias de captura entre el 70-90%) siempre y cuando haya un cierto inventario en el reactor (entre 10 y 40 mbar) y una alimentación continua de CaO activo (flujos de circulación de sólidos en torno 1-4 kg/m²s).

- ⊙ El balance de carbono entre el CO_2 desaparecido de la fase gas y el CaCO_3 formado en la corriente de circulación de sólidos se cierra de manera satisfactoria en muchos de los estados estacionarios estudiados.
- ⊙ La comparación de los resultados experimentales con las predicciones del modelo de reacción del carbonatador aplicado a las muestras de sólidos extraídas del sistema, muestra un factor de efectividad del carbonatador de 0.87. De esta manera, se puede considerar las partículas de CaO en el carbonatador de la planta piloto son un 87% tan efectivas para capturar CO_2 como si estuviesen reaccionando en un reactor diferencial a la misma concentración media de CO_2 . Este alto valor de efectividad del carbonatador indica que la reacción de carbonatación en el lecho está controlada por la relativamente lenta cinética de reacción.
- ⊙ El parámetro clave para interpretar la eficacia de captura de CO_2 es la cantidad de CaO activo en el lecho, que es el producto de dos factores: inventario de sólidos (W_{CaO}) y fracción de fase activa (X_{active}). Para alcanzar altas eficacias de captura de CO_2 es necesario al menos, que uno de los dos parámetros sea suficientemente alto.

Referencias

- Abanades, J. C. (2002). "The maximum capture efficiency of CO₂ using a carbonation/calcination cycle of CaO/CaCO₃." *Chemical Engineering Journal* 90(3): 303-306.
- Abanades, J. C., Alvarez, D. (2003). "Conversion limits in the reaction of CO₂ with lime." *Energy & Fuels* 17(2): 308-315.
- Abanades, J. C., Anthony, E. J., Lu, D. Y., Salvador, C., Alvarez, D. (2004a). "Capture of CO₂ from combustion gases in a fluidized bed of CaO." *Aiche Journal* 50(7): 1614-1622.
- Abanades, J. C., Anthony, E. J., Wang, J. S., Oakey, J. E. (2005). "Fluidized bed combustion systems integrating CO₂ capture with CaO." *Environmental Science & Technology* 39(8): 2861-2866.
- Abanades, J. C., Rubin, E. S., Anthony, E. J. (2004b). "Sorbent cost and performance in CO₂ capture systems." *Industrial & Engineering Chemistry Research* 43(13): 3462-3466.
- Alvarez, D., Abanades, J. C. (2005). "Determination of the critical product layer thickness in the reaction of CaO with CO₂." *Industrial & Engineering Chemistry Research* 44(15): 5608-5615.
- Baker, E. H. (1962). "The calcium oxide-calcium dioxide system in the pressure range 1-300 atmospheres." *J Chem Soc*: 464-470.
- Bhatia, S. K., Perlmutter, D. D. (1983). "Effect of the product layer on the kinetics of the CO₂-lime reaction." *AIChE Journal* 29(1): 79-86.

- CENITCO2 (diciembre 2007). Informe sobre el diseño conceptual de un prototipo de demostración de un sistema de combustión de biomasa con captura "in situ" de CO₂ mediante carbonatación. MOD3-INC-IT-T34-001. Grupo de captura de CO₂ del INCAR-CSIC.
- CENITCO2 (junio 2008). Resultados experimentales en planta de laboratorio con captura de CO₂ y regeneración continua de sorbente. MOD3-INC-IT-T23-001. Grupo de captura de CO₂ del INCAR-CSIC.
- CENITCO2 (mayo 2007). Presentación primeros resultados planta de laboratorio con captura de CO₂. MOD3-INC-IT-T22-001. Grupo de captura de CO₂ del INCAR-CSIC.
- Cohen, J. E. (1995). *How many people can the earth support?* New York, W. W. Norton & Company.
- Curran, G. P., Fink, C. E., Gorin, E. (1967). "CO₂ acceptor gasification process. Studies of acceptor properties." *Adv. Chem. Ser.* 69: 141-161.
- Duarte, C. M., Abanades, J. C., Agustí, S., Alonso, S., Benito, G., Ciscar, J. C., Dachs, J., Grimalt, J. O., López, I., Montes, C., Pardo, M., Ríos, A. F., Simó, R., Valladares, F. (2009). *Cambio Global: Impacto de la actividad humana sobre el sistema Tierra*, Editorial: CSIC y Catarata.
- Ebner, A. D., Ritter, J. A. (2009). *State-of-the-art Adsorption and Membrane Separation Processes for Carbon Dioxide Production from Carbon Dioxide Emitting Industries*, Taylor & Francis. 44: 1273 - 1421.
- Eide, L. I., Anheden, M., Lyngfelt, A., Abanades, C., Younes, M., Clodic, D., Bill, A. A., Feron, P. H. M., Rojey, A., Giroudiere, F. (2005). "Novel capture processes." *Oil & Gas Science and Technology-Revue De L Institut Francais Du Petrole* 60(3): 497-508.
- Fauth, D. J., Frommell, E. A., Hoffman, J. S., Reasbeck, R. P., Pennline, H. W. (2005). "Eutectic salt promoted lithium zirconate: Novel high temperature sorbent for CO₂ capture." *Fuel Processing Technology* 86(14-15): 1503-1521.
- Feron, P. H. M. (1994). *Membranes for carbon dioxide recovery from power plants. Carbon Dioxide Chemistry: Environmental Issues*, The Royal

- Society of Chemistry. J. Paul and C.M. Pradier (Eds.). Cambridge: 236-249.
- Gartner, E. (2004). "Industrially interesting approaches to "low-CO₂" cements." *Cement and Concrete Research* 34(9): 1489-1498.
- González, B., Grasa, G. S., Alonso, M., Abanades, J. C. (2008). "Modeling of the deactivation of CaO in a carbonate loop at high temperatures of calcination." *Industrial and Engineering Chemistry Research* 47(23): 9256-9262.
- Grasa, G. S., Abanades, J. C. (2006). "CO₂ capture capacity of CaO in long series of carbonation/calcination cycles." *Industrial & Engineering Chemistry Research* 45(26): 8846-8851.
- HUNOSA-CSIC (diciembre 2007). Comportamiento de calizas de Hunosa en ciclos de carbonatación-calcinación y ensayos preliminares de captura de CO₂ en postcombustión en prototipo de laboratorio de lechos fluidizados circulantes interconectados. Grupo de Captura de CO₂ del INCAR-CSIC.
- HUNOSA-CSIC (diciembre 2008). Acuerdo ENDESA-HUNOSA-CSIC para el desarrollo de tecnologías de captura de CO₂ en postcombustión mediante ciclos de carbonatación-calcinación. Grupo de Captura de CO₂ del INCAR-CSIC.
- IEA (2008). Greenhouse Gas R&D Programme (IEA GHG), CO₂ Capture in the Cement Industry, July 2008/3.
- IEA (2009). World Energy Outlook 2009.
- IPCC-AR4 (2007). Climate Change 2007. Mitigation. Fourth Assessment Report. B. Metz, O. Davidson, P. Bosch, R. Dave and L. (Eds.) Meyer. Cambridge University Press.
- IPCC (2005). Special Report on Carbon Dioxide Capture and Storage. B. Metz, O. Davidson, H. Coninck, M. de Loos and L. (Eds.) Meyer. Cambridge University Press. New York, (United States).
- Kato, M., Nakagawa, K., Essaki, K., Maezawa, Y., Takeda, S., Kogo, R., Hagiwara, Y. (2005). Novel CO₂ Absorbents Using Lithium-Containing Oxide. 2: 467-475.

- Li, Y., Buchi, S., Grace, J. R., Lim, C. J. (2005). "SO₂ removal and CO₂ capture by limestone resulting from calcination/sulfation/carbonation cycles." *Energy & Fuels* 19(5): 1927-1934.
- Martínez, I., Murillo, R., Grasa, G., Rodríguez, N., Abanades, J. C. (2010). "Conceptual design of a three bed fluidized bed combustion system capturing CO₂ with CaO." *International Journal of Greenhouse Gas Control* (en prensa).
- National Energy Technology Laboratory (NETL) (2007). The cost and performance baseline for fossil energy power plants study Volume 1: Bituminous coal and natural gas to electricity. DOE/NETL-2007/1281
- Nsakala ya, N., Gregory, N. L., David, G. T. (2007). Commercialization Development of Oxygen Fired CFB for Greenhouse Gas Control.
- Seo, Y., Jo, S. H., Ryu, C. K., Yi, C. K. (2009). "Effect of Reaction Temperature on CO₂ Capture Using Potassium-Based Solid Sorbent in Bubbling Fluidized-Bed Reactor." *Journal of Environmental Engineering-Asce* 135(6): 473-477.
- Shimizu, T., Hiramata, T., Hosoda, H., Kitano, K., Inagaki, M., Tejima, K. (1999). "A Twin Fluid-Bed Reactor for Removal of CO₂ from Combustion Processes." *Trans. Inst. Chem. Eng.* 77(1): 62-68.
- Siriwardane, R. V., Robinson, C., Shen, M., Simonyi, T. (2007). "Novel regenerable sodium-based sorbents for CO₂ capture at warm gas temperatures." *Energy & Fuels* 21(4): 2088-2097.
- TheCopenhagenDiagnosis (2009). : Updating the World on the Latest Climate Science I. Allison, N. L. Bindoff, R. A. Bindshadler et al. The University of New South Wales Climate Change Research Centre (CCRC). Sidney, Australia 60 pp. .
- Wang, J. S., Anthony, E. J., Abanades, J. C. (2004). "Clean and efficient use of petroleum coke for combustion and power generation." *Fuel* 83(10): 1341-1348.
- Yang, H., Xu, Z., Fan, M., Gupta, R., Slimane, R. B., Bland, A. E., Wright, I. (2008). "Progress in carbon dioxide separation and capture: A review." *Journal of Environmental Sciences* 20(1): 14-27.

- Yong, Z., Mata, V., Rodrigues, A. E. (2002). "Adsorption of carbon dioxide at high temperature--a review." *Separation and Purification Technology* 26(2-3): 195-205.